Engineering and Evaluating Fibrin-Targeted Biomaterials for Hemostasis

Robert James Lamm

A disseration

submitted in partial fulfillment of the

requirements for the degree of

Doctor of Philosophy

University of Washington

2018

Reading Committee:

Suzie H. Pun, Chair

Lilo D. Pozzo

Nathan J. White

Program Authorized to Offer Degree:

Bioengineering

University of Washington

Abstract

Engineering and Evaluating Fibrin-Targeted Biomaterials for Hemostasis

Robert James Lamm

Chair of the Supervisory Committee:

Suzie H. Pun

Department of Bioengineering

Traumatic injury incurs a heavy burden on both civilian and military populations throughout the world, and a large proportion of these deaths are due to hemorrhage, or uncontrolled bleeding. Current interventions are not ideal as topical agents are not capable of treating non-compressible injury and biological coagulation products have short shelf-lives and stringent storage conditions. A synthetic, injectable hemostat can overcome the downsides of current interventions. This led to the development of PolySTAT, a polymer-peptide conjugate which crosslinks fibrin at the wound site. This thesis aims to optimize PolySTAT and determine its safety in large animals, with the ultimate goal of moving PolySTAT towards clinical translation. Optimization includes a structure-function study focused on varying the peptide content of the material and exploration of alternative synthesis strategies. Large animal data demonstrates safety of PolySTAT infusions in swine, which have notoriously strong adverse effects to infusion treatments.

Dedication

This is dedicated to two individuals, Keelan and Mom. Keelan put me in a 3-point stance for the first time and picked me up when I was the worst player on the team. Mom has been my biggest fan in everything in my life. These two were paramount in my success as they always listened, and they always smiled. Keelan and Mom remind me to have fun every day and for that I am eternally grateful.

Acknowledgments

I have countless individuals to thank, and words will not do them justice:

Suzie, who is much, much more than an academic advisor and supports her students relentlessly.
Leslie, who is a patient, kind, and exciting mentor. Her ingenuity and desire made PolySTAT.
Nathan, whose creativity and optimism regularly pushes us engineers to think outside of the box.
Drew, who is a bottomless well of knowledge and new ideas.
Nataly, who rules with an iron fist and always has the best Halloween costumes.
Dave, who taught me, encouraged me, and reminded me to stay level-headed in research.
Maryelise, who was always a fun, supportive elder student.
Kevin, who taught me to how to pipette and is my source for insider info from 2010-infinity.
Christine, who reminded me not to eat sugar packets and is always willing to talk through things.
Chayanon, who inspires me with his creativity and helpfulness.
Brynn & Gary, who I owe so much for keeping me laughing and smiling through this journey.
David, who forwarded countless papers and who has been fun grow with.
Albert, who is inquisitive and insightful and keeps me on my toes.
Alex, who is an endless source of thoughtful conversation.
Dan, who brings a very different perspective and enriches the way I think about materials.
Meilyn, who is a thoughtful, caring labmate and friend.
Ian, who brings fun and positivity with him into the lab (and seemingly everywhere).
Emmeline, who manages to always get things done and smiles the whole time.
Audrey, who is invested in both the science and the people of Pun Lab.
Trey, for reminding me to be excited about my work even in tough times. Good luck!

And many, many others including: Heather, Tony, Selvi, Hua, Yilong, Tianyu, Paul, Shixian, Eric, Joe, Ian, Leslie, Sarah, Jon, David, Blake, Jason, Andrew, Randolph, Anna, Mal, Mango.

And of course, Mom & Dad, without whom I would be nowhere.

TABLE OF CONTENTS

Executive Summary 1

Specific Aims 3

Part 1: Introduction 5

Chapter 1. Hemorrhage During Traumatic Injury 7

1.1 Impact of Traumatic Injury 7

1.2 Hemostasis 8

1.3 Coagulopathy in Trauma 10

Chapter 2. Hemorrhage Interventions 12

2.1 Hemostats Currently Approved or in Clinical Trials 12

2.1.1 Human-derived Blood Components 12

2.1.2 Recombinant FVIIa 13

2.1.3 Tranexamic Acid (TXA) 13

2.2 Biomaterials for the Treatment of Hemorrhage 14

2.2.1 Naturally-Derived Materials: The Pioneers of Injectable Hemostats 14

2.2.2 Synthetic Platelets 15

2.2.3 Fibrin-modulating Synthetic Particles 17

2.2.4 Polymer-based Fibrin Clot Modulation 18

2.3 PolySTAT 20

2.3.1 Design and Synthesis of PolySTAT 20

2.3.2 In Vitro Study of PolySTAT's Effects on Clot Formation 21

2.3.3 In Vivo Efficacy and Biodistribution of PolySTAT 23

2.3.4 In Vitro Comparison of PolySTAT to rFVIIa and TXA 24

2.3.5 Summary 25

2.4 References 26

Part 2: Optimizing the Synthesis of PolySTAT 41

Chapter 3. Peptide Valency Plays an Important Role in the Activity of a Synthetic Fibrin-Crosslinking Polymer 43
3.1 Introduction 44
3.2 Materials and Methods 46
3.2.1 Materials 46
3.2.2 Poly(HEMA-st-NHSMA) Synthesis and Characterization 47
3.2.3 Synthesis of PolySTATs Containing Varying Peptide Valencies 47
3.2.4 Rotational Thromboelastometry 48
3.2.5 PolySTAT Evaluation in a Rat Femoral Artery Injury and Fluid Resuscitation Model 49
3.2.6 Neutron Scattering Characterization 50
3.3 Results 52
3.3.1 Synthesis and Characterization of PolySTATs with Varying Peptide Valencies 52
3.3.2 In Vitro Evaluation of PolySTATs by ROTEM 54
3.3.3 In Vivo Performance of PolySTATs in Femoral Artery Injury and Fluid Resuscitation Model 56
3.3.4 Neutron Scattering Measurements of Fibrin Gels with PolySTAT 57
3.4 Discussion 60
3.5 Conclusions 63
3.6 Acknowledgments 64
3.7 References 64
3.8 Supplemental 78
Chapter 4. Improved water solubility and synthetic efficiency of a fibrin-crosslinking polymer 84
4.1 Introduction 85
4.2 Materials and Methods 87
4.2.1 Materials 87
4.2.2 Hydrolysis of Glycidyl methacrylate to Glycerol monomethacrylate 87
4.2.3 Synthesis of pHEMA and pGmMA 88
4.2.4 Polymerization kinetics of p(HEMA-co-NHSMA) and p(GmMA-co-NHSMA) 88
4.2.5 Synthesis of PolySTAT via conjugation 89

4.2.6 Synthesis of FBP-containing methacrylamide monomer, FBP-methacrylamide 89
4.2.7 Synthesis of PolySTAT via FBP-methacrylamide 90
4.2.8 Synthesis of FBP-containing methacrylate monomer, FBP-methacrylate 90
4.2.9 Synthesis of PolySTAT via FBP-methacrylate..... 91
4.2.10 Solubility testing 91
4.2.11 ROTEM Characterization of PolySTATs from various synthesis strategies..... 91
4.3 Results..... 92
4.3.1 Monomer Synthesis 92
4.3.2 Methacrylamide Polymer Synthesis 92
4.3.3 Methacrylate Polymer Synthesis..... 94
4.3.4 Solubility of pHEMA and pGmMA 94
4.3.5 Polymerization kinetics of p(HEMA-co-NHSMA) and p(GmMA-co-NHSMA) 95
4.3.6 ROTEM Characterization of PolySTATs from various synthesis strategies..... 96
4.4 Discussion and Conclusions 98
4.5 References..... 99

Part 3: Evaluate PolySTAT in A large animal model..... 114

Chapter 5. PolySTAT Administration is Safe in a Swine Model of Aortic Tear. 116

5.1 Introduction..... 117
5.2 Materials and Methods..... 118
5.2.1 Materials 118
5.2.2 Synthesis of HEMA backbone polymer 118
5.2.3 PolySTAT Synthesis..... 119
5.2.4 Evaluation of PolySTAT Administration in Uninjured Swine..... 119
5.2.5 Evaluation of PolySTAT Administration in a Swine Model of Trauma via Aortic Tear 120
5.3 Results..... 121
5.3.1 PolySTAT Synthesis..... 121
5.3.2 Evaluation of PolySTAT Administration in Uninjured Swine..... 121
5.3.3 Evaluation of PolySTAT Administration in a Swine Model of Trauma via Aortic Tear 122

5.4 Discussion and Conclusions 126
5.5 *References* 127

Chapter 6. Chapter 6: Proposed Future work 141

6.1 Introduction 142
6.2 Pursuit of a water-soluble Fibrin-Binding Peptide 142
6.3 Fibrin-targeted modulation of tumor metastatic environment 144
6.4 A targeting platform for *Staphylococcus Aureas* 146
6.5 References 151

EXECUTIVE SUMMARY

Traumatic injury is a large burden globally. It is a leading cause of death for both civilians and members of the military. A significant proportion of these deaths are due to hemorrhage, or uncontrolled bleeding. Hemorrhage is initiated by injury and exacerbated by coagulopathy when hemostasis is not reached quickly. Hemostasis, the stoppage of bleeding, normally occurs in the body through complex cellular and protein mechanisms resulting in a strong clot. However, under the hyperfibrinolytic conditions of acute trauma coagulopathy and sustained hemodilution associated with resuscitation fluids, many trauma patients struggle to reach hemostasis due to trauma-induced coagulopathy. Current methods to enhance hemostasis in the clinic, such as human blood components and recombinant clotting factors, can improve outcomes but are not ideal. These interventions require strict storage conditions, preventing their general field use, and provide the potential for immune response resulting in organ failure. Thus, there is an unmet need for synthetic materials able to treat non-compressible hemorrhage that can be administered intravenously.

Early work in the field of injectable hemostats focused on primary hemostasis, the aggregation of platelets at the site of the wound. Another key component of clots is the cross-linked insoluble fibrin gel that strengthens the primitive platelet plug. Fibrin is an attractive target for an injectable hemostat due to its down-stream placement in hemostasis, allowing for the material to be active only where coagulation is activated. Additionally, fibrin-binding ligands have been utilized for the imaging of clots providing ready-to-use targeting moieties.

Seeing this opportunity and inspired by the natural fibrin cross-linking activity of factor XIIIa, PolySTAT was created through a collaboration between the Pun and White groups at the University of Washington. PolySTAT consists of a linear polymer backbone decorated with fibrin-binding peptides (FBPs). Due to the multivalent display of FBP, PolySTAT integrates into fibrin clots and crosslinks the gel, resulting in improved clotting times, clot strength, and most notably a decrease in clot breakdown in the presence of hyperfibrinolytic conditions. PolySTAT has also been shown to increase survival in a model of femoral artery injury and fluid resuscitation in rats.

As PolySTAT is a very promising biomaterial solution for the enhancement of hemostasis in trauma patients, it is the aim of this dissertation work to advance the material towards translation to the clinic. Throughout this work, PolySTAT is scrutinized to determine the effects of the

material structure on the function and mechanism of clot enhancement, the potential for improved synthetic efficiency, its potential to benefit patients in multiple modes of traumatic injury, and its benefits in large animals. Through the lens of PolySTAT, this work is translatable to understanding mechanisms and effects of fibrin gel modulation and the potential benefits of fibrin-crosslinking for enhancing hemostasis.

The last chapter in this thesis focuses on work that can be expanded from the thesis. The first of these proposed projects, improving the solubility of the fibrin-binding peptide in water will drastically improve the synthesis of fibrin-targeted materials and increase the applications for which the peptide can be applied. The next utilizes the fact that PolySTAT is the beginning of a fibrin-targeting platform that can be used for many disease states. The last proposed project will utilize an early project in the Pun Lab which 'failed' to launch a targeting platform for *Staphylococcus aureas*. In this project, a peptide sequence from fibrinogen will be used to target clumping factor A on the bacteria and deliver non-traditional antibiotics as a treatment against MRSA that should not increase antibiotic resistance risks.

SPECIFIC AIMS

Specific Aim 1: Optimize the Synthesis of PolySTAT

Before translation of PolySTAT to the clinic, we must understand the effects of peptide valency on the material. Additionally, peptides make up a large proportion of the cost which is relevant to ultimate translation. First, peptide valency was studied by synthesizing polymers with varied valency and studying the effects on fibrin gels formed with these materials. ROTEM and neutron scattering was utilized to determine strong candidates with low peptide valency for *in vivo* evaluation in a rat model of femoral artery injury and fluid resuscitation. Secondly, alternative strategies for synthesis were considered. A direct polymerization of FBP into the backbone was pursued to avoid the low efficiency of the current graft-to approach. Additionally, water-soluble comonomers were copolymerized to improve the solubility and synthetic efficiency of PolySTAT.

Aim 1 Chapters:

Peptide Valency Plays and Important Role in the Activity of a Synthetic Fibrin Cross-linking Polymer. [Part 2, Chapter 3]

Improved water solubility and synthetic efficiency of a fibrin-crosslinking polymer. [Part 2, Chapter 4]

Publications:

R.J. Lamm, E.B. Lim, K.M. Weigandt, L.D. Pozzo, N.J. White, and S.H. Pun. "Peptide valency plays an important role in the activity of a synthetic fibrin-crosslinking polymer" Biomaterials. July 2017, vol. 132, pp96-104.

R.J. Lamm, F. Huyan, N.J. White, S.H. Pun. "Improved water solubility and synthetic efficiency of a fibrin-crosslinking polymer" *In preparation.*

Specific Aim 2: Evaluate PolySTAT in a large animal model

Traumatic injury occurs in two main forms, penetrating injury and blunt injury. Each type of injury has a unique effect physiologically, and a clinically relevant hemostatic material must consequently be effective in treating both. Additionally, the FDA requires efficacy data in two species before an investigational new drug (IND) filing may be submitted. To meet these criteria,

we developed a blunt trauma injury model in rats. Blunt injuries are commonly veinous/artierolar bleeds at low pressures in organs, therefore a liver resection model was used to mimic blunt injury. Next, PolySTAT was evaluated in a swine model of aortic tear. Swine are an attractive model due to a cardiovascular system similar to humans and large volume of blood which provides the ability for extensive testing on the condition of the animal.

Aim 2 Chapters:

PolySTAT Administration is Safe in Swine Models of Aortic Tear. [Part 3, Chapter 5]

PART 1: INTRODUCTION

CHAPTER 1: HEMORRHAGE DURING TRAUMATIC INJURY

1.1 IMPACT OF TRAUMATIC INJURY

Physical injuries to the body, also known as traumatic injuries, affect many lives throughout the US and the world. According to the Centers for Disease Control and Prevention, unintentional traumatic injury is the leading cause of death for Americans ages 1 to 44[1]. Additionally, traumatic injuries result in the greatest years of potential life lost in the US[2]. According to World Health Organization reports, injuries from road traffic accidents alone accounted for about 2% of deaths globally in 2000 and in 2015, ranking this subset of traumatic injury in the top-10 causes of death worldwide[3,4].

After suffering a potentially fatal traumatic injury, more than one-third of patients are dead upon arrival to the hospital[5]. This emphasizes the generally accepted, while sometimes refuted concept, of the "golden hour" in trauma treatment coined by R Adams Cowley which suggests that treatment within 60 minutes of severe injury will determine the survival of a trauma patient[6].

Traumatic injuries are complex; the term describes wounds from gunshots, stabbings, car accidents, and any other situations which result in one of the three categories of trauma as defined by the National Institutes of Health: blunt force trauma, penetrating trauma, or controlled injury (i.e. surgery). These injuries may occur internally and/or externally throughout the body, affecting various organs and structures, and often incurring significant blood loss. The complexity of these injuries make traumatic injury and the associated causes of death challenging to treat. Hemorrhage, or uncontrolled bleeding, is responsible for 30 to 40% of deaths within the first 24 hours post-injury[7]. This represents a large proportion of deaths that can be alleviated by an improvement in treatments that promote hemostasis.

It is worth noting that to this point, the impacts discussed do not represent the increased severity of injuries faced by deployed military members and the prolonged times to reach treatment in the military arena[8]. Faced with these challenges, hemorrhage plays a large role in combat deaths, accounting for 80% of deaths due to potentially survivable injuries[9]. In fact, the U.S. Army Institute of Surgical Research, reported that improved methods for intravenous non-compressible hemostasis as the main proposed method by which to improve survival of soldiers based on observational data from the War on Terrorism, 2001-2004[9].

1.2 HEMOSTASIS

When the vasculature suffers an injury, the body regulates bleeding through what is known as hemostasis. A robust clot containing proteins, cells, and platelets is formed. The clot must be strong enough to staunch bleeding, be constantly remodeled, and ultimately broken down for proper wound healing at the site of injury. A complex biological function with many steps acting concurrently, hemostasis is generally divided into two phases. Primary hemostasis refers to formation of the platelet plug (Fig. 1.1, left)[10]. Secondary hemostasis describes the formation of a polymerized fibrin clot network (Fig. 1.1, right)[10].

Primary hemostasis begins at the site of injury, where damage to the endothelium results in contact between the subendothelial matrix and blood components. Circulating at a low concentration in the blood, multimeric protein von Willebrand Factor (vWF) binds collagen, a major component in the subendothelial matrix[11]. Additional vWF is released from damaged endothelial cells, and upon binding collagen, vWF acts as an anchor which platelets use to localize to the wound site[12].

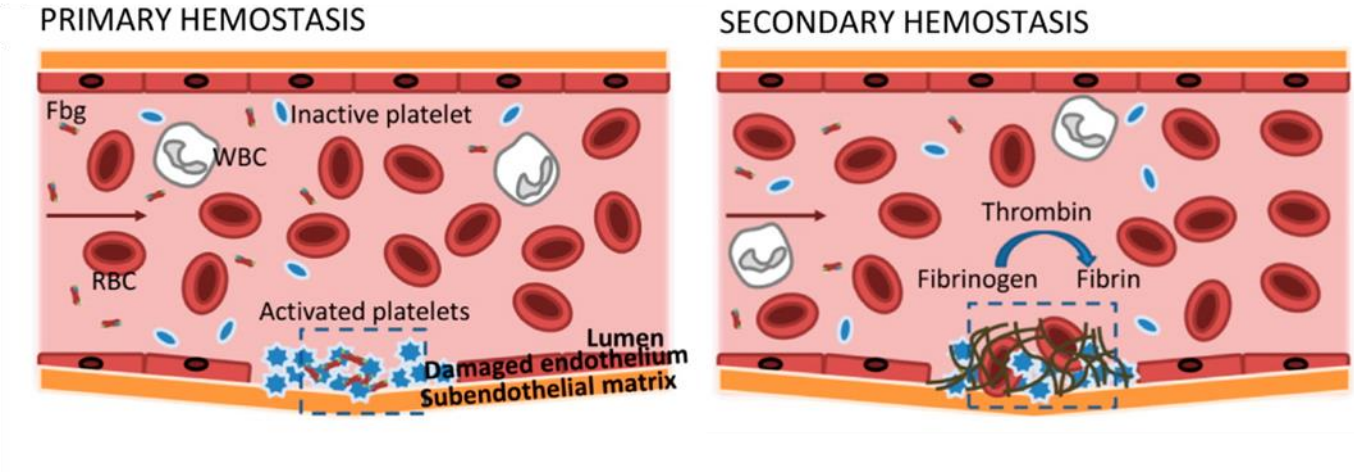

Figure 1.1. Schematic of Hemostasis. Left, Primary hemostasis consists of platelet adhesion and activation. Right, secondary hemostasis consists of clotting cascade activation and ultimate formation of fibrin from fibrinogen and a stabilized fibrin clot. This clot will then undergo remodeling and breakdown by the fibrin-cleaving enzyme plasmin. Figure adapted from Chan *et al*[10]. Copyright 2015 American Chemical Society.

Quiescent platelets bind vWF via the platelet glycoprotein receptor GP Ib-IX complex in a sheer-dependent manner. Additional receptors are implicated in the localization of platelets to the

wound site, including platelet surface receptor GP VI which has affinity for collagen[11]. Localized at the wound site, platelets are exposed to activating stimulants thrombin and adenosine diphosphate which trigger a morphological and biochemical change[12]. In their quiescent state, platelets exhibit a discoid shape, but upon activation platelets protrude pseudopods and their shape becomes irregular[13]. Additionally, GP IIb/IIIa undergoes a conformational change allowing for binding of the circulating blood protein fibrinogen. Due to fibrinogen's symmetrical structure, allowing GP IIB/IIIa to bind at multiple sites, platelets begin to be cross-linked by fibrinogen at the wound site[14–16]. The result of primary hemostasis is a platelet plug that is anchored through interactions of collagen and vWF, and further cross-linked by fibrinogen.

Concurrently, secondary hemostasis is underway; the serine proteases of the clotting cascade undergo a series of cleavages, the final product being a cross-linked fibrin clot (Fig 1.2). Secondary hemostasis is initiated by exposure of tissue factor, naturally found in the tissue adventitia bound to phospholipid, to circulating Factor VII (FVII). This calcium-dependent reaction results in activation to FVIIa[17]. The TF-FVIIa complex can generate FXa, which forms the prothrombinase complex with FVa present on the surface of platelets[17]. The prothrombinase complex generates FIIa, otherwise known as thrombin. This arm of secondary hemostasis is known as the extrinsic pathway, and acts a "sparkplug" to generate thrombin to strengthen kickstart the intrinsic pathway and generate initial fibrin (FIa) from fibrinogen (FI). The most basic understanding of the intrinsic pathway follows that polyphosphate and phospholipids at the site of injury activate FXIIa, which can generate FXIa. FIX is the substrate for FXIa, generating FIXa, which with FVIIIa leads to the generation of FXa in a mechanism orthogonal to that of the extrinsic pathway[18,19]. Decades of research aiming to fully elucidate the mechanisms of clotting have revealed great levels of redundancy and feedback in secondary hemostasis. The TF-FVIIa complex of the extrinsic pathway was found to also activate FIX of the intrinsic pathway, linking it to another mechanism by which to generate FXa[20]. Additionally, FXI has been shown to be activated by thrombin and FXa[19,21]. Importantly, thrombin is considered a master regulator of clotting and is implicated in generation of procoagulatory elements FVIIIa, FXIa, FVa, FXIIIa, as well as the cascade-inhibiting protein C pathway.

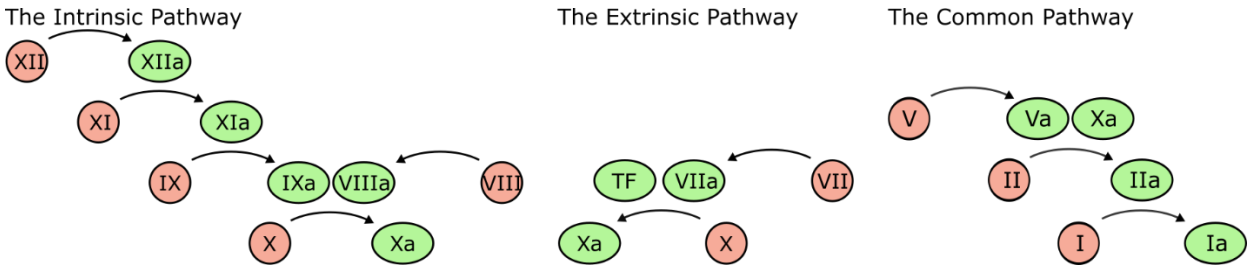

Figure 1.2. The Coagulation Cascade. A simple diagram of the basic clotting cascade, containing the core factors and their primary substrates.

Once significant thrombin is generated, fibrinogen is cleaved into fibrin and self-assembles to form the fibrin clot (Fig. 1.1, right)[10]. The final step in the clotting cascade is the generation of factor XIIIa which covalently crosslinks fibrin fibers through its transglutaminase activity. At this stage, bleeding is decreased and rebleeding is dependent on the condition of the clot. The clot will undergo lysis and remodeling over the course of hemostasis. Ultimately, it will be broken down by plasmin, a fibrin-cleaving enzyme.

1.3 Coagulopathy in Trauma

After traumatic injury, the body faces a greater obstacle to reach hemostasis in comparison to cuts, scrapes, and minor injuries. Additionally, there are physiological conditions, both congenital and acquired, that can further decrease the body's ability to clot, known as coagulopathies. Many of the congenital conditions are dysregulations in proteins involved in the clotting cascade; hemophilia A is a dysregulation in FVIII, hemophilia B is a dysregulation in FIX, and von Willebrand Disease is a dysregulation of vWF. Acquired coagulopathies can directly affect clotting such as those associated with liver failure and the autoimmune disorder known as acquired hemophilia. These congenital and acquired conditions are often regulated through treatments over time. A common and deadly acquired coagulopathy that is not present pre-injury is known as trauma-induced coagulopathy[22,23]. This term describes the combination of the hyperfibrinolytic and hypocoagulative effects of acute trauma coagulopathy present in 25% of trauma patients upon arrival at the hospital as well as the effects of fluid resusciation[23,24]. Fluid resuscitation, while important for maintaining blood pressure in patients to prevent shock, leads to dilution of clotting factors and 70% of patients who receive 4L or more of resuscitation fluid experience coagulopathy[25]. Additionally, patients suffer from acidemia due to insufficient perfusion and

hypothermia due to blood loss, which decrease the function of clotting factors[26]. Overall, these factors make hemostasis difficult after traumatic injury, and are associated with increased mortality[27]. Thus, treatments capable of improving hemostasis, specifically replenishing clotting factors and/or their functions, are necessary to combat what has been hailed the “triad of death”: coagulopathy, acidemia, and hypothermia.

CHAPTER 2: HEMORRHAGE INTERVENTIONS

Many interventions are currently available for treating patients suffering hemorrhage. In the cases of minor injuries and injuries to the extremities, pressure tourniquets are useful and impactful. Additionally, topical agents such as fibrin glue and Quikclot® have shown to be effective for external hemorrhage. The prevalence and impact of non-compressible, uncontrolled bleeding however, has spurred vast improvements in technologies and treatment strategies in the last two decades. Many intervention options are available now, with many more exciting intervention technologies in development.

2.1 HEMOSTATS CURRENTLY APPROVED OR IN CLINICAL TRIALS

2.1.1 *Human-derived Blood Components*

Transfusions of blood products from human donors have been used to treat hemorrhage for nearly a century, with the first use estimated at the end of World War I[28]. Patients may receive whole blood, fresh frozen plasma (FFP), frozen platelets, a red blood cell concentrate known as packed red blood cells (PRBCs), or cryoprecipitate. Whole blood provides hemostatic benefits as well as red blood cells to ensure oxygen delivery throughout the body. FFP, platelets, and cryoprecipitate contain components found in the blood specifically related to hemostasis. PRBCs are utilized to ensure oxygen delivery throughout the body. Whole blood provides the benefits of FFP & PRBCs, however it was surmised that by splitting the components into whole blood, each component could be used rationally which would result in the efficient use of a valuable resource[29].

The overall goal of transfusions of large volumes of blood products, known as massive transfusions (MTs) is to balance hemostasis and oxygen delivery with blood components, specifically to counteract the dilutive effects of fluid resuscitation, which aims to keep a patient out of shock. It is generally considered that a unit ratio of 1:1:1 FFP:PRBC:platelets provides the best outcome for patients[29,30]. A retrospective study observing trauma patients in New Orleans concluded that a 1:1 ratio of FFP:PRBC conferred a survival advantage over a group those that received

1:>2 FFP:PRBC, and this data corroborated reports from the military arena[30]. The military uses whole blood transfusion presently under circumstances where component treatment is not possible, generally due to shortage borne out of the stringent storage conditions necessary for platelets[31].

MT has also been implicated in numerous negative effects including, but not limited to, citrate toxicity, hypocalcemia, hyperkalemia, multiple organ failure, immune response, and potential for infection[31,32]. Additionally, these components require strict storage conditions. Overall, MT is a strategy that is administered in a non-standardized fashion patient-by-patient and, despite advances, retains many weaknesses biologically as well as technically.

2.1.2 *Recombinant FVIIa*

NovoSeven®, marketed by NovoNordisk Pharmaceutical, Inc., is a recombinantly manufactured active form of human factor VII. The original indication for NovoSeven® was for the treatment of hemophilia since FVIIa activates the extrinsic pathway in the presence of TF at the site of the wound which compensates for the weakened intrinsic pathway in hemophiliacs. NovoSeven has entered trials for use as a treatment for traumatic injury. It has shown a good safety profile, with no increase in thromboembolic events, and a reduction in multiple organ failure[33,34]. However, NovoSeven is not yet an approved for trauma as it has not shown a robust, significant improvement in survival.

2.1.3 *Tranexamic Acid (TXA)*

A key aspect of coagulopathy is the hyperfibrinolytic environment during large bleeds. In a healthy clotting event, coagulation is initiated to staunch bleeding, and the release of tissue plasminogen activator (tPA) activates plasmin to both ensure that no off-target thrombosis occurs as well as break down the clot to allow for proper wound healing. In a large injury, however, tPA is released by damaged endothelial cells resulting in significant amounts of plasmin generated and consequently creating a hyperfibrinolytic state near the wound site[35]. Tranexamic acid (TXA) is a lysine analogue that has been used to combat hyperfibronlysis for its ability to inactivate

plasmin[35]. The effects of TXA during trauma treatment has been studied in civilian (CRASH-2) and military (MATTERS) settings and reported in 2010 and 2012, respectively. In both cases, treatment with TXA showed improved survival compared to a placebo with no increase in negative effects[36,37]. While it is not currently approved for trauma treatment, these large studies in the last 10 years coupled with hundreds of current clinical trials in the US alone[38] suggest a promising a future for TXA.

2.2 BIOMATERIALS FOR THE TREATMENT OF HEMORRHAGE

With the elucidation of clotting mechanisms and the advancement of nanotechnology, biomaterials able to promote hemostasis have become a promising solution. These materials, often taking a drug delivery approach, aim to enhance different aspects of clotting while providing a targeted therapy that enhances clotting only at the wound site.

2.2.1 *Naturally-Derived Materials: The Pioneers of Injectable Hemostats*

Early work in this field saw the use of natural materials. One of the first natural/synthetic hemostatic materials originated in 1980 when Barry S. Coller demonstrated that platelets aggregated in an ADP-dependent fashion in the presence of fibrinogen-coated acrylonitrile microbeads[39]. This was shortly followed by Coller and coworkers developing thromboerythrocytes, studied in the 1990s. The decoration of red blood cells (RBCs) to the Ac-CGGRGDF-NH_2 peptide, a sequence found in fibrinogen and involved in GPIIb/IIIa binding, allowed thromboerythrocytes to take advantage of the biocompatibility of RBCs, but add hemostatic effects[40]. *In vitro* studies confirmed thromboeythrocytes aggregate platelets in the presence of ADP.

Shortly thereafter, Levi *et al* studied the ability of a fibrinogen-coated albumin microparticle, coined the Synthocyte, to improve hemostasis. These particles were successful in decreasing bleeding in an ear injury model in platelet-deficient rabbits[41].

This early work showed the ability of particles with fibrinogen, or peptides containing fibrinogen sequences such as RGD, to aggregate platelets and decrease bleeding. Despite advantages of biocompatibility, these technologies retain the

inherent weaknesses of blood products, namely storage potential and potential for immune response.

2.2.2 *Synthetic Platelets*

Significant work in the realm of drug delivery revealed that nanoparticles exhibit improved biodistribution over larger particles and provide improved delivery of cargo to sites of interest. Additionally, particles on the micron-scale, such as the Synthocytes of the 1990s, are filtered out quickly in lung capillary beds and can lead to significant toxicity[42]. Synthetic nanoparticles allow for control over the size and composition of the material and can have more favorable storage conditions in comparison to naturally-derived materials.

Liposomes, lipid bilayers forming spherical vesicles, are attractive delivery vehicles for their ability to delivery hydrophilic and/or hydrophobic cargo, ease of surface functionalization, and controlled formation strategies. Okamura *et al.* utilized these characteristics in a PEGylated phospholipid liposome system decorated with a 12-residue peptide found at the C-terminus of the gamma chain of fibrinogen, known as H12[43]. These particles were found to interact specifically with platelets and decrease tail bleed times in a model of platelet-deficient mice[43]. This early work showed promise of this system, and later the platelet agonist ADP was loaded into the liposomes to further improve pro-coagulatory effects. ADP-loaded H12-liposomes provided a similar decrease in bleeding time and non-loaded H12-liposomes at one-fourth the concentration in a model of thrombocytopenic mice[44].

Polymeric nanoparticles have been utilized for drug delivery due similar benefits as liposomes, but with the ability for greater tunability of the particle characteristics based on the polymers used in the formulation. The Lavik group developed a PEGylated poly(lactic-co-glycolic acid) (PLGA) nanoparticle system decorated with RGD peptides found in fibrinogen. These particles were shown to interact specifically with activated platelets, promoting aggregation, and increase survival in a model of traumatic femoral artery injury in rats[45]. This elegant design was further improved by tuning ligand density, where studies showed that increased RGD on the surface of particles resulted in similar improvement of survival at lower doses administered in

a liver injury model in rats[46]. Additionally, the polymer core was altered to a poly(lactic acid) core with a mixture of isomers D-lactic acid and L-lactic acid, conferring improved stability during storage at elevated temperatures[47]. The Lavik group's hemostatic nanoparticles, through tunability and design, show promise in models of penetrating trauma, blunt trauma, as well as blast injuries as well as robust storage properties[45,48]. The hemostatic nanoparticles were loaded with steroid dexamethasone and found to decrease inflammation in the lung after blast trauma[49]. Earlier this year, the Lavik group reported results in swine[50]. Here, they demonstrated their hemostatic nanoparticles led to complement-related massive exsanguination. They were able to alter their design, introducing a neutral form of the RGD peptide to decrease the complement-related psuedoallergy response and subsequently demonstrated decreased blood loss in pigs. Notably, bleeding ceased within 10 minutes. The Lavik group continues to be a forerunner in the intravenous hemostat field and their synthetic platelets show immense promise.

Another promising synthetic platelet is the liposome-based SynthoPlate developed by the Sen Gupta group. Early work from their group investigated the use of RGD-decorated liposomes as drug delivery systems to platelets and their ability to increase platelet aggregation[51,52]. This pro-coagulatory system has evolved over time to more accurately recapitulate multiple functions of platelets. Heteromultivalent display of peptides binding vWF and collagen were shown to improve localization of the synthetic platelets to the wound site[53]. This was incorporated into the overall design of the system, and synthetic platelets consisting of liposomes decorated with RGD peptide, a vWF binding peptide, and a collagen binding peptide have been shown to decrease bleeding time in a tail transection mouse model[54]. Earlier this year, the Sen Gupta group also reported results in swine[55]. Here, they demonstrated that Synthoplates retain activity after sterilization techniques (filtration and E-beam), exhibit limited complement activation, and decrease blood loss in a swine model of traumatic injury. Haima Therapeutics is currently pursuing development and commercialization of the SynthoPlate system[56].

Synthetic platelets have utilized the targeting ability of peptides and the ease of surface conjugation to develop sophisticated systems that are able to interact

specifically with platelets, effectively cross-linking at the site of injury. Depending on the system used, delivery potential has been utilized to give these systems the ability to activate platelets or promote wound healing. Tunability of cores has allowed for the improvement of stability during storage. The ease of surface conjugation has allowed for the use of multiple ligands and the tuning of ligand density for optimal efficacy. Nanoparticles still have some weaknesses in ultimate use, notably significant uptake in the liver and the potential for complement activation related pseudoallergy (CARPA), the immune response to particulates observed by the Lavik group which can be deadly if not mediated and was observed in treatments with the first FDA-approved nanotechnology drug, Doxil[57,58].

2.2.3 *Fibrin-modulating Synthetic Particles*

Synthetic platelets mimic the form of activated platelets bound to fibrinogen and cross-link platelets at the wound site, boosting primary hemostasis and formation of the platelet plug. However, there has been less work in synthetic materials for the enhancement of secondary hemostasis. At the end of secondary hemostasis, there is a cross-linked insoluble fibrin gel that forms a robust clot. Assisting this process may improve the ability for the body to staunch bleeding.

The Barker group has thoroughly studied fibrin gels, fibrin-based biomaterials and the effects of materials on fibrin and fibrin gel formation. The group entered the field of synthetic hemostats with platelet-like particles (PLPs) consisting of ultra-low crosslinked microgel particles decorated with fibrin-targeted single domain variable fragments (sdFvs) that were identified through phage display[59]. These particles were shown to associate with fibrin clots via sdFv targeting, and based on their poly(N-isopropylacrylamide-co-acrylic acid) core, these particles deform once bound to the fibrin. PLPs were shown to decrease bleeding time in a femoral vein injury model in rats, due to the ability of PLPs to bind and stabilize clots at the wound site. A large role of platelets within the established fibrin clot is to physically pull inward and "collapse" the clot[60]. PLPs were shown to collapse clots on a time scale of 24-48 h. Naturally, this occurs on the scale of minutes to hours, but this shows the potential for creating materials capable of binding, stabilizing, and collapsing fibrin clots. PLPs

have been shown to promote clot properties while still allowing for diffusion of bioactive molecules, an important observation for combined treatments[61].

2.2.4 *Polymer-based Fibrin Clot Modulation*

The formation of the fibrin network in a clot is initiated at the activation of fibrinogen from fibrin (Fig 2.1)[10]. Enzymatic cleavage by thrombin exposes peptide strands that can insert into domains of symmetric fibrin(ogen) monomers forming protofibrils. Lorand *et al* hypothesized that a double-headed linker with a peptide sequence found in knob A (Gly-Pro-Arg-Pro, GPRP) at either end of PEG would be able to cross-link fibrin, altering properties. This was the case, and the double-headed linker was able to cross-link D domains in a non-covalent fashion reminiscent of the covalent cross-linking observed by FXIIa[62]. Cross-linking was shown to be productive at low concentrations, but this benefit was ablated as concentration was increased, a result that was true for both purified D domains and purified gamma chains of fibrinogen.

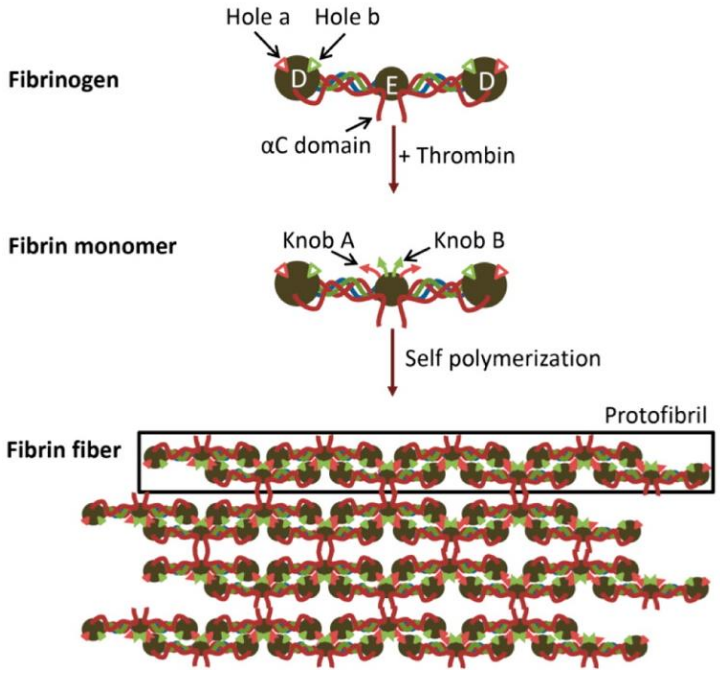

Figure 2.1. Activation and Assembly of Fibrin. Thrombin cleaves peptides at the Aα and Bβ strands of fibrinogen, revealing knobs A & B, respectively. These peptide strands have affinity for holes a and b, respectively inserting and forming protofibrils. Interactions of αC domains of nearby protofibrils result in lateral aggregation and greater fibrin fiber is formed. Figure adapted from Chan *et al*[10]. Copyright 2015 American Chemical Society.

Work by the Barker group in fibrin gels for biomaterials applications led to further pursuit of this strategy. Four-arm PEGs decorated with GPRP peptides were synthesized and the effects on fibrin clot formation were observed[63]. Similar to the work by Lorand *et al*, the studies by Soon *et al* demonstrated four-armed GPRP increased crosslinking of fibrinogen, but this effect was lost at high concentrations. High concentrations of four-armed GPRP was also shown to increase clotting times and decrease elastic modulus. It is hypothesized the decrease in clotting properties is due to GPRP peptides competing with fibrin monomers for polymerization sites, in contrast to FXIIIa cross-linking which occurs elsewhere on the D domain. The work

of Lorand *et al* and Soon *et al* were groundbreaking to show that fibrin could be non-covalently crosslinked by multivalent display of peptides that bind fibrin.

2.3 PolySTAT

Inspired by the concept of crosslinking fibrin demonstrated by Lorand *et al* & Soon *et al* and applying drug delivery approaches to hemostasis utilized by the Lavik and Sen Gupta groups, the Pun Lab has developed a polymer-peptide material that cross-links fibrin at the site of injury.

The Caravan group reported the phage display identification and subsequent affinity and stability optimization of a fibrin-binding peptide (FBP) utilized for MRI imaging of clots[64,65]. By utilizing a targeting ligand that does not interfere with the standard knob-hole interaction of fibrin polymerization, the potential to obtain productive cross-linking of fibrin seems more likely. In 2015, Chan *et al* reported the development of a fibrin cross-linking polymer capable of modulating clot properties as a treatment for promoting hemostasis[66]. The elegant design, FBP grafted onto a poly(hydroxyethyl methacrylate) (pHEMA) backbone, showed strong results both *in vitro* and *in vivo*.

2.3.1 *Design and Synthesis of PolySTAT*

Due to advances in polymer chemistry, controlled radical polymerizations such as reversible addition-fragmentation chain transfer (RAFT) polymerization allow for the synthesis of well-controlled polymers at desired molecular weights[67,68]. Polymers can experience prolonged circulation properties over nanoparticles when of the correct size and composition[69], making them attractive for use in biomedical applications. When designing PolySTAT, a RAFT-amenable pHEMA backbone was chosen for its hydrophilic nature and previous use in biomaterials[70]. Additionally, n-hydroxysuccinimide methacrylate (NHSMA) was copolymerized to allow for the grafting of the Caravan group's FBP to the material.

Chan *et al* reported control over the base polymer synthesis and that PolySTAT was synthesized with 16 peptides per polymer, on average[66].

2.3.2 *In Vitro Study of PolySTAT's Effects on Clot Formation*

PolySTAT significantly enhanced clotting in purified fibrin systems. Laser-scanning confocal microscopy demonstrated that fluorescein-labeled PolySTAT co-localized with fibrin in clots, compared to little-to-no colocalization of a control polymer with a scrambled form of FBP, PolySCRAM (Fig. 2.2A)[66]. Cone-and-plate rheometry demonstrated that fibrin clots formed with PolySTAT were able to retain storage modulus at one-third the concentration of fibrinogen. (Fig 2.2B). Thromboelastography (TEG), a clinical assay of clotting, indicated that clots under hyperfibrinolytic conditions formed more quickly and stronger, while preventing clot lysis (Fig. 2.2B).

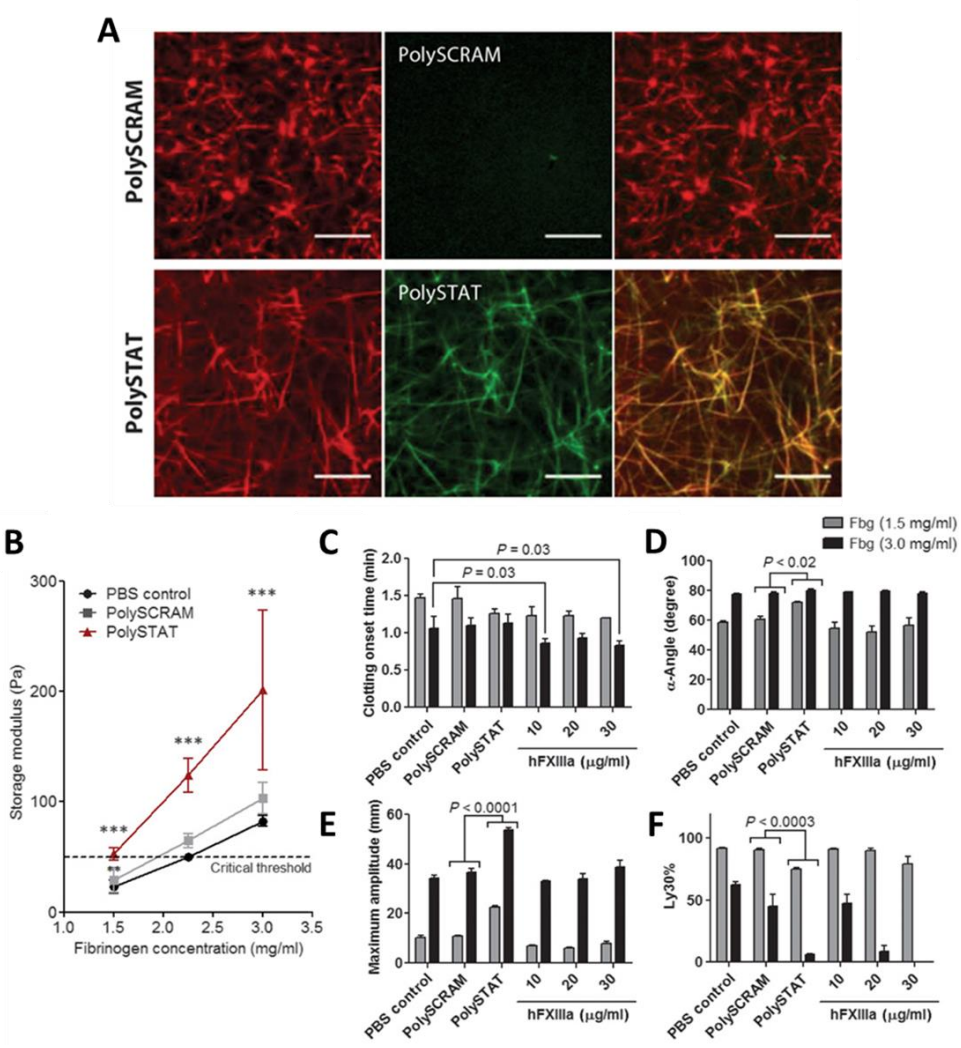

Fig 2.2 In vitro characterization of PolySTAT. A, Confocal microscopy of fluorescein-labeled PolySTAT and PolySCRAM (green) in fluorescently-labeled fibrin (red) clots. Left panes are fibrin, middle panes are polymer, and right panes are merged channels. PolySTAT was shown to colocalize with fibrin whereas PolySCRAM had little-to-no colocalization. B, Cone-and-plate rheometry of fibrin clots formed with varying concentrations of fibrinogen with PolySTAT or PBS and PolySCRAM as controls. PolySTAT improved storage modulus, rescuing low concentration fibrinogen gels. C-F, TEG analysis of fibrin gels formed in the presence of PolySTAT. Clot kinetics (D) and stiffness (E) were increased and clotting time and fibrinolysis (F) were decreased in comparison to PBS and PolySCRAM controls. Figure adapted from Chan *et al*[66]. Reprinted with permission from AAAS.

2.3.3 *In Vivo Efficacy and Biodistribution of PolySTAT*

PolySTAT was evaluated in a rat model of femoral artery injury and fluid resuscitation. A diagram explaining the procedure is present in Figure 2.3A adapted from Chan *et al*[66]. Over the 75-minute time course of the study, the PolySTAT group survived 100% of the time, in comparison to 0-40% for controls (saline, PolySCRAM, albumin as an oncotic pressure control, and hFXIIa) (Fig. 2.3B). Notably, rats treated with PolySTAT required smaller volumes of resuscitation fluid over the course of the study, suggesting the benefit of early hemostasis in trauma (Fig 2.3C).

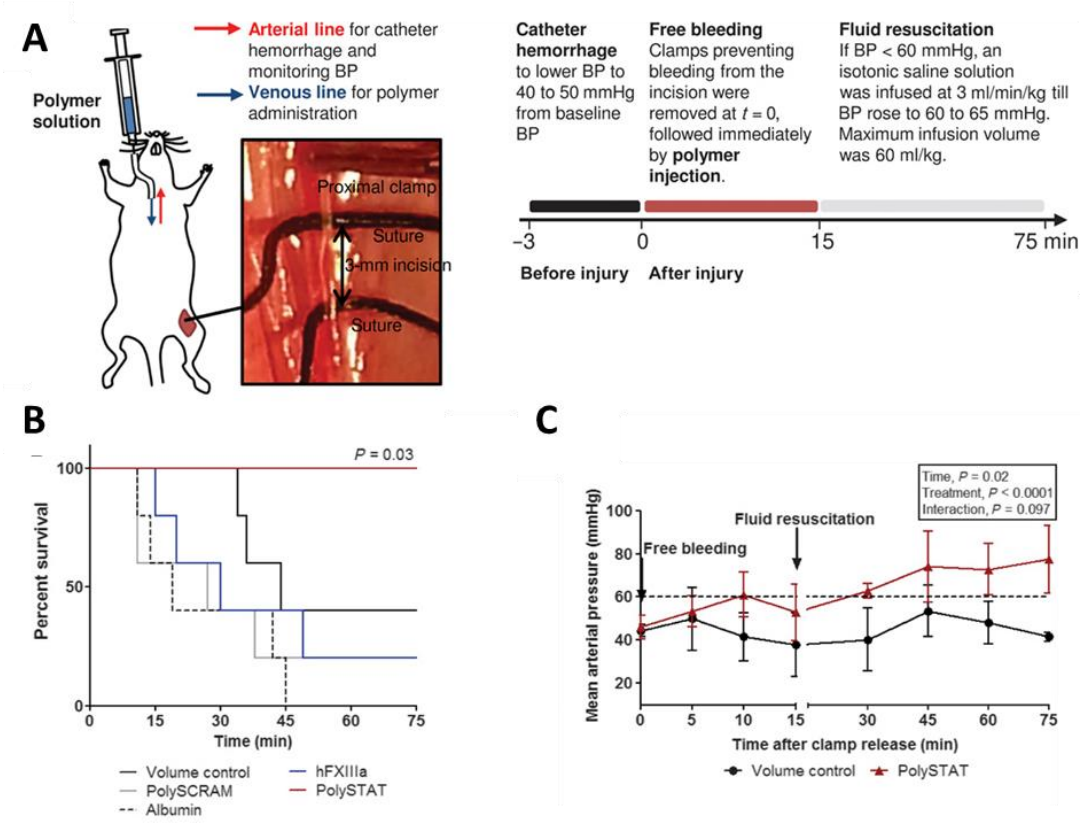

Fig 2.3 In vivo characterization of PolySTAT. A, schematic of femoral artery injury and fluid resuscitation model. B, survival of animals over the 75-minute time course of the study. PolySTAT rats survived 100% of the time, compared to 0-40% survival for control groups. C, mean arterial pressure (MAP) of PolySTAT and saline-treated animals. Rats treated with PolySTAT required less resuscitation fluid to reach a goal MAP of 60 mm Hg. Figure adapted from Chan *et al*[66]. Reprinted with permission from AAAS.

In biodistribution studies, >50% of PolySTAT administered was removed from the body within in hour. Through 20 min, the area with the largest % of injected dose (ID) was the plasma, which is favorable for a material that performs its function in the blood. Over long periods (1 d, 1 week) remaining ID is present in liver and kidney. Notably, when %ID is normalized to mass of organ, accumulatin in the liver is similar to that in the spleen, suggesting PolySTAT is cleared primarily through the kidneys (Fig 2.4).

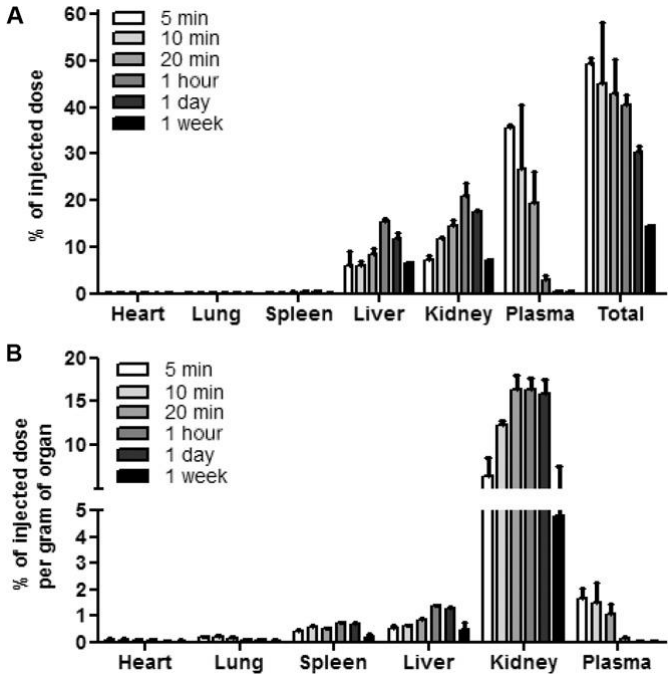

Fig 2.4 Biodistribution of PolySTAT. Figure adapted from Chan *et al*[66]. Reprinted with permission from AAAS.

2.3.4 *In Vitro Comparison of PolySTAT to rFVIIa and TXA*

In another report, Chan *et al* compared the effects of PolySTAT in a simulated trauma-induced coagulopathy (sTIC) model to that of clinically used treatments NovoSeven® and TXA[71]. PolySTAT was shown to decrease clot breakdown to a similar degree to the antifibrinolytic TXA, as well as improve clotting to a similar

degree as rFVIIa. Demonstrative rotational thromboelastometry (ROTEM) traces are provided in Figure 2.5.

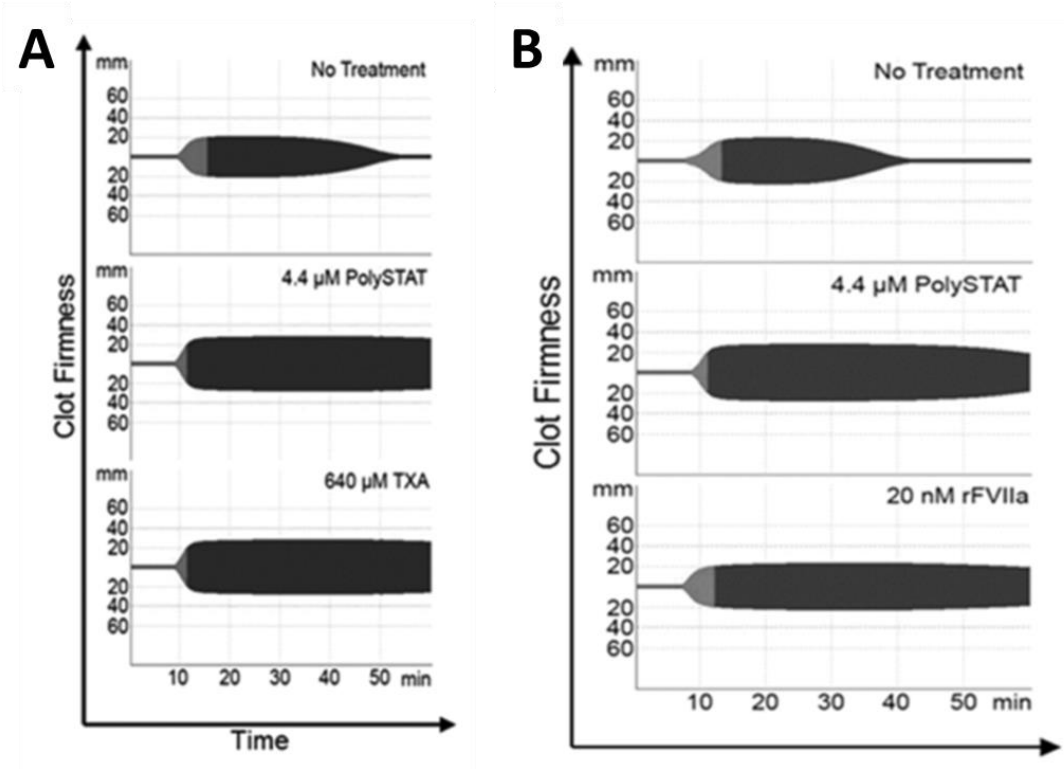

Fig 2.5 ROTEM traces comparing PolySTAT to TXA and rFVIIa. A, a sTIC plasma model was used to develop weakly forming clots. Both PolySTAT and TXA were shown to significantly reduce clot lysis over 60 min. B, both PolySTAT and rFVIIa increased and prolonged clot firmness. Figure adapted from Chan *et al*[66]. Copyright 2016 American Chemical Society.

2.3.5 *Summary*

PolySTAT, developed in a collaboration between the Pun and White labs at the University of Washington, is a promising biomaterial solution for promoting hemostasis. A multivalent display of fibrin-binding peptides on a polymer, PolySTAT utilizes strategies of drug delivery and polymer cross-linking for hemostasis, similar to those used in the pioneering materials in the field of injectable hemostats, to enhance hemostasis by forming clots stronger, more quickly, and with

less breakdown. By improving hemostasis, especially shortly after injury, the outcomes of traumatic injury patients can be greatly improved and the numbers of deaths can be decreased.

2.4 REFERENCES

1. WISQARS: Leading Causes of Death Reports. *Centers for Disease Control and Prevention* (2015).
2. WISQARS: Years of Potential Life Lost. *Centers for Disease Control and Prevention* (2015).
3. Murray, C. J. L., Lopez, A. D., Mathers, C. D. & Stein, C. *The Global Burden of Disease 2000 project: aims, methods and data sources*. (2001).
4. World Health Organization: The top 10 causes of death. (2017). Available at: http://www.who.int/mediacentre/factsheets/fs310/en/.
5. Sauaia, A. *et al.* Epidemiology of Trauma Deaths: A Reassessment. *J. Trauma* **38,** 185–193 (1995).
6. Lerner, E. B. & Moscati, R. M. The Golden Hour : Scientific Fact or Medical 'Urban Legend'. *Am. Emerg. Med.* **8,** 758–760 (2001).
7. Kauvar, D. S., Lefering, R. & Wade, C. E. Impact of Hemorrhage on Trauma Outcome : An Overview of Epidemiology, Clinical Presentations, and Therapeutic Considerations. *J. Trauma* **60,** 3–11 (2006).
8. Champion, H. R. *et al.* A Profile of Combat Injury. *J. Trauma* **54,** 513–519 (2003).
9. Holcomb, J. B. *et al.* Causes of Death in U . S . Special Operations Forces in the Global War on Terrorism. **245,** 986–991 (2007).
10. Chan, L. W., White, N. J. & Pun, S. H. Synthetic Strategies for Engineering Intravenous Hemostats. *Bioconjug. Chem.* **26,** 1224–1236 (2015).
11. Chen, H., Locke, D., Liu, Y., Liu, C. & Kahn, M. L. The Platelet Receptor GPVI Mediates Both Adhesion and Signaling Responses to Collagen in a Receptor Density-dependent Fashion*. **277,** 3011–3019 (2002).
12. Daniel, J. L. *et al.* Molecular Basis for ADP-induced Platelet Activation. **273,** 2024–2029 (1998).
13. Klinik, M. *et al.* Molecular Mechanisms of Platelet Activation. *Pharm. Rev.* **69,** 58–141

(1989).

14. Shattil, S. J., Hoxie, J. A., Cunningham, M. & Brass, L. F. Changes in the Platelet Membrane Glycoprotein IIb * IIIa Complex during Platelet Activation *. **260,** (1985).
15. Takeoka, S. *et al.* Function of fibrinogen. **312,** 773–779 (2003).
16. Tomiyama, Y., Tsubakio, T. & Kurata, Y. The Arg-Gly-Asp (RGD) recognition site of platelet glycoprotein IIb- IIIa on nonactivated platelets is accessible to high-affinity macromolecules. *Blood* **79,** 2303–2312 (2011).
17. Davie, E. W., Fujikawa, K. & Kisiel, W. The Coagulation Cascade: Initiation, Maintenance, and Regulation. *Biochemistry* **30,** 10363–10370 (1991).
18. Morrison, D. C. & Cochrane, C. G. Direct Evidence For Hageman Factor (Factor XII) Activation by Bacterial Lipopolysaccharides. *J. Exp. Med.* **140,** 797–811 (1974).
19. Bouma, B. N. & Griffin, J. H. Human blood coagulation factor XI . Purification , properties , and mechanism of activation by activated factor XII. *J. Biol. Chem.* **252,** 6432–6437 (1977).
20. Hoffman, M., Monroe, D. M. & Roberts, H. R. Activated factor VII activates factors IX and X on the surface of activated platelets : thoughts on the mechanism of action of ... *Blood Coagul. Fibrinolysis* **9,** S61–S65 (1998).
21. Mann, K. G., Brummel, K. & Butenas, S. What is all that thrombin for? *J Thromb Haemost* **1,** 1504–1514 (2003).
22. White, N. J. Mechanisms of trauma-induced coagulopathy. *Haematology* 660–663 (2013).
23. Kushimoto, S., Kudo, D. & Kawazoe, Y. Acute traumatic coagulopathy and trauma-induced coagulopathy : an overview. *J. Intensive Care* 1–7 (2017). doi:10.1186/s40560-016-0196-6
24. Brohi, K., Singh, J., Heron, M. & Coats, T. Acute traumatic coagulopathy. *J. Trauma* **54,** 1127–1130 (2003).
25. Kaafarani, H. M. a & Velmahos, G. C. Damage control resuscitation in trauma. *Scand. J. Surg.* **103,** 81–88 (2014).
26. Mikhail, J. The trauma triad of death: hypothermia, acidosis, and coagulopathy. *AACN clinical issues* **10,** 85–94 (1999).
27. Niles, S. E. *et al.* Increased Mortality Associated With the Early Coagulopathy of Trauma in Combat Casualties. *J. Trauma Inj. Infect. Crit. Care* **64,** 1459–1465 (2008).

28. Standbury, L. G. & Hess, J. R. Blood Transfusion in World War I : The Roles of Lawrence Bruce. *Transfus. Med. Rev.* **23,** 232–236 (2009).
29. Boyle, R., Willis, T. & Wren, C. The History of Blood Transfusion. *Br. J. Haemotology* **110,** 758–767 (2000).
30. Duchesne, J. C., Hunt, J. P., Wahl, G. & Marr, A. B. Review of Current Blood Transfusions Strategies in a Mature Level I Trauma Center : Were We Wrong for the Last 60. *J. Trauma* **65,** 272–278 (2008).
31. Repine, T. B., Perkins, J. G., Kauvar, D. S. & Blackborne, L. The Use of Fresh Whole Blood in Massive Transfusion. **60,** (2005).
32. Sihler, K. C. & Napolitano, L. M. Complications of Massive Transfusion. *Chest* **137,** 209–220 (2010).
33. Riou, B. *et al.* Recombinant factor VIIa (Novoseven) as adjunctive therapy for bleeding contorl in trauma - a randomized. placebo-controlled trial. in *Shock* 228 (2004).
34. Rizoli, S. B. *et al.* Recombinant activated factor VII as an adjunctive therapy for bleeding control in severe trauma patients with coagulopathy : subgroup analysis from two randomized trials. *Crit. Care* **10,** 1–11 (2006).
35. Raza, I. *et al.* The incidence and magnitude of fibrinolytic activation in trauma patients. *J. Thromb. Haemost.* **11,** 307–314 (2013).
36. Williams-johnson, J. A., Mcdonald, A. H., Strachan, G. G. & Williams, E. W. Effects of Tranexamic Acid on Death, Vascular Occlusive Events, and Blood Transfusion in Trauma Patients with Significant Haemorrhage (CRASH-2) A Randomised, Placebo-Controlled Trial. *West Indian Med J* **59,** 612–624 (2010).
37. Houston, F. S. Military Application of Tranexamic Acid in Trauma Emergency Resuscitation (MATTERs) Study. **147,** 113–119 (2012).
38. Search Results: tranexamic acid. *ClinicalTrials.gov* (2018).
39. Coller, B. S. Interaction of normal, thrombathemis, and Bernard-Soulier platelets with immobilized fibrinogen: defective platelet-fibrinogen interaction in thrombastatin. *Blood* **55,** 169–179 (1980).
40. Coller, B. S. *et al.* Thromboerythrocytes In Vitro Studies of a Potential Autologous , Semi-artificial Alternative to Platelet Transfusions. *J Clin Invest* **98,** 546–555 (1992).
41. Ten, O. Fibrinogen-coated albumin microcapsules reduce bleeding in severely

thrombocytopenic rabbits. **9,** 107–111 (1999).

42. Illum, L. *et al.* Blood clearance and organ deposition of intravenously administered colloidal particles . The effects of particle size , nature and shape. **12,** 135–146 (1982).
43. Okamura, Y. *et al.* Hemostatic effects of phospholipid vesicles carrying fibrinogen gamma chain dodecapeptide in vitro and in vivo. *Bioconjug. Chem.* **16,** 1589–96 (2005).
44. Okamura, Y. *et al.* Development of fibrinogen gamma-chain peptide-coated, adenosine diphosphate-encapsulated liposomes as a synthetic platelet substitute. *J. Thromb. Haemost.* **7,** 470–7 (2009).
45. Bertram, J. P. *et al.* Intravenous Hemostat : Nanotechnology to Halt Bleeding. *Sci. Transl. Med.* **1,** 11–22 (2009).
46. Shoffstall, A. J. *et al.* Tuning ligand density on intravenous hemostatic nanoparticles dramatically increases survival following blunt trauma. *Biomacromolecules* **14,** 2790–2797 (2013).
47. Lashof-sullivan, M. *et al.* Hemostatic Nanoparticles Improve Survival Following Blunt Trauma Even after 1 Week Incubation at 50 °C. *ACS Biomater. Sci. Eng.* **2,** 385–392 (2016).
48. Shoffstall, A. J. *et al.* Intravenous hemostatic nanoparticles increase survival following blunt trauma injury. *Biomacromolecules* **13,** 3850–3857 (2012).
49. Hubbard, W. B., Lashof-Sullivan, M. M., Lavik, E. B. & Vandevord, P. J. Steroid-loaded hemostatic nanoparticles combat lung injury after blast trauma. *ACS Macro Lett.* **4,** 387–391 (2015).
50. Onwukwe, C. *et al.* Engineering Intravenously Administered Nanoparticles to Reduce Infusion Reaction and Stop Bleeding in a Large Animal Model of Trauma. (2018). doi:10.1021/acs.bioconjchem.8b00335
51. Gupta, A. Sen, Huang, G., Lestini, B. J., Sagnella, S. & Kottke-marchant, K. RGD-modified liposomes targeted to activated platelets as a potential vascular drug delivery system RGD-modified liposomes targeted to activated platelets as a potential vascular drug delivery system. *Thromb Haemost* **93,** 106–114 (2005).
52. Ravikumar, M., Modery, C. L., Wong, T. L. & Gupta, A. Sen. Peptide-Decorated Liposomes Promote Arrest and Aggregation of Activated Platelets under Flow on Vascular Injury Relevant Protein Surfaces in Vitro. *Biomacromolecules* **13,** 1495–1502

(2012).

53. Ravikumar, M. *et al.* Mimicking Adhesive Functionalities of Blood Platelets using Ligand- Decorated Liposomes. *Bioconjug. Chem.* **23,** 1266–1275 (2012).
54. Modery-Pawlowski, C. L., Tian, L. L., Ravikumar, M., Wong, T. L. & Gupta, A. Sen. In vitro and in vivo hemostatic capabilities of a functionally integrated platelet-mimetic liposomal nanoconstruct. *Biomaterials* **34,** 3031–3041 (2013).
55. Hickman, D. A. *et al.* Intravenous synthetic platelet (SynthoPlate) nanoconstructs reduce bleeding and improve ‘ golden hour ’ survival in a porcine model of traumatic arterial hemorrhage. *Sci. Rep.* 1–14 (2018). doi:10.1038/s41598-018-21384-z
56. Shukla, M., Sekhon, U. D. S., Li, W. & Hickman, D. A. In vitro characterization of SynthoPlate (synthetic platelet) technology and its in vivo evaluation in severely thrombocytopenic mice. *J Thromb Haemost* **15,** 375–387 (2016).
57. Lashof-sullivan, M., Sho, A. & Lavik, E. Intravenous hemostats : challenges in translation to patients. *Nanoscale* **5,** 10719–10728 (2013).
58. Szebeni, J. *et al.* Prevention of infusion reactions to PEGylated liposomal doxorubicin via tachyphylaxis induction by placebo vesicles: A porcine model. *J. Control. Release* **160,** 382–387 (2012).
59. Brown, A. C. *et al.* Ultrasoft microgels displaying emergent platelet-like behaviours. *Nat. Mater.* **13,** 1–7 (2014).
60. Niewlarowski, S., Regoeczi, E., Stewart, G. J., Senyi, A. F. & Mustard, J. F. Platelet Interaction with Polymerizing Fibrin. **51,** 685–700 (1972).
61. Welsch, N., Brown, A. C., Barker, T. H. & Lyon, L. A. Colloids and Surfaces B : Biointerfaces Enhancing clot properties through fibrin-specific self-cross-linked PEG side-chain microgels. *Colloids Surfaces B Biointerfaces* **166,** 89–97 (2018).
62. Lorand, L. A double-headed Gly-Pro-Arg-Pro ligand mimics the functions of the E domain of fibrin for promoting the end-to-end crosslinking of □ chains by factor XIII a. **95,** 537–541 (1998).
63. Soon, A. S. C., Lee, C. S. & Barker, T. H. Modulation of fibrin matrix properties via knob:hole affinity interactions using peptide-PEG conjugates. *Biomaterials* **32,** 4406–4414 (2011).
64. Kolodziej, A. F. *et al.* Fibrin Specific Peptides Derived by Phage Display:

Characterization of Peptides and Conjugates for Imaging. *Bioconjug. Chem.* **23,** 548–556 (2012).

65. Kolodziej, A. F., Zhang, Z., Overoye-chan, K., Jacques, V. & Caravan, P. Peptide Optimization and Conjugation Strategies Magnetic Resonance Imaging Contrast Agents. **1088,** 185–211
66. Chan, L. W. *et al.* A synthetic fibrin cross-linking polymer for modulating clot properties and inducing hemostasis. *Sci. Transl. Med.* **7,** (2015).
67. Chiefari, J. *et al.* Living Free-Radical Polymerization by Reversible Addition - Fragmentation Chain Transfer : The RAFT Process We wish to report a new living free-radical polymer- ization of exceptional effectiveness and versatility . 1 The living character is conferred by . **9297,** 5559–5562 (1998).
68. Chu, D. S. H. *et al.* Application of living free radical polymerization for nucleic acid delivery. *Acc. Chem. Res.* **45,** 1089–1099 (2012).
69. Kopeček, J., Kopečková, P., Minko, T., Lu, Z. R. & Peterson, C. M. Water soluble polymers in tumor targeted delivery. *J. Control. Release* **74,** 147–158 (2001).
70. Barrett, G. D., Constable, I. J. & Stewart, A. D. Clinical results of hydrogel lens implantation. *J. Cataract Refract. Surg.* **12,** 623–631 (1986).
71. Chan, L. W., White, N. J. & Pun, S. H. A Fibrin Cross-linking Polymer Enhances Clot Formation Similar to Factor Concentrates and Tranexamic Acid in an in Vitro Model of Coagulopathy. *ACS Biomater. Sci. Eng.* (2016). doi:10.1021/acsbiomaterials.5b00536
72. Maegele, M. *et al.* Early coagulopathy in multiple injury: An analysis from the German Trauma Registry on 8724 patients. *Injury* **38,** 298–304 (2007).
73. 6 Factor VIII Concentrates, Factor VIII/von Willebrand Factor Concentrates, Factor IX Concentrates, Activated Prothrombin Complex Concentrates. *Transfus. Med. Hemotherapy* **36,** 409–418 (2009).
74. Okamura, Y. *et al.* Development of fibrinogen c-chain peptide-coated, adenosine diphosphate-encapsulated liposomes as a synthetic platelet substitute. *J Thromb Haemost* **7,** 470–477 (2009).
75. Fasting, C. *et al.* Multivalency as a Chemical Organization and Action Principle. *Angew. Rev.* **51,** 10472–10498 (2012).
76. Spain, S. G. & Cameron, N. R. A spoonful of sugar : the application of glycopolymers in

therapeutics. *Polym. Chem.* **2,** 60–68 (2011).

77. Weigandt, K. M., Pozzo, D. C. & Porcar, L. Structure of high density fibrin networks probed with neutron scattering and rheology. *Soft Matter* **5,** 4321–4330 (2009).
78. Weigandt, K. M., Porcar, L. & Pozzo, D. C. In situ neutron scattering study of structural transitions in fibrin networks under shear deformation. *Soft Matter* **7,** 9992–10000 (2011).
79. Yanjarappa, M. J., Gujraty, K. V, Joshi, A., Saraph, A. & Kane, R. S. Synthesis of Copolymers Containing an Active Ester of Methacrylic Acid by RAFT : Controlled Molecular Weight Scaffolds for Biofunctionalization. *Biomacromolecules* **7,** 1665–1670 (2006).
80. Kirby, N. M. *et al.* research papers A low-background-intensity focusing small-angle X-ray scattering undulator beamline. 1670–1680 (2013). doi:10.1107/S002188981302774X
81. Hammouda, B., Ho, D. L. & Kline, S. Insight into Clustering in Poly (ethylene oxide) Solutions. *Macromolecules* **37,** 6932–6937 (2004).
82. Glinka, C. J. *et al.* The 30 m Small-Angle Neutron Scattering Instruments at the National Institute of Standards and Technology. *J. Appl. Crystallogr.* **31,** 430–445 (1998).
83. Kline, S. R. Reduction and analysis of SANS and USANS data using IGOR Pro. *J. Appl. Crystallogr.* **39,** 895–900 (2006).
84. Barker, J. G. *et al.* Design and performance of a thermal-neutron double-crystal diffractometer for USANS at NIST. *J. Appl. Crystallogr.* **38,** 1004–1011 (2005).
85. Terech, P. Structural Study of Cholesteryl Anthraquinone-2-carboxylate (CAQ) Physical Organogels by Neutron and X-ray Small Angle Scattering. *J. Phys. Chem.* **100,** 3759–3766 (1996).
86. Teixeira, J. Small-Angle Scattering by Fractal Systems. *J. Appl. Crystallogr.* **21,** 781–785 (1988).
87. Hammouda, B. & Horkay, F. Clustering and Solvation in Poly(acrylic acid) Polyelectrolyte Solutions. *Macromolecules* **38,** 2019–2021 (2005).
88. Dowling, M. B. *et al.* Biomaterials A self-assembling hydrophobically modi fi ed chitosan capable of reversible hemostatic action. *Biomaterials* **32,** 3351–3357 (2011).
89. Laudano, A. P. & Doolittle, R. F. Studies on synthetic peptides that bind to fibrinogen and prevent fibrin polymerization. Structural requirements, number of binding sites, and species differences. *Biochemistry* **19,** 1013–1019 (1980).

90. Lukyanov, A. N. & Torchilin, V. P. Micelles from lipid derivatives of water-soluble polymers as delivery systems for poorly soluble drugs. **56,** 1273–1289 (2004).
91. Rizvi, S. A. A. & Saleh, A. M. Applications of nanoparticle systems in drug delivery technology. *Saudi Pharm. J.* **26,** 64–70 (2018).
92. Kieler-ferguson, H. M. & Fr, J. M. J. Clinical developments of chemotherapeutic nanomedicines : polymers and liposomes for delivery of camptothecins and platinum (II). **5,** (2013).
93. Press, D. Effective use of nanocarriers as drug delivery systems for the treatment of selected tumors. 7291–7309 (2017).
94. Langer, R. Drug delivery and targeting. **392,** 5–10 (1998).
95. Montet, X., Funovics, M., Montet-abou, K., Weissleder, R. & Josephson, L. Multivalent Effects of RGD Peptides Obtained by Nanoparticle Display. 6087–6093 (2006). doi:10.1021/jm060515m
96. Lee, H., Fonge, H., Hoang, B., Reilly, R. M. & Allen, C. articles The Effects of Particle Size and Molecular Targeting on the Intratumoral and Subcellular Distribution of Polymeric Nanoparticles. **7,** 1195–1208 (2010).
97. Lamm, R. J. *et al.* Peptide valency plays an important role in the activity of a synthetic fibrin-crosslinking polymer. *Biomaterials* **132,** 96–104 (2017).
98. Devlin, J., Panganiban, L. & Devlin, P. Random peptide libraries: a sourse of specific protein binding molecules. *Science (80-.).* **249,** 404–406 (1990).
99. Fan, S. *et al.* Curcumin-loaded PLGA-PEG nanoparticles conjugated with B6 peptide for potential use in Alzheimer ' s disease. *Drug Deliv.* **25,** 1044–1055 (2018).
100. Duvall, C. L., Convertine, A. J., Benoit, D. S. W., Hoffman, A. S. & Stayton, P. S. articles Intracellular Delivery of a Proapoptotic Peptide via Conjugation to a RAFT Synthesized Endosomolytic Polymer. (2010).
101. Chu, D. S. *et al.* As featured in : Biomaterials Science. (2015). doi:10.1039/c4bm00259h
102. Johnson, R. N. *et al.* Synthesis of Statistical Copolymers Containing Multiple Functional Peptides for Nucleic Acid Delivery. *Biomacromolecules* **11,** 3007–13 (2010).
103. Chu, D. S. H., Schellinger, J. G., Bocek, M. J., Johnson, R. N. & Pun, S. H. Optimization of Tet1 ligand density in HPMA-co-oligolysine copolymers for targeted neuronal gene delivery. *Biomaterials* **34,** 9632–9637 (2013).

104. Schellinger, J. G. *et al.* Melittin-grafted HPMA-oligolysine based copolymers for gene delivery. *Biomaterials* **34,** 2318–2326 (2013).
105. Kanaide, H. & Shainoff, J. R. Cross-linking of fibrinogen and fibrin by fibrin-stabilizing factor (factor XIIIa). *Transl. Res.* **85,** 574–597 (1975).
106. O'Brien-Simpson, N. M., Ede, N. J., Brown, L. E., Swan, J. & Jackson, D. C. Polymerization of unprotected synthetic peptides: A view toward synthetic peptide vaccines. *J. Am. Chem. Soc.* **119,** 1183–1188 (1997).
107. Hasson, C. J., Caldwell, G. E. & Emmerik, R. E. A. Van. NIH Public Access. *Motor Control* **27,** 590–609 (2009).
108. Studenovská, H., Šlouf, M. & Rypáček, F. Poly(HEMA) hydrogels with controlled pore architecture for tissue regeneration applications. *J. Mater. Sci. Mater. Med.* **19,** 615–621 (2008).
109. Kopeckova, P. Water soluble polymers in tumor targeted delivery. *J. Control. Release* **74,** 147–158 (2001).
110. Cunningham, V. J. *et al.* Poly(glycerol monomethacrylate) − Poly(benzyl methacrylate) Diblock Copolymer Nanoparticles via RAFT Emulsion Polymerization: Synthesis, Characterization, and Interfacial Activity. (2014). doi:10.1021/ma501140h
111. Save, M., Weaver, J. V. M., Armes, S. P. & Mckenna, P. Atom Transfer Radical Polymerization of Hydroxy-Functional Methacrylates at Ambient Temperature: Comparison of Glycerol Monomethacrylate with 2-Hydroxypropyl Methacrylate. 1152–1159 (2002). doi:10.1021/ma011541r
112. Das, D. *et al.* RAFT polymerization of ciprofloxacin prodrug monomers for the controlled intracellular delivery of antibiotics. *Polym. Chem* **7,** 826–837 (2016).
113. Shin, H. C., Alani, A. W. G., Rao, D. A., Rockich, N. C. & Kwon, G. S. Multi-drug loaded polymeric micelles for simultaneous delivery of poorly soluble anticancer drugs. *J. Control. Release* **140,** 294–300 (2009).
114. Hughes, H. C. Swine in cardiovascular research. *Lab Anim. Sci.* **36,** 348–350 (1986).
115. Swindle, M. M., Makin, A., Herron, A. J., Clubb, F. J. & Frazier, K. S. Swine as Models in Biomedical Research and Toxicology Testing. *Vet. Pathol.* **49,** 344–356 (2012).
116. Pusateri, A. E. *et al.* Effect of a Chitosan-Based Hemostatic Dressing on Blood Loss and Survival in a Model of Severe Venous Hemorrhage and Hepatic Injury in Swine. *J trauma*

54, 177–182 (2003).

117. Pusateri, A. E. *et al.* Advanced Hemostatic Dressing Development Program : Animal Model Selection Criteria and Results of a Study of Nine Hemostatic Dressings in a Model of Severe Large Venous Hemorrhage and Hepatic Injury in Swine. *J Trauma* **55,** 518–526 (2003).
118. Stern, S. *et al.* RESUSCITATION WITH THE HEMOGLOBIN-BASED OXYGEN CARRIER , HBOC-201 , IN A SWINE MODEL OF SEVERE UNCONTROLLED HEMORRHAGE AND TRAUMATIC BRAIN INJURY. *Shock* **31,** 64–79 (2009).
119. White, N. J., Wang, X., Liles, W. C. & Stern, S. Fibrinogen Concentrate Improves Survival During Limited Resuscitation of Uncontrolled Hemorrhagic Shock in a Swine Model. *Shock* **42,** 456–463 (2014).
120. Szebeni, J., Bed, P. & Rozsnyay, Z. Liposome-induced complement activation and related cardiopulmonary distress in pigs : factors promoting reactogenicity of Doxil and AmBisome. **8,** 176–184 (2012).
121. Szebeni, J. *et al.* A porcine model of complement-mediated infusion reactions to drug carrier nanosystems and other medicines ☆. **64,** 1706–1716 (2012).
122. Bertram, J. P. *et al.* Intravenous Hemostat : Nanotechnology to Halt Bleeding. (2009).
123. Boldt, J., Haisch, G., Suttner, S., Kumle, B. & Schellhaass, A. Effects of a new modifed, balanced hydroxyethyl starch preparation (Hextend). *Br. J. Anaesth.* **89,** 722–728 (2002).
124. Landskroner, K., Olson, N. & Jesmok, G. Cross-species pharmacologic evaluation of plasmin as a direct-acting thrombolytic agent: Ex vivo evaluation for large animal model development. *J. Vasc. Interv. Radiol.* **16,** 369–377 (2005).
125. Mitterlechner, T. *et al.* Prothrombin complex concentrate and recombinant prothrombin alone or in combination with recombinant factor X and FVIIa in dilutional coagulopathy: A porcine model. *J. Thromb. Haemost.* **9,** 729–737 (2011).
126. R. Baylis, J. *et al.* Rapid hemostasis in a sheep model using particles that propel thrombin and tranexamic acid. *Laryngoscope* **127,** 787–793 (2017).
127. Ngambenjawong, C., Gustafson, H. H., Sylvestre, M. & Pun, S. H. A Facile Cyclization Method Improves Peptide Serum Stability and Confers Intrinsic Fluorescence. *ChemBioChem* **18,** 2395–2398 (2017).
128. Von Maltzahn, G. *et al.* Nanoparticles that communicate in vivo to amplify tumour

targeting. *Nat. Mater.* **10,** 545–552 (2011).

129. Liu, G. W. *et al.* Glomerular disease augments kidney accumulation of synthetic anionic polymers. *Biomaterials* **178,** 317–325 (2018).
130. Tabata, Y. & Ikada, Y. Effect of the size and surface charge of polymer microspheres on their phagocytosis by macrophage. *Biomaterials* **9,** 356–362 (1988).
131. Caliceti, P. & Veronese, F. P harmacokinetic and biodistribution properties of poly(ethylene glycol)–protein conjugates Paolo. *Adv. Drug Deliv. Rev.* **55,** 1261–1277 (2003).
132. Beier, J. I. *et al.* Fibrin accumulation plays a critical role in the sensitization to lipopolyccharide-induced liver injury caused by ethanol in mice. *Hepatology* **49,** 1545–1553 (2009).
133. Imokawa, S. *et al.* Tissue factor expression and fibrin deposition in the lungs of patients with idiopathic pulmonary fibrosis and systemic sclerosis. *Am. J. Respir. Crit. Care Med.* **156,** 631–636 (1997).
134. Brown, L. F., Dvorak, A. M. & Dvorak, H. F. Leaky vessels, fibrin deposition, and fibrosis: a sequence of events common to solid tumors and to many other types of disease. *Am. Rev. Respir. Dis.* **140,** 1104–7 (1989).
135. Hiramoto, R., Bernecky, J., Jurandowski, J. & Pressman, D. Fibrin in Human Tumors. *Cancer Res.* **20,** 592–593 (1960).
136. Fernandez, P. M., Patierno, S. R. & Rickles, F. R. Tissue factor and fibrin in tumor angiogenesis. *Semin. Thromb. Hemost.* **30,** 31–44 (2004).
137. Wallace, A. C. Demonstration of Fibrin in Early Stages of Experimental Metastases. *Cancer Res.* **36,** 1904–1909 (1976).
138. Dirix, L. Y. *et al.* Plasma fibrin D-dimer levels correlate with tumour volume, progression rate and survival in patients with metastatic breast cancer. *Br. J. Cancer* **86,** 389–395 (2002).
139. Chu, D. S. *et al.* MMP9-sensitive polymers mediate environmentally-responsive bivalirudin release and thrombin inhibition. *Biomater. Sci.* **3,** 41–45 (2015).
140. Warkentin, T. E., Greinacher, A. & Koster, A. Bivalirudin. *Thromb. Haemost.* **99,** 830–839 (2008).
141. Hejna, M., Raderer, M. & Zielinski, C. C. Inhibition of metastases by anticoagulants. *J.*

Natl. Cancer Inst. **91,** 22–36 (1999).

142. Amirkhosravi, A. *et al.* Tissue factor pathway inhibitor reduces experimental lung metastasis of B16 melanoma. *Thromb. Haemost.* **87,** 930–936 (2002).
143. Kondapaka, S. B., Fridman, R. & Reddy, K. B. Epidermal growth factor and amphiregulin up-regulate matrix metalloproteinase-9 (MMP-9) in human breast cancer cells. *Int. J. Cancer* **70,** 722–726 (1997).
144. Svendsen, L., Blombäck, B., Blombäck, M. & Olsson, P. I. Synthetic chromogenic substrates for determination of trypsin, thrombin and thrombin-like enzymes. *Thromb. Res.* **1,** 267–278 (1972).
145. Reinhard, J., Brösicke, N., Theocharidis, U. & Faissner, A. The extracellular matrix niche microenvironment of neural and cancer stem cells in the brain. *Int. J. Biochem. Cell Biol.* **81,** 174–183 (2016).
146. Palumbo, J. S. *et al.* Platelets and fibrin(ogen) increase metastatic potential by impeding natural killer cell-mediated elimination of tumor cells. *Blood* **105,** 178–185 (2005).
147. Ogston, A. OGSTON, M.D., Surgeon. *J. Anat.* **16,** 526–567 (1882).
148. Lowry, F. D. Staphylococcus aureus Infections. *N. Engl. J. Med.* **339,** 520–532 (1998).
149. Lake, J. G. *et al.* Pathogen distribution and antimicrobial resistance among pediatric healthcare-associated infections reported to the National Healthcare Safety Network, 2011-2014. *Infect. Control Hosp. Epidemiol.* **39,** 1–11 (2018).
150. Weiner, L. M. *et al.* Antimicrobial-Resistant Pathogens Associated with Healthcare-Associated Infections: Summary of Data Reported to the National Healthcare Safety Network at the Centers for Disease Control and Prevention, 2011-2014. *Infect. Control Hosp. Epidemiol.* **37,** 1288–1301 (2016).
151. Lee, A. S. *et al.* Methicillin-resistant Staphylococcus aureus. *Nat. Rev. Dis. Prim.* **4,** (2018).
152. Jevons, P. M. 'Celbenin'-resistant Staphylococci. *Br. Med. J.* **1,** 124–125 (1961).
153. Hiramatsu, K. *et al.* Methicillin-resistant Staphylococcus aureus clinical strani with reduced vancomycin susceptibility. *J. Antimicrob. Chemother.* **40,** 135–146 (1997).
154. Huh, A. J. & Kwon, Y. J. 'Nanoantibiotics': A new paradigm for treating infectious diseases using nanomaterials in the antibiotics resistant era. *J. Control. Release* **156,** 128–145 (2011).

155. Loughman, A. *et al.* Roles for fibrinogen, immunoglobulin and complement in platelet activation promoted by Staphylococcus aureus clumping factor A. *Mol. Microbiol.* **57,** 804–818 (2005).
156. Mcdevitt, D. *et al.* Characterization of the interaction between the Staphylococcus aureus clumping factor (ClfA) and fibrinogen. *Eur. J. Biochem.* **247,** 416–424 (1997).
157. Que, Y. *et al.* Reassessing the Role of Staphylococcus aureus Clumping Factor and Fibronectin-Binding Protein by Expression in Lactococcus. *Infect. Immun.* **69,** 6296–6302 (2001).
158. Patti, J. M. A humanized monoclonal antibody targeting Staphylococcus aureus. *Vaccine* **22,** (2004).
159. Takeoka, S. *et al.* Function of fibrinogen gamma-chain dodecapeptide-conjugated latex beads under flow. *Biochem. Biophys. Res. Commun.* **312,** 773–9 (2003).
160. Okamura, Y. *et al.* Hemostatic effects of fibrinogen gamma-chain dodecapeptide-conjugated polymerized albumin particles in vitro and in vivo. *Transfusion* **45,** 1221–8 (2005).
161. Okamura, Y., Maekawa, I., Teramura, Y., Maruyama, H. & Handa, M. Hemostatic Effects of Phospholipid Vesicles Carrying Fibrinogen γ Chain Dodecapeptide in Vitro and in Vivo. 30–33 (2005).
162. Pease, D. C. An Electron Microscopy Study of Red Bone Marrow. *Blood* **11,** 501–526 (1956).
163. Wagner, B. C. L. *et al.* Analysis of GPIIb/IIIa Receptor Number by Quantification of 7E3 Binding to Human Platelets. (2015).
164. Nilsson, I. M., Patti, J. M., Bremell, T., Höök, M. & Tarkowski, A. Vaccination with a recombinant fragment of collagen adhesin provides protection against Staphylococcus aureus-mediated septic death. *J. Clin. Invest.* **101,** 2640–2649 (1998).
165. Stevens, K. A., Sheldon, B. W., Klapes, N. A. & Klaenhammer, T. R. Nisin treatment for inactivation of Salmonella species and other gram- negative bacteria. *Appl. Environ. Microbiol.* **57,** 3613–3615 (1991).
166. Millette, M., Le Tien, C., Smoragiewicz, W. & Lacroix, M. Inhibition of Staphylococcus aureus on beef by nisin-containing modified alginate films and beads. *Food Control* **18,** 878–884 (2007).

167. Hancock, R. E. W. Peptide antibiotics. *Lancet* **349,** 418–422 (1997).
168. Biscola, V. *et al.* Isolation and characterization of a nisin-like bacteriocin produced by a Lactococcus lactis strain isolated from charqui, a Brazilian fermented, salted and dried meat product. *Meat Sci.* **93,** 607–613 (2013).
169. Miao, J. *et al.* Membrane disruption and DNA binding of Staphylococcus aureus cell induced by a novel antimicrobial peptide produced by Lactobacillus paracasei subsp. tolerans FX-6. *Food Control* **59,** 609–613 (2016).

PART 2: OPTIMIZING THE SYNTHESIS OF POLYSTAT

The synthesis method for PolySTAT currently uses a conjugation step that reproducibly grafts FBP at an efficiency of ~25%. While solid-phase peptide synthesis has made peptides an affordable option for nanotechnology, the cost of polymer materials is far less. Peptides make up 90% of the total cost of PolySTAT. Thus, we aim to study the function of peptide valency in the material and improve the synthetic efficiency towards the goal of translating PolySTAT to the clinic.

CHAPTER 3: PEPTIDE VALENCY PLAYS AN IMPORTANT ROLE IN THE ACTIVITY OF A SYNTHETIC FIBRIN-CROSSLINKING POLYMER

Robert J. Lamm, Esther B. Lim, Katie M. Weigandt,

Lilo D. Pozzo, Nathan J. White, Suzie H. Pun

Synopsis: Therapeutic polymers have the potential to improve the standard of care for hemorrhage, or uncontrolled bleeding, as synthetic hemostats. PolySTAT, a fibrin-crosslinking peptide-polymer conjugate, has the capacity to rescue fibrin clot formation and improve survival in a model of acute traumatic bleeding. PolySTAT consists of a synthetic polymer backbone to which targeting fibrin-binding peptides are linked. For translation of PolySTAT, the optimal valency of peptides must be determined. Grafting of fibrin-binding peptides to the poly(hydroxyethyl methacrylate)-based backbone was controlled to produce peptide valencies ranging from 0 to 10 peptides per polymer. PolySTATs with valencies of ≈4 or greater resulted in increased clot firmness, kinetics, and decreased breakdown as measured by thromboelastometry. A valency of ≈4 increased clot firmness 57% and decreased clot breakdown 69% compared to phosphate-buffered saline. This trend was characterized by neutron scattering, which probed the structure of clots formed in the presence of PolySTAT. Finally, PolySTAT with valencies of 4 (100% survival; $p = 0.013$) and 8 (80% survival; $p = 0.063$) improved survival compared to an albumin control in a femoral artery injury model (20% survival). This work demonstrates tunability of hemostatic polymers and the ability of in vitro assays to predict in vivo efficacy.

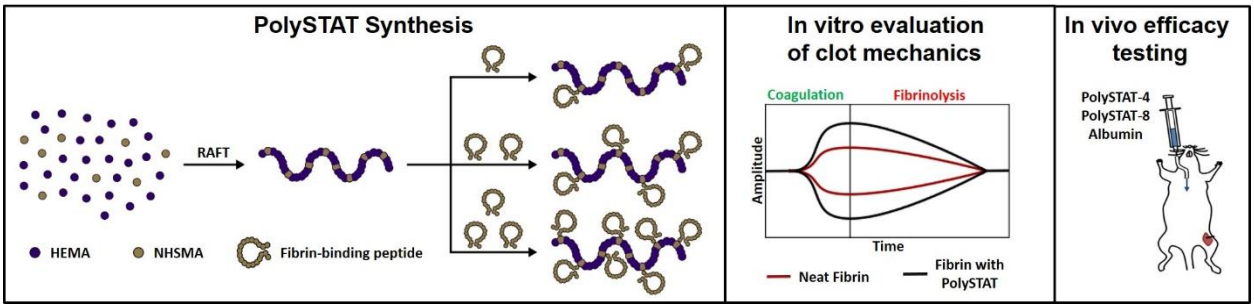

This work has resulted in a publication: Lamm *et al*. *Biomaterials.* (2017) **130:**96-104.

3.1 INTRODUCTION

Traumatic injury is the leading cause of death for Americans ages 1 to 44,[7] and hemorrhage, or uncontrolled bleeding, is responsible for 30% to 40% of these fatalities[5,7]. Bleeding is naturally managed through hemostasis, which occurs in two main steps. Primary hemostasis describes the process of quiescent circulating platelets undergoing a morphological and biochemical change upon activation in response to damaged endothelium. Activated platelets express the membrane receptor complex GPIIb/IIIa which binds fibrinogen, resulting in formation of the primary platelet plug. Secondary hemostasis describes the process by which the serine proteases of the clotting cascade undergo a number of activating cleavages. Downstream in the cascade, fibrinogen is cleaved by thrombin to form fibrin, which is able to self-assemble into a fibrous network. Thrombin also activates FXIIIa, which covalently crosslinks the fibrin network resulting in strengthening of the initial platelet plug. The formation of robust clots is critical for stopping blood loss and preventing hemorrhagic shock and death; however, the loss of blood also depletes critical blood proteins necessary for hemostasis[24]. An additional complication is the development of coagulopathy, or impaired clot formation, that occurs in up to 30% of trauma patients. Patients with trauma-induced coagulopathy (TIC) form clots that are weaker and have shorter half-lives due to enzymatic clot breakdown by the enzyme plasmin (hyperfibrinolysis),[35] resulting in 4 to 6 fold increase in mortality when TIC is present upon patient's arrival to the hospital[27,72].

To combat these effects, human-derived products (whole blood, fresh frozen plasma, and factor concentrates) as well as recombinant factors are used as systemic treatments. While effective, a number of limitations plague these therapies such as short shelf-lives, stringent storage conditions, microbial contamination risks, and the risk of immunogenicity in patients[73]. Synthetic hemostats are therefore in development as an alternative approach to improve clotting function while avoiding the limitations of current treatments.

Several synthetic, platelet-mimicking technologies have been reported to have efficacy in inducing hemostasis in rodent bleeding models. For example, the Lavik group has demonstrated that poly(lactic acid-co-glycolic acid) (PLGA) nanoparticles decorated with platelet-binding RGD moieties decrease bleeding times in animal models of various injuries including sharp, blunt, and blast traumas[45,48,49]. Liposome-based platelet-recruiting technologies have also shown success. Okamura et al. showed that adenosine diphosphate-loaded liposomes modified with a platelet-

binding H12 peptide can have procoagulatory effects, decreasing bleeding times in mice and rabbits,[74] and the Sen Gupta group has reported that multifunctional liposomes that bind von Willebrand factor, collagen, and platelet integrins have hemostatic properties when administered to murine bleeding models[54].

Synthetic materials targeting secondary hemostasis have also been reported. The Barker group reported a procoagulant microgel formulation that binds fibrin and collapses clot structure based on unique material properties of the microgel[59]. In addition, our lab recently reported a polymeric hemostat, PolySTAT, that mimics the activity of FXIIIa by physically crosslinking fibrin fibers through its multivalent display of fibrin-binding peptides[64] (FBPs) along a hydrophilic polymer backbone[66]. PolySTAT integrates into forming clots, decreases clotting time, and prevents clot lysis while also increasing clot strength. When administered intravenously, PolySTAT also improved survival outcomes in a rat model of femoral artery hemorrhage and fluid resuscitation. Additionally, PolySTAT has been shown to enhance clots in similar fashion to standards of care such as factor concentrates and tranexamic acid[71]. During initial development, various polymer lengths were investigated, with a degree of polymerization of 200 showing optimal clot-enhancing properties using thromboelastography (TEG). Based on the material's performance *in vivo*, further optimization of the material is being pursued towards ultimate translation.

One previously unexplored property of PolySTAT is FBP valency. When considering targeting ligand display there is a non-obvious balance between potential binding sites, saturating targets, and the effects of ligands on the material structure itself. Notably, multivalency is used to increase binding to target substrates[75]. Conversely, it has been found in some applications that too high a ligand density can result in decreased binding[76]. Specifically, ligand density has been shown to play an important role in nanoparticle-based injectable hemostats[46]. In addition to the efficacy of the material, the peptide valency of the final formulation has significant impact on the production costs.

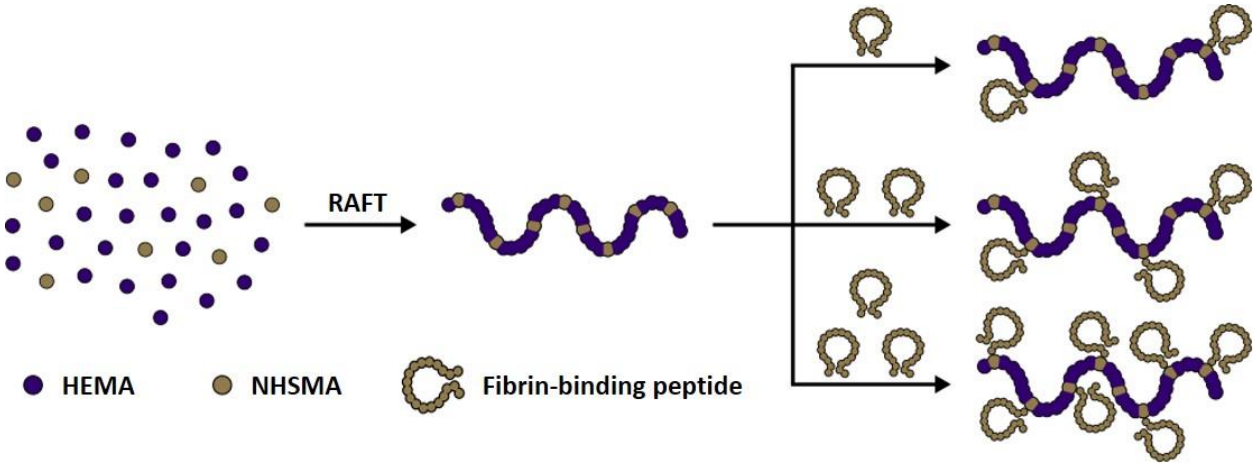

Figure 3.1. Diagram of synthesis strategy for PolySTAT with varied peptide valencies. Base polymers were synthesized by polymerizing hydroxyethyl methacrylate (HEMA), n-hydroxysuccinimide methacrylate (NHSMA), CTP, and AIBN at an 80:20:1:3 ratio and allowing to react for 24 h at 70 °C. Fibrin-binding peptide (FBP) was grafted to the backbone at varying ratios of peptide:NHS in presence of organic base and reacted 24 h at 50 °C.

This work reports a structure-function study important for the optimization of PolySTAT composition. PolySTATs with various peptide valencies were synthesized by reversible addition-fragmentation chain transfer (RAFT) polymerization followed by peptide grafting (Fig. 1). The effect of PolySTAT peptide valency on clot mechanics was determined by rotational thromboelastometry (ROTEM) experiments. High performing valencies were tested to confirm efficacy in a femoral artery and fluid resuscitation model in rats. Finally, neutron scattering, which has been demonstrated as a powerful tool for fibrin structure analysis,[77,78] was used to probe the effects of PolySTAT with varying peptide valencies on the structure of fibrin gels.

3.2 Materials and Methods

3.2.1 *Materials*

2,2′-Azobis(2-methylpropionitrile) (AIBN), 4-cyanopentanoic acid dithiobenzoate (CTP), 2-hydroxyethyl methacrylate (HEMA), and all other reagents were purchased from Sigma-Aldrich (Saint Louis, MO) unless noted otherwise. N-hydroxysuccinimide methacrylate (NHSMA) was purchased from TCI America

(Portland, OR). The fibrin binding peptide (FBP; Sequence: Ac-Y(DGl)C(HPr)YGLCYIQGK),[64] developed by the Caravan group, was purchased as a custom order from GL Biochem (Shanghai, China). Thrombin (Fibri-Prest Automate 5) was purchased from Stago (Asnières sur Seine, France). Fibrinogen and plasmin were purchased from Enzyme Research Laboratories (South Bend, IN). Male Sprague-Dawley rats (300 to 360 g) were obtained from Charles River Laboratories (Wilmington, MA). Certain commercial equipment, instruments, or materials are identified in this paper to foster understanding. Such identification does not imply recommendation or endorsement by the National Institute of Standards and Technology, nor does it imply that the materials or equipment identified are necessarily the best available for the purpose.

3.2.2 *Poly(HEMA-st-NHSMA) Synthesis and Characterization*

Poly(HEMA-st-NHSMA) was synthesized by reversible addition-fragmentation chain transfer (RAFT) polymerization as described previously[66]. A final composition of 80% HEMA and degree of polymerization of 200 was targeted by combining HEMA, NHSMA, CTP, and AIBN at a 160:40:1:0.33 ratio in dimethylacetamide (DMAc) under nitrogen for 24 h at 70 °C. The desired product was purified from unreacted monomer by 2x precipitation in diethyl ether, with DMAc as the intermediate solvent, precipitated polymer was collected by centrifugation at 4500 x g. Dithiobenzoate groups were removed via an end capping reaction with 20x molar excess AIBN at 70 °C for 24 hours. Polymers were characterized via gel permeation chromatography (GPC) with static light scattering and refractive index detectors (MiniDawn Treos and OptilabRex, respectively, both Wyatt Technology, Santa Barbara, CA) to determine molecular weight and polydispersity index (PDI). ^{1}H Nuclear magnetic resonance (NMR) was utilized to determine NHSMA content of the polymer and confirm removal of dithiobenzoate groups.

3.2.3 *Synthesis of PolySTATs Containing Varying Peptide Valencies*

Poly(HEMA-st-NHSMA) was reacted with FBP via the primary amine present in the peptide's lysine residue at the C-terminus under organic basic conditions described

by Yanjarappa *et al*[79]. Briefly, polymer and peptide were combined with diisopropylethylamine in dimethylsulfoxide and allowed to react at 50 °C for 24 hours. The molar feed ratios of peptide:NHS were ranged from 0 to 1.5 to target PolySTATs with differing amounts of peptide per polymer. Unreacted NHS groups were then capped with a 10x molar feed of 3-aminopropanol. Polymers were purified by extensive dialysis as follows. First, the product was dialyzed against phosphate-buffered saline (PBS) for 24 h (3 buffer changes, 4 L of buffer) during which unreacted peptide precipitates. Contents of the dialysis bag were collected and centrifuged at 4500 x g for 8 min to remove unreacted peptide; the supernatant was collected and moved to a fresh dialysis bag. Dialysis continued for 24 h (3 buffer changes), followed by water for 48 h (6 dialysate changes) to remove PBS salts. Peptide content of materials was determined using the extinction coefficient of FBP and the materials' absorbance at a wavelength of 280 nm using a NanoDrop 2000 UV-Vis spectrophotometer (Thermo Fisher Scientific, Waltham, MA).

Small-angle x-ray scattering (SAXS) measurements were performed on PolySTATs with varying peptide valency using the standard measurement settings on the SAXS instrument at the Australian Synchrotron[80]. Polymers were prepared in phosphate-buffered saline, loaded into capillaries. Scattering profiles were fitted to the correlation length model, with an additional clustering term, as described by Hammouda et al[81]:

$$I(Q) = \frac{A}{Q^n} + \frac{C}{1 + (QL)^m} + B$$

3.2.4 *Rotational Thromboelastometry*

ROTEM experiments consisted of 300 µL of clotting solution in a standard ROTEM cup placed in a ROTEM whole blood hemostasis analyzer (ROTEM, Basel, Switzerland). Final concentrations in the ROTEM cup were 1.5 mg/mL fibrinogen, 0.5 IU/mL thrombin, 4 µg/mL plasmin, 0.1 mmol/L CaCl2, and 5 or 20 µmol/L PolySTAT. Measured parameters in ROTEM include: (i) the clotting time (CT), measured as the time between reagent addition to clot formation; (ii) α-angle, which

reflects the rate of clot formation, (iii) the maximum clot firmness (MCF), the highest strength observed for the clot, (iv) the lysis index-30 minutes (LI-30), the percentage of MCF retained 30 minutes after initiation of clot formation, and (v) maximum lysis (ML), the percentage of clot strength lost compared to the MCF at the end of analysis.

3.2.5 *PolySTAT Evaluation in a Rat Femoral Artery Injury and Fluid Resuscitation Model*

Animal use was carried out in accordance with protocols approved by the University of Washington Institutional Animal Care and Use Committee. The rat femoral artery injury and fluid resuscitation model was performed as described previously[66]. Sprague-Dawley rats weighing 300-360 g were randomized into one of three treatment groups (albumin, PolySTAT-4, and PolySTAT-8). Rats were anesthetized with isoflurane followed by ketamine-xylazine cocktail injection in the hindlimb. Catheters were placed in the carotid artery and jugular vein for blood pressure measurement and administration of polymers, respectively. Blood gas and metabolites were measured to maintain healthy baseline respiration and lactate levels (carbon dioxide, $\leq$ 55 mm Hg; O_2 saturation, $\geq$ 95%; lactate, $\leq$ 1.0 mM).

After baseline blood gas and metabolites were confirmed appropriate, the femoral artery in the left hindlimb was identified and isolated. Microsurgical clamps were placed at the proximal and distal ends of the isolated vessel to prevent bleeding while a 3 mm longitudinal incision was made using microscissors. Once the injury was made, a controlled catheter bleed was completed to ensure that all animals started at a normalized mean arterial pressure of 40-50 mm Hg. Clamps were removed and the treatment injected immediately. Depending on treatment group, albumin, PolySTAT-4, or PolySTAT-8 solution (10 mg/mL) were injected over 1.5 min at a dose of 15 mg/kg.

For the first 15 minutes, animals bled freely from the femoral artery wound. After t = 15, animals received saline infusion at a rate of 3 mL/min per kilogram to restore mean arterial pressure to at least 60 mm Hg up to a total of 60 mL/kg.

Blood loss over time was measured by collection of blood at 5 minute intervals in pre-weighed gauze by the blinded researcher at the wound edges with care not to disturb the femoral artery or the clot.

3.2.6 *Neutron Scattering Characterization*

Samples for small-angle neutron scattering (SANS) and ultra-small-angle neutron scattering (USANS) were prepared as described previously[77]. Briefly, deuterated water containing 99.9% D_2O obtained from Cambridge Isotope Laboratories (Andover, MA) was used to prepare PBS containing 0.5 mol/L NaCl. Fibrinogen was dialyzed against the deuterated buffer. Stock PolySTAT solutions were prepared in deuterated buffer as well. Fibrinogen solutions were degassed under vacuum to prevent signal-altering bubbles. 0.5 IU/mL of thrombin was added to each sample, mixed, and immediately loaded it into the SANS or USANS cells in the presence of 5 μmol/L PolySTAT or a volume control of deuterated PBS.

Small-angle neutron scattering (SANS) and ultra-small-angle neutron scattering (USANS) measurements were performed on the same samples at the Center for Neutron Research at NIST in Gaithersburg, Maryland as described previously[77]. SANS measurements were performed on the NG7 30-meter instrument[82]. Measurements were performed at detector distances of 1.3 m, 7 m, and 13.2 m to allow for a q range of 0.002 $Å^{-1}$ to 0.3 $Å^{-1}$. Neutron wavelengths were 5 Å and 8.4 Å. All SANS data were corrected for background and empty cell scattering. Data were measured on an absolute scale relative to flux of the direct beam[83]. USANS measurements were performed on the BT5 perfect crystal diffractometer[84]. All SANS data were reduced and desmeared using the NIST macros in Igor[83].

Data were then analyzed using previously established methods for fibrin gels[77]. A modified Guinier fit for one-dimensional structures was used to determine the cross-sectional fiber radius of fibrin fibers within the protein gels. Moreover, a fractal model was used to measure the correlation length and fractal dimension of the fractal structure corresponding to branching of fibrin fibers within the protein gels[77].

The Guinier fit was performed on the region that includes the turnover to low-q and the intermediate Porod region (0.001 $Å^{-1} < q < 0.01$ $Å^{-1}$). The intensity and q in the

Guinier region are related to the cross-sectional radius of gyration by the following equation[85]:

$$(qI)_{Q\to 0} = (qI)_0 \exp\left(-\left(\frac{R_g^2}{2}\right)q^2\right)$$

where q is scattering vector, I is scattering intensity, and R_g is the cross-sectional radius of gyration. Using this approach, an average radius of gyration is determined and the assuming cylindrical structure of fibrin fibers, as previously, the fiber radius can be determined by the following equation[77,85]:

$$R = R_g\sqrt{2}$$

where R is the true radius of the fiber and R_g is the cross-sectional radius of gyration from the Guinier fit. The fiber radius was found to increase with increasing peptide valency (Table 2).

The network structure was modeled using a fractal model that utilizes spherical building blocks based on the work of Teixeira[86]. The data from the USANS range (q < 0.001 Å^{-1}) was fitted through least-squares to the fractal described by the following three equations[86]:

$$I(q) = P(q)S(q)$$

where *I(q)* is the total intensity, which is made up of the form factor, *P(q)*, and the structure factor, *S(q)*. The form factor is described as[86]:

$$P(q) = \varphi V_P^2 \Delta\rho^2 \left(\frac{sin(qR_0) - qR_0 cos(qR_0)}{3(qR_0)^3}\right)^2$$

where φ is the volume fraction of spherical building blocks, V_P is the volume of the spheres, $\Delta\rho$ is the difference in scattering length density, q is the scattering vector, and R_0 is the sphere radius. The structure factor is described as[86]:

$$S(q) = 1 + \frac{sin\left[\left(D_f - 1\right)tan^{-1}(q\xi)\right]}{(qR_0)^{D_f}} \frac{D_f \Gamma\left(D_f - 1\right)}{[1 + 1/(q^2\xi^2)]^{(D_f-1)/2}}$$

where D_f is the fractal dimension and ξ is the correlation length. The difference in scattering length density was determined through measurements performed by Weigandt *et al*[77]. The radius of the spheres was defined as the radius found from the

Guinier model. During fitting, D_f, ξ, and φ were allowed to vary with while minimizing χ^2.

3.3 RESULTS

3.3.1 *Synthesis and Characterization of PolySTATs with Varying Peptide Valencies*

PolySTATs with varying peptide valencies were synthesized by first preparing a backbone polymer, poly(HEMA-st-NHSMA), by RAFT polymerization followed by peptide grafting and conversion of unreacted NHSMA to alcohols. All polymers were synthesized using the same backbone polymer to ensure that the degree of polymerization of all materials is held constant. Polymers were synthesized with molecular weight (31.7 kDa) and NHSMA content (19%) similar to theoretical values (28.2 kDa and 20%) as confirmed by GPC and 1H NMR, respectively. Degree of polymerization was 225.

Table 3.1. Variation of Peptide Valencies

Peptide:NHS Molar Feed	Peptides per Polymer	Title
1.5	10.4	PolySTAT-10
1.0	7.9	PolySTAT-8
0.5	4.2	PolySTAT-4
0.25	2.9	PolySTAT-3
0.1	1.4	PolySTAT-1
0.0	0.3	PolySTAT-0

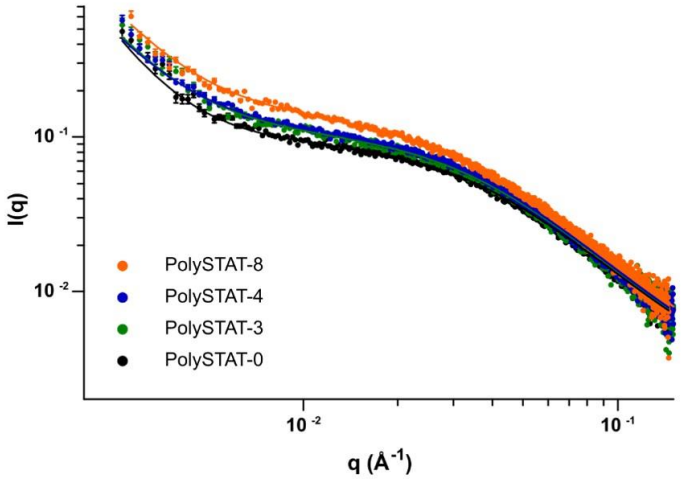

Figure 3.2. X-ray scattering of PolySTAT with various peptide valencies. PolySTATs were dissolved in phosphate-buffered saline. Measurements were taken using the SAXS instrument at the Australian Synchrotron. Experimental data are displayed as averages as points with uncertainty from reduction as error bars that are often hidden behind data points and fit lines. Correlation length model fits for each condition are shown as solid lines

Polymers with increasing FBP valencies were obtained by increasing peptide feed ratios during peptide grafting. The peptide valency, in average peptides per polymer, for the various reaction feeds are shown in Table 1. Polymer conjugates with average peptide content of 0 to 10 peptides per polymer were synthesized. The pHEMA backbone and PolySTATs with a range of peptide valencies showed no lysis of red blood cells at 25 µM concentrations suggesting hemocompatibility at approximately 5-fold greater than the administered in vivo dose of 15 mg/kg (5.2 µM) (Fig. S1).

Table 3.2. PolySTAT radii of gyration

Sample	Rg (Å)
PolySTAT-8	115.9
PolySTAT-4	105.0
PolySTAT-3	104.7
PolySTAT-0	97.1

SAXS measurements and fits (Fig. 2) demonstrated that with an increase in peptide content, the radius of gyration of the polymer-peptide conjugate increased (Table 2). Additionally, an increase in low-q scattering intensity was observed for all samples. This is likely due to clustering effects of the pHEMA backbone of the material.

Clustering of water-soluble polymers due to hydrophobic interactions has been observed to give similar low-q features to those observed in these meaurements[81,87].

3.3.2 *In Vitro Evaluation of PolySTATs by ROTEM*

Rotational thromboelastometry (ROTEM), a clinically used method to characterize coagulation, was used to determine the effect of polymers on clot mechanics. Two PolySTAT concentrations tested, 5 μmol/L and 20 μmol/L, were used. The lower 5 μM concentration mimics the conditions of the previous PolySTAT studies and corresponds to ≈15 mg/kg *in vivo* dose for the various polymers. The higher 20 μM concentration corresponds to about two PolySTAT polymers per potential binding site on fibrin. A distinct threshold of peptide valency necessary for PolySTAT to impact clot half-life or formation rate was observed (Fig. 3A, 3B). Polymers with fewer than an average of 3 peptides/polymer did not impact LI-30 or α-angle; in contrast, polymers with greater than an average of 4 peptides/polymer showed significantly increased kinetics of clot formation and delay in clot breakdown. It is interesting to note that at a higher concentration of PolySTAT (20 μmol/L), the kinetics of clot formation are slightly decreased for the clots formed in the presence of PolySTATs with more than 4 peptides per polymer on average. Thus, the threshold peptide valency required for clot strengthening activity by ROTEM was determined to be ≈4 peptides per polymer on average.

Based on these results, the effect of 5 μM PolySTAT-4 on clot mechanics was fully tested against a PBS volume control. Fig. 3C-E show the effects of PolySTAT-4 on CT, MCF and ML. There was a decrease, though not statistically significant, in the CT in the presence of PolySTAT-4 at 5 μM ($p = 0.086$). The MCF was increased 57% (12.7 mm to 20.0 mm, $p = 0.007$), indicating stronger clot formation in the

presence of PolySTAT-4 (Fig. 3D). The ML at 50 minutes was decreased 69% (79.3% to 24.3%, $p < 0.001$) for fibrin clots formed with PolySTAT-4, confirming the antifibrinolytic activity of PolySTAT.

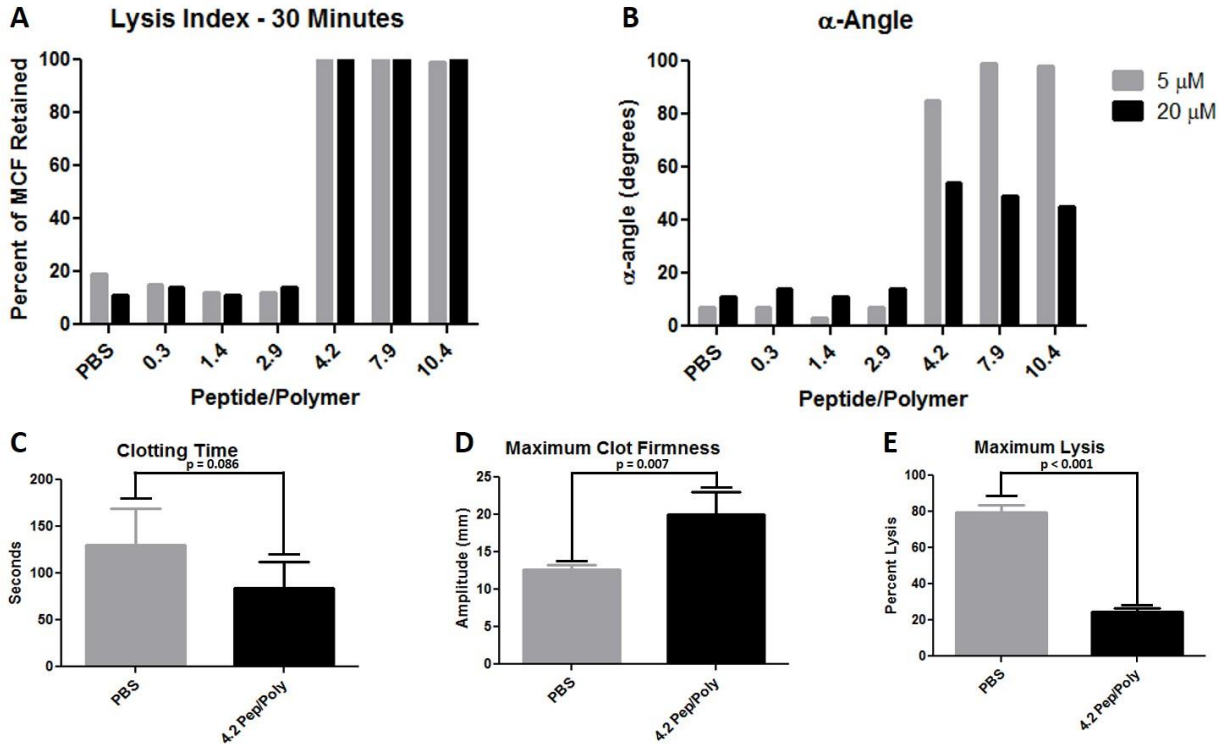

Figure 3.3. *In vitro* characterization of fibrin clot kinetics, clot strength, and fibrinolysis. The effect of PolySTAT with various peptide valencies was tested in a hyperfibrinolytic model using ROTEM. The amount of clot firmness retained 30 minutes after clot initiation **(A)** and the clot kinetics **(B)** were tested for all peptide valencies at concentrations of 5 μM PolySTAT and 20 μM PolySTAT ($n = 1$). **(C-E)** Clotting time, clot strength, and total fibrinolysis of fibrin clots in presence of either a PBS control or the PolySTAT variant containing 4.2 peptides per polymer. Data are averages $\pm$ standard deviation ($n = 3$). *P* values were determined using the student's t-test.

3.3.3 *In Vivo Performance of PolySTATs in Femoral Artery Injury and Fluid Resuscitation Model*

In the previously reported development and characterization of PolySTAT, rats treated with PolySTAT-16 in a femoral artery and fluid resuscitation model showed significantly improved survival over scrambled peptide controls, an oncotic control (albumin), a volume control (saline), and the body's natural fibrin crosslinker hFXIIIa.[66] Here, PolySTATs with average valencies of 4 and 8 were found to also be effective in comparison to animals treated with albumin as an osmotic control (Fig. 4B). Animals in the albumin group showed 20% survival over the entire model with deaths occurring within the first twenty minutes. All animals treated with PolySTAT-4 survived through the 75-minute model; this translates to a statistically significant increase in survival in comparison to albumin ($p = 0.013$). Of the 5 rats treated with PolySTAT-8, a single animal did not survive, resulting in 80% survival, a non-significant increase in survival in comparison to albumin-treated animals ($p = 0.063$). Hemorrhage volumes were measured for each animal and are reported as milliliter of blood lost per kilogram (mL/kg). Animals treated with albumin (Fig. 4C) generally did not clot well at the injury site, demonstrated by a lack of plateau in blood loss. The exception is the lone surviving rat that clotted and kept its clot strength throughout the experiment. All rats treated with PolySTAT-4 exhibited clotting with no rebleeding events (Fig. 4D). All rats treated with PolySTAT-8 clotted within 15 minutes. There was one minor rebleeding event. Notably, the animal that did not survive did not appear to hemorrhage greatly, but was deemed a clinical death with a prolonged mean arterial blood less than 20 mm Hg.

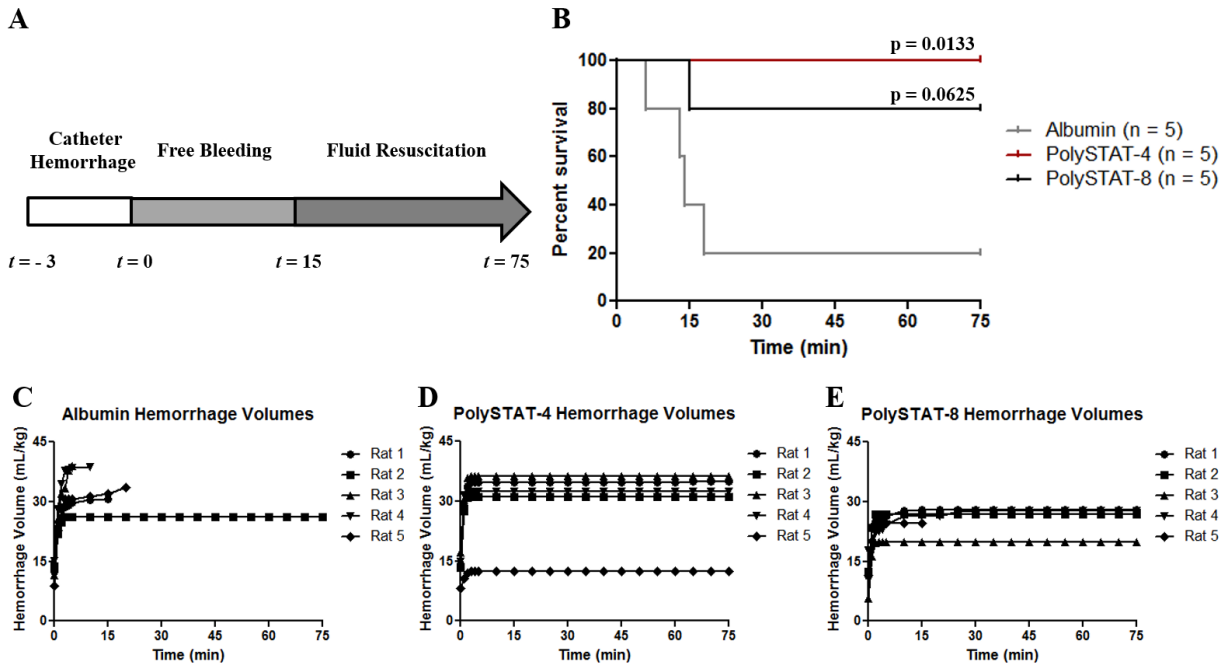

Figure 3.4. ***In vivo*** **evaluation of PolySTAT with different valencies in a rat traumatic injury model. (A)** Outline of the experiment. Rats underwent catheter hemorrhage to normalize starting blood pressures. Subsequently, clamps proximal and distal to the wound were removed and the treatment was injected. The injury was allowed to bleed freely for 15 minutes, at which point fluid resuscitation began in the form of 0.9% saline infusion. **(B)** Survival of animals over 75-minute experiment (n = 5 per condition). *P* values determined by log-rank Mantel-Cox test with comparisons against albumin control. **(C-E).** Cumulative hemorrhage volumes for individual animals in each condition.

3.3.4 *Neutron Scattering Measurements of Fibrin Gels with PolySTAT*

Neutron scattering was used to determine the effect of PolySTAT on fibrin structure. Fibrin clots were formed in the presence of PolySTATs with peptide valencies of approximately 0, 2, 4, and 8. Despite full solubility at 10 mg/mL in H_2O PBS, PolySTAT did not fully dissolve in the deuterated buffer used for neutron scattering studies, therefore the soluble fraction of PolySTAT was collected as supernatant after centrifugation and used. These samples were characterized by UV spectroscopy to determine peptide content and polymer concentration, which are reported in

Supplementary Table 3. Due to the hydrophobic nature of FBP, polymer populations with lower peptide grafting ratios resulted in higher solubility (Table S3). Thus, the average peptide valency of polymers dissolved in D_2O was different from the parent populations. The true peptide valency is used to label the conditions in Figure 5.

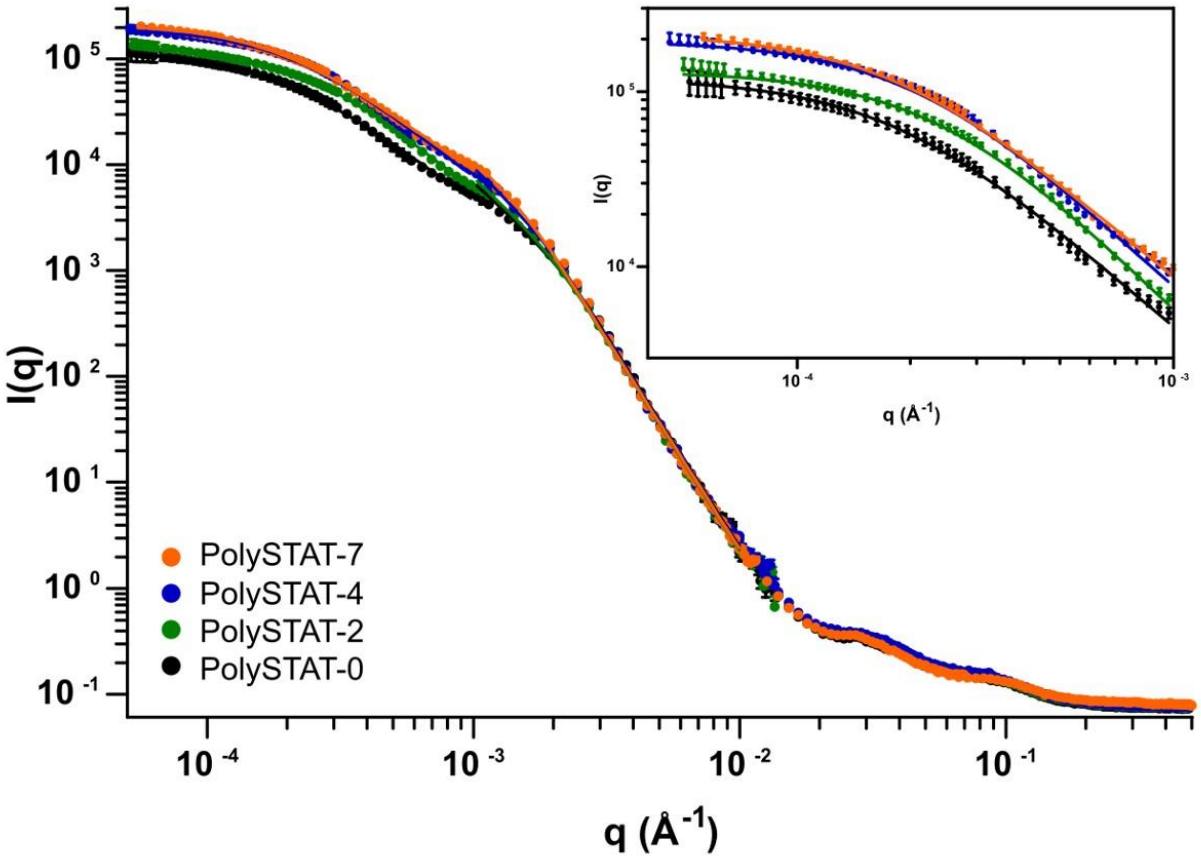

Figure 3.5. Neutron scattering of fibrin gels with various PolySTATs. Fibrin gels were formed in deuterated solvent by activation with thrombin in the presence of PolySTAT variants. Measurements were taken on SANS and USANS instruments. The data were desmeared and combined into a single scattering profile per sample. Experimental data are displayed as averages points with error bars from the reduction that are often hidden behind data points and fit lines. Guinier model fits for each condition are shown as solid lines for the region ($0.008 < q < 0.01$ Å^{-1}). Fractal model fits for various conditions are shown as solid lines for the region ($0.00005 < 0.008$ Å^{-1}). **Inset,** Fractal model fits and data within the fractal model range.

Table 3.3 Guinier model fit results: fiber radius

Sample	R_g (nm)	R (nm)
PolySTAT-0	34.1 ± 0.4	48.2 ± 0.6
PolySTAT-2	37.9 ± 0.5	53.6 ± 0.7
PolySTAT-4	41.7 ± 0.5	59.0 ± 0.7
PolySTAT-7	46.9 ± 0.6	66.3 ± 0.8

Samples were prepared in uniform fashion with degassed solutions in SANS and USANS sample cells. Scattering data were fully reduced, desmeared, and combined into a single scattering profile (Fig. 5). Signals for neat fibrinogen and PolySTAT-0 appear similar throughout the entire q range. Additionally, PolySTAT-2, -4, and -8 overlap with these samples throughout the SANS regime of high- and mid-q. However, there is a change in scattering intensity for PolySTAT with 8 and 4 peptides/polymer in the low-q USANS regime. Using strategies previously used to analyze neutron scattering data of fibrin gels, a modified Guinier fit for one-dimensional structures was used to determine the cross-sectional fiber radius of fibrin fibers within the protein gels. Moreover, a fractal model was to measure the correlation length and fractal dimension of the fractal structure corresponding to branching of fibrin fibers within the protein gels[77].

The correlation length describes the distance over which the fractal dimension is accurate. From the fits, both the correlation length and the fractal dimension have no distinct trend with ξ ranging from 281 to 529 nm and D_f ranging from 1.92 to 2.21 (Table 4).

Table 3.4. Fractal model fit results: fractal structure

Sample	Correlation Length (nm)	Fractal Dimension
PolySTAT-0	529.4 ± 31.3	1.92 ± 0.05
PolySTAT-2	381.1 ± 18.3	2.21 ± 0.05
PolySTAT-4	451.1 ± 18.8	2.11 ± 0.04
PolySTAT-7	519.6 ± 22.2	1.99 ± 0.03

3.4 DISCUSSION

While synthetic materials that mimic the effects of platelets have seen success, there is currently little work creating synthetic materials mimicking other components of clot formation. Our initial design of a FXIIIa-inspired polymeric hemostat that physically crosslinks fibrin consisted of a polyHEMA backbone with an average of 16 FBP grafted per polymer[66]. In this initial work, effects of polymer length were investigated, but not the amount of peptide per polymer. Varying the peptide valency could potentially vastly alter the interaction between PolySTAT and the fibrin clot. Increasing peptide valency could allow for increased fibrin crosslinking; however, there is likely a saturation point at which increasing peptide content does not increase the positive effect of PolySTAT. Additionally, increased peptide content could lead to instability of the conjugate as the peptide is highly hydrophobic. Furthermore, minimizing the peptide content per polymer without sacrificing efficacy would aide translation to clinical use.

To investigate the effect of peptide valency on PolySTAT efficacy for hemostasis, PolySTAT polymers were synthesized with varying amounts of peptide per polymer. First, a poly(HEMA-*st*-NHSMA) backbone was synthesized, controlling the degree of polymerization and NHSMA content via the monomer:CTA and HEMA:NHSMA ratios, respectively. PolySTATs with various FBP valencies ranging from 0 to 10 were then synthesized from the poly(HEMA-*st*-NHSMA) backbone by grafting FBP to the polymer at various mole ratios of peptide: polymer. Importantly, this reaction is reproducible and scalable. Larger batches of PolySTAT-4 and PolySTAT-8 with similar polymer properties were prepared for animal studies (SI Tables S1 & S2).

ROTEM of fibrin clots formed under lytic conditions with the various PolySTATs showed a threshold of biological activity at ≈4 peptides per polymer. It was not surprising that polymer backbones lacking peptides had no effect on clotting. It was also predictable that conjugates with valencies of ≈2 did not influence clotting, as these lack the ability to bind the fibrin network in a multivalent fashion in independent locations. These results demonstrate the importance of including greater than 2 binding ligands in cross-linking materials. This agrees with the observation by Soon et al. that 4-arm PEG decorated with 4 fibrin knob-mimetic glycine-proline-arginine-proline (GPRP) peptides significantly increased fibrin chain-crosslinking compared to a similarly decorated bifunctional PEG with 2 GPRP peptides conjugated[63].

Another potential explanation for enhanced clotting with increased peptide valency is due to the increased amphiphile character due to incorporation of the hydrophobic FBP. Amphiphilic materials have been shown to promote hemostasis through non-specific interactions[88]. However, previous work with PolySTAT compared it against PolySCRAM, which substitutes FBP with a scrambled peptide sequence. This scrambled sequence retains the peptide's highly hydrophobic nature while changing the amino acid sequence which ablates specific binding to fibrin. As PolySCRAM performed similar to PBS controls in vitro and in vivo, amphiphilicity has little to no contribution to PolySTAT's activity.

It is also interesting to note that *in vitro* results shown here provide possible insight into the unknown binding site of FBP. FBP was developed through initial phage display discovery followed by engineering for stability and binding affinity,[64] although the exact binding site to fibrin was not determined. GPRP peptides, as knob mimetics, are known to interact with fibrin at the knob-hole interactions.[63,89] Despite similar crosslinking activity of GPRP-PEG and PolySTAT, the functional outcome for GPRP-PEG and PolySTAT are very different. While PolySTAT at different valencies can increase fibrin gel strength, decrease clotting time, and strongly decrease fibrinolysis,[66] 4-arm GPRP-PEG had minimal effects of clotting time and fibrinolysis, and decreased fibrin gel elastic modulus due to GPRP peptides binding at a site which disrupts natural fibrin polymerization[63]. These data suggest that FBP does not interact nor interfere with the knob-hole interactions that are integral to fibrin self-assembly.

This hypothesis is further supported by the results from the neutron scattering experiments. Probing the high- to mid-q range correlates to investigating the fibrin monomer to individual coarse fiber length scale[77]. Nearly identical scattering signals for all samples throughout this range suggests little to no deviation in internal fiber structure of the fibrin gel in respect to the neat fibrin gel (Fig. 5).

The difference in scattering signals were observed in the mid- to low-q regimes, and through fitting it was determined that the greatest effects were at the fiber radius level. The radius of fibrin fibers was found to increase with increasing peptide valency, and trended linearly with peptide valency with an R^2 of 0.9992 (Supplemental S5). This may be due to the greater PolySTAT valencies leading to the recruitment of additional fibrin, or adding to the mass of individual fibers. It is worth noting that in these experiments the fiber radii are similar to those observed by Weigandt *et al* but systematically smaller[77]. Finally, the fits related to the network structure showed no

consistent difference in the network. The correlation length and fractal dimension were similar to those observed for neat fibrin by Weigandt *et al*[77]. This suggests that the changes PolySTAT incurs on the fibrin gel is primarily at the individual fiber length scale. These results give insight into the mechanism by which PolySTAT promotes clotting, suggesting that PolySTAT conducts its effects on the fiber structure of fibrin gels, and also the potential binding site for FBP. A possible explanation for the observation that PolySTAT does not affect fibrin gel structure at small length scales despite its presence at the onset of fibrinogen activation could be that FBP binds at regions where fibrin monomers have self-assembled, perhaps overlapping two or more fibrin monomers.

ROTEM characterization of clot mechanics revealed that PolySTAT with a valency greater or equal to 4 peptides per polymer (4, 8, and 10) showed enhanced clot properties in contrast to PolySTAT with valencies lower than 4 (0, 1, and 3). Similarly, Shoffstall et al showed that for their platelet-mimicking RGD-modified PLGA nanoparticles, an increased number of RGD ligands presented by PLGA nanoparticles resulted in a lower concentration necessary to promote clotting in a liver trauma model. At increased concentrations, we observed a saturating effect on clot kinetics (alpha angle) by the high valency PolySTATs. This is likely due to saturation of binding sites in the early steps of clot formation when fibrin is being generated by thrombin's cleavage of fibrinogen. This observation agrees with those by Shoffstall et al. that high concentrations of particles with high ligand densities resulted in a loss of procoagulatory effects[46].

Previously, ROTEM characterization has been a good predictor of *in vivo* success for injectable hemostats[48,66]. Furthermore, the Lavik group's ligand density work provided evidence for ROTEM as a method for screening different formulations of hemostatic materials[46]. The results in this study further support ROTEM-based prediction for *in vivo* success in femoral artery bleeding models. Intravenous administration of both PolySTAT-4 and PolySTAT-8 improved survival rates over 75 minutes in the rat femoral artery injury model. An endpoint of 75 minutes was chosen to allow ample time for rebleeding to occur. In our previous work with the model, all rebleeds began before 30 minutes post-injury,[66] and the same was observed in these studies. Investigation of hemorrhage rate of the animals suggests that animals treated with PolySTAT-4 did tend to lose more blood (Fig. 4D & 4E, S4A). This is especially true when focusing on the 4 very similar animals in each treatment group. For both treatments, however, it appears that blood loss ceased quickly and contributed to survival. Notably, the animal that did not survive in the PolySTAT-8 group did not show greater hemorrhage than its cohort. This suggests that this animal

did not die due to blood loss and additional circumstances such as heart arrhythmia may have contributed. Animals treated with albumin as an oncotic non-hemostatic protein control in general did not stop bleeding or experienced rebleeding. This suggests that in the femoral artery injury model, there may be a clot strength that can be attained by both PolySTAT-4 and -8, but more slowly by PolySTAT-4, that promotes survival. Since PolySTAT assists most dramatically with retaining clot strength by decreasing fibrinolysis, other models of trauma that are less prone to rebleeding and require faster clotting may provide greater insight to the feasibility of PolySTAT-4 in comparison to variants with higher valency.

While PolySTAT-4 and -8 both performed well in the femoral injury model, there are subtle differences between the two and PolySTAT-16 that require further investigation prior to translation. Notably, decreasing peptide valency decreases the overall molecular weight of the material and may therefore lead to an increased rate of clearance and altered biodistribution. If, in future work this rate is found to be too great, the polymer backbone molecular weight can be increased to counteract lost mass with decreased peptide valency. Despite these differences, to date only one animal treated with a formulation of PolySTAT in the femoral artery injury model has died, resulting in 93% survival, compared to all control animals (scrambled peptide, albumin, hFXIIIa, and saline) ranging from 0% to 40% survival, with an aggregate 20% survival. Additionally, some insight into the potential mechanism for how PolySTAT interacts with the fibrin has been provided through coagulation assays and neutron scattering experiments. Neutron scattering has also been used to observe structure changes in fibrin during rheological experiments[78]. This versatility is promising as a tool for gaining additional understanding of the hemostatic mechanisms in general.

3.5 CONCLUSIONS

PolySTAT polymers containing 4 or more peptides per polymer on average were effective to restore clot formation and improve survival in a rat bleeding model. The threshold observed in these studies may be due to a minimal average distance between cross-links for multivalency and effective clot strengthening, or, as shown by neutron scattering, a minimum valency necessary for additional recruitment of fibrin. Synthetic fibrin-targeting hemostats have great potential to significantly improve survival from traumatic bleeding.

3.6 ACKNOWLEDGMENTS

This work was supported by NIH R21EB018637. RJL was supported by an NSF Graduate Fellowship (2013163249) and NIH Training Grant NIBIB T32EB1650. NJW was supported by Grant Number KL2 TR000421 from the National Center for Advancing Translational Sciences (NCATS), a component of the National Institutes of Health (NIH). Its contents are solely the responsibility of the authors and do not necessarily represent the official view of NCATS or NIH. We acknowledge the support of the National Institute of Standards and Technology, U.S. Department of Commerce, in providing the neutron research facilities used in this work and invitational travel support for RJL. This work utilized facilities supported in part by the National Science Foundation under Agreement No. DMR-1508249. We thank James Carothers for use of his Nanodrop 2000. We thank Dr. Xu Wang, and Dr. Susan Stern of the Emergency Medicine Research Laboratory for their technical assistance and expertise. We thank Dr. Leslie Chan for contributing her time and expertise to the PolySTAT project. We thank Dr. Yilong Cheng and Gary Liu for advice and assistance with RBC hemolysis.

3.7 REFERENCES

1. WISQARS: Leading Causes of Death Reports. *Centers for Disease Control and Prevention* (2015).
2. WISQARS: Years of Potential Life Lost. *Centers for Disease Control and Prevention* (2015).
3. Murray, C. J. L., Lopez, A. D., Mathers, C. D. & Stein, C. *The Global Burden of Disease 2000 project: aims, methods and data sources*. (2001).
4. World Health Organization: The top 10 causes of death. (2017). Available at: http://www.who.int/mediacentre/factsheets/fs310/en/.
5. Sauaia, A. *et al.* Epidemiology of Trauma Deaths: A Reassessment. *J. Trauma* **38,** 185–193 (1995).
6. Lerner, E. B. & Moscati, R. M. The Golden Hour : Scientific Fact or Medical 'Urban Legend'. *Am. Emerg. Med.* **8,** 758–760 (2001).
7. Kauvar, D. S., Lefering, R. & Wade, C. E. Impact of Hemorrhage on Trauma Outcome : An Overview of Epidemiology, Clinical Presentations, and Therapeutic Considerations. *J.*

Trauma **60,** 3–11 (2006).

8. Champion, H. R. *et al.* A Profile of Combat Injury. *J. Trauma* **54,** 513–519 (2003).
9. Holcomb, J. B. *et al.* Causes of Death in U . S . Special Operations Forces in the Global War on Terrorism. **245,** 986–991 (2007).
10. Chan, L. W., White, N. J. & Pun, S. H. Synthetic Strategies for Engineering Intravenous Hemostats. *Bioconjug. Chem.* **26,** 1224–1236 (2015).
11. Chen, H., Locke, D., Liu, Y., Liu, C. & Kahn, M. L. The Platelet Receptor GPVI Mediates Both Adhesion and Signaling Responses to Collagen in a Receptor Density-dependent Fashion*. **277,** 3011–3019 (2002).
12. Daniel, J. L. *et al.* Molecular Basis for ADP-induced Platelet Activation. **273,** 2024–2029 (1998).
13. Klinik, M. *et al.* Molecular Mechanisms of Platelet Activation. *Pharm. Rev.* **69,** 58–141 (1989).
14. Shattil, S. J., Hoxie, J. A., Cunningham, M. & Brass, L. F. Changes in the Platelet Membrane Glycoprotein IIb * IIIa Complex during Platelet Activation *. **260,** (1985).
15. Takeoka, S. *et al.* Function of fibrinogen. **312,** 773–779 (2003).
16. Tomiyama, Y., Tsubakio, T. & Kurata, Y. The Arg-Gly-Asp (RGD) recognition site of platelet glycoprotein IIb- IIIa on nonactivated platelets is accessible to high-affinity macromolecules. *Blood* **79,** 2303–2312 (2011).
17. Davie, E. W., Fujikawa, K. & Kisiel, W. The Coagulation Cascade: Initiation, Maintenance, and Regulation. *Biochemistry* **30,** 10363–10370 (1991).
18. Morrison, D. C. & Cochrane, C. G. Direct Evidence For Hageman Factor (Factor XII) Activation by Bacterial Lipopolysaccharides. *J. Exp. Med.* **140,** 797–811 (1974).
19. Bouma, B. N. & Griffin, J. H. Human blood coagulation factor XI . Purification , properties , and mechanism of activation by activated factor XII. *J. Biol. Chem.* **252,** 6432–6437 (1977).
20. Hoffman, M., Monroe, D. M. & Roberts, H. R. Activated factor VII activates factors IX and X on the surface of activated platelets : thoughts on the mechanism of action of ... *Blood Coagul. Fibrinolysis* **9,** S61–S65 (1998).
21. Mann, K. G., Brummel, K. & Butenas, S. What is all that thrombin for? *J Thromb Haemost* **1,** 1504–1514 (2003).

22. White, N. J. Mechanisms of trauma-induced coagulopathy. *Haematology* 660–663 (2013).
23. Kushimoto, S., Kudo, D. & Kawazoe, Y. Acute traumatic coagulopathy and trauma-induced coagulopathy : an overview. *J. Intensive Care* 1–7 (2017). doi:10.1186/s40560-016-0196-6
24. Brohi, K., Singh, J., Heron, M. & Coats, T. Acute traumatic coagulopathy. *J. Trauma* **54,** 1127–1130 (2003).
25. Kaafarani, H. M. a & Velmahos, G. C. Damage control resuscitation in trauma. *Scand. J. Surg.* **103,** 81–88 (2014).
26. Mikhail, J. The trauma triad of death: hypothermia, acidosis, and coagulopathy. *AACN clinical issues* **10,** 85–94 (1999).
27. Niles, S. E. *et al.* Increased Mortality Associated With the Early Coagulopathy of Trauma in Combat Casualties. *J. Trauma Inj. Infect. Crit. Care* **64,** 1459–1465 (2008).
28. Standbury, L. G. & Hess, J. R. Blood Transfusion in World War I : The Roles of Lawrence Bruce. *Transfus. Med. Rev.* **23,** 232–236 (2009).
29. Boyle, R., Willis, T. & Wren, C. The History of Blood Transfusion. *Br. J. Haemotology* **110,** 758–767 (2000).
30. Duchesne, J. C., Hunt, J. P., Wahl, G. & Marr, A. B. Review of Current Blood Transfusions Strategies in a Mature Level I Trauma Center : Were We Wrong for the Last 60. *J. Trauma* **65,** 272–278 (2008).
31. Repine, T. B., Perkins, J. G., Kauvar, D. S. & Blackborne, L. The Use of Fresh Whole Blood in Massive Transfusion. **60,** (2005).
32. Sihler, K. C. & Napolitano, L. M. Complications of Massive Transfusion. *Chest* **137,** 209–220 (2010).
33. Riou, B. *et al.* Recombinant factor VIIa (Novoseven) as adjunctive therapy for bleeding contorl in trauma - a randomized. placebo-controlled trial. in *Shock* 228 (2004).
34. Rizoli, S. B. *et al.* Recombinant activated factor VII as an adjunctive therapy for bleeding control in severe trauma patients with coagulopathy : subgroup analysis from two randomized trials. *Crit. Care* **10,** 1–11 (2006).
35. Raza, I. *et al.* The incidence and magnitude of fibrinolytic activation in trauma patients. *J. Thromb. Haemost.* **11,** 307–314 (2013).
36. Williams-johnson, J. A., Mcdonald, A. H., Strachan, G. G. & Williams, E. W. Effects of

Tranexamic Acid on Death, Vascular Occlusive Events, and Blood Transfusion in Trauma Patients with Significant Haemorrhage (CRASH-2) A Randomised, Placebo-Controlled Trial. *West Indian Med J* **59,** 612–624 (2010).

37. Houston, F. S. Military Application of Tranexamic Acid in Trauma Emergency Resuscitation (MATTERs) Study. **147,** 113–119 (2012).
38. Search Results: tranexamic acid. *ClinicalTrials.gov* (2018).
39. Coller, B. S. Interaction of normal, thrombathemis, and Bernard-Soulier platelets with immobilized fibrinogen: defective platelet-fibrinogen interaction in thrombastatin. *Blood* **55,** 169–179 (1980).
40. Coller, B. S. *et al.* Thromboerythrocytes In Vitro Studies of a Potential Autologous , Semi-artificial Alternative to Platelet Transfusions. *J Clin Invest* **98,** 546–555 (1992).
41. Ten, O. Fibrinogen-coated albumin microcapsules reduce bleeding in severely thrombocytopenic rabbits. **9,** 107–111 (1999).
42. Illum, L. *et al.* Blood clearance and organ deposition of intravenously administered colloidal particles . The effects of particle size , nature and shape. **12,** 135–146 (1982).
43. Okamura, Y. *et al.* Hemostatic effects of phospholipid vesicles carrying fibrinogen gamma chain dodecapeptide in vitro and in vivo. *Bioconjug. Chem.* **16,** 1589–96 (2005).
44. Okamura, Y. *et al.* Development of fibrinogen gamma-chain peptide-coated, adenosine diphosphate-encapsulated liposomes as a synthetic platelet substitute. *J. Thromb. Haemost.* **7,** 470–7 (2009).
45. Bertram, J. P. *et al.* Intravenous Hemostat : Nanotechnology to Halt Bleeding. *Sci. Transl. Med.* **1,** 11–22 (2009).
46. Shoffstall, A. J. *et al.* Tuning ligand density on intravenous hemostatic nanoparticles dramatically increases survival following blunt trauma. *Biomacromolecules* **14,** 2790–2797 (2013).
47. Lashof-sullivan, M. *et al.* Hemostatic Nanoparticles Improve Survival Following Blunt Trauma Even after 1 Week Incubation at 50 °C. *ACS Biomater. Sci. Eng.* **2,** 385–392 (2016).
48. Shoffstall, A. J. *et al.* Intravenous hemostatic nanoparticles increase survival following blunt trauma injury. *Biomacromolecules* **13,** 3850–3857 (2012).
49. Hubbard, W. B., Lashof-Sullivan, M. M., Lavik, E. B. & Vandevord, P. J. Steroid-loaded

hemostatic nanoparticles combat lung injury after blast trauma. *ACS Macro Lett.* **4,** 387–391 (2015).

50. Onwukwe, C. *et al.* Engineering Intravenously Administered Nanoparticles to Reduce Infusion Reaction and Stop Bleeding in a Large Animal Model of Trauma. (2018). doi:10.1021/acs.bioconjchem.8b00335
51. Gupta, A. Sen, Huang, G., Lestini, B. J., Sagnella, S. & Kottke-marchant, K. RGD-modified liposomes targeted to activated platelets as a potential vascular drug delivery system RGD-modified liposomes targeted to activated platelets as a potential vascular drug delivery system. *Thromb Haemost* **93,** 106–114 (2005).
52. Ravikumar, M., Modery, C. L., Wong, T. L. & Gupta, A. Sen. Peptide-Decorated Liposomes Promote Arrest and Aggregation of Activated Platelets under Flow on Vascular Injury Relevant Protein Surfaces in Vitro. *Biomacromolecules* **13,** 1495–1502 (2012).
53. Ravikumar, M. *et al.* Mimicking Adhesive Functionalities of Blood Platelets using Ligand- Decorated Liposomes. *Bioconjug. Chem.* **23,** 1266–1275 (2012).
54. Modery-Pawlowski, C. L., Tian, L. L., Ravikumar, M., Wong, T. L. & Gupta, A. Sen. In vitro and in vivo hemostatic capabilities of a functionally integrated platelet-mimetic liposomal nanoconstruct. *Biomaterials* **34,** 3031–3041 (2013).
55. Hickman, D. A. *et al.* Intravenous synthetic platelet (SynthoPlate) nanoconstructs reduce bleeding and improve ‘ golden hour ’ survival in a porcine model of traumatic arterial hemorrhage. *Sci. Rep.* 1–14 (2018). doi:10.1038/s41598-018-21384-z
56. Shukla, M., Sekhon, U. D. S., Li, W. & Hickman, D. A. In vitro characterization of SynthoPlate (synthetic platelet) technology and its in vivo evaluation in severely thrombocytopenic mice. *J Thromb Haemost* **15,** 375–387 (2016).
57. Lashof-sullivan, M., Sho, A. & Lavik, E. Intravenous hemostats : challenges in translation to patients. *Nanoscale* **5,** 10719–10728 (2013).
58. Szebeni, J. *et al.* Prevention of infusion reactions to PEGylated liposomal doxorubicin via tachyphylaxis induction by placebo vesicles: A porcine model. *J. Control. Release* **160,** 382–387 (2012).
59. Brown, A. C. *et al.* Ultrasoft microgels displaying emergent platelet-like behaviours. *Nat. Mater.* **13,** 1–7 (2014).

60. Niewlarowski, S., Regoeczi, E., Stewart, G. J., Senyi, A. F. & Mustard, J. F. Platelet Interaction with Polymerizing Fibrin. **51,** 685–700 (1972).
61. Welsch, N., Brown, A. C., Barker, T. H. & Lyon, L. A. Colloids and Surfaces B : Biointerfaces Enhancing clot properties through fibrin-specific self-cross-linked PEG side-chain microgels. *Colloids Surfaces B Biointerfaces* **166,** 89–97 (2018).
62. Lorand, L. A double-headed Gly-Pro-Arg-Pro ligand mimics the functions of the E domain of fibrin for promoting the end-to-end crosslinking of chains by factor XIII a. **95,** 537–541 (1998).
63. Soon, A. S. C., Lee, C. S. & Barker, T. H. Modulation of fibrin matrix properties via knob:hole affinity interactions using peptide-PEG conjugates. *Biomaterials* **32,** 4406–4414 (2011).
64. Kolodziej, A. F. *et al.* Fibrin Specific Peptides Derived by Phage Display: Characterization of Peptides and Conjugates for Imaging. *Bioconjug. Chem.* **23,** 548–556 (2012).
65. Kolodziej, A. F., Zhang, Z., Overoye-chan, K., Jacques, V. & Caravan, P. Peptide Optimization and Conjugation Strategies Magnetic Resonance Imaging Contrast Agents. **1088,** 185–211
66. Chan, L. W. *et al.* A synthetic fibrin cross-linking polymer for modulating clot properties and inducing hemostasis. *Sci. Transl. Med.* **7,** (2015).
67. Chiefari, J. *et al.* Living Free-Radical Polymerization by Reversible Addition - Fragmentation Chain Transfer : The RAFT Process We wish to report a new living free-radical polymer- ization of exceptional effectiveness and versatility . 1 The living character is conferred by . **9297,** 5559–5562 (1998).
68. Chu, D. S. H. *et al.* Application of living free radical polymerization for nucleic acid delivery. *Acc. Chem. Res.* **45,** 1089–1099 (2012).
69. Kopeček, J., Kopečková, P., Minko, T., Lu, Z. R. & Peterson, C. M. Water soluble polymers in tumor targeted delivery. *J. Control. Release* **74,** 147–158 (2001).
70. Barrett, G. D., Constable, I. J. & Stewart, A. D. Clinical results of hydrogel lens implantation. *J. Cataract Refract. Surg.* **12,** 623–631 (1986).
71. Chan, L. W., White, N. J. & Pun, S. H. A Fibrin Cross-linking Polymer Enhances Clot Formation Similar to Factor Concentrates and Tranexamic Acid in an in Vitro Model of

Coagulopathy. *ACS Biomater. Sci. Eng.* (2016). doi:10.1021/acsbiomaterials.5b00536

72. Maegele, M. *et al.* Early coagulopathy in multiple injury: An analysis from the German Trauma Registry on 8724 patients. *Injury* **38,** 298–304 (2007).
73. 6 Factor VIII Concentrates, Factor VIII/von Willebrand Factor Concentrates, Factor IX Concentrates, Activated Prothrombin Complex Concentrates. *Transfus. Med. Hemotherapy* **36,** 409–418 (2009).
74. Okamura, Y. *et al.* Development of fibrinogen c-chain peptide-coated, adenosine diphosphate-encapsulated liposomes as a synthetic platelet substitute. *J Thromb Haemost* **7,** 470–477 (2009).
75. Fasting, C. *et al.* Multivalency as a Chemical Organization and Action Principle. *Angew. Rev.* **51,** 10472–10498 (2012).
76. Spain, S. G. & Cameron, N. R. A spoonful of sugar : the application of glycopolymers in therapeutics. *Polym. Chem.* **2,** 60–68 (2011).
77. Weigandt, K. M., Pozzo, D. C. & Porcar, L. Structure of high density fibrin networks probed with neutron scattering and rheology. *Soft Matter* **5,** 4321–4330 (2009).
78. Weigandt, K. M., Porcar, L. & Pozzo, D. C. In situ neutron scattering study of structural transitions in fibrin networks under shear deformation. *Soft Matter* **7,** 9992–10000 (2011).
79. Yanjarappa, M. J., Gujraty, K. V, Joshi, A., Saraph, A. & Kane, R. S. Synthesis of Copolymers Containing an Active Ester of Methacrylic Acid by RAFT : Controlled Molecular Weight Scaffolds for Biofunctionalization. *Biomacromolecules* **7,** 1665–1670 (2006).
80. Kirby, N. M. *et al.* research papers A low-background-intensity focusing small-angle X-ray scattering undulator beamline. 1670–1680 (2013). doi:10.1107/S002188981302774X
81. Hammouda, B., Ho, D. L. & Kline, S. Insight into Clustering in Poly (ethylene oxide) Solutions. *Macromolecules* **37,** 6932–6937 (2004).
82. Glinka, C. J. *et al.* The 30 m Small-Angle Neutron Scattering Instruments at the National Institute of Standards and Technology. *J. Appl. Crystallogr.* **31,** 430–445 (1998).
83. Kline, S. R. Reduction and analysis of SANS and USANS data using IGOR Pro. *J. Appl. Crystallogr.* **39,** 895–900 (2006).
84. Barker, J. G. *et al.* Design and performance of a thermal-neutron double-crystal diffractometer for USANS at NIST. *J. Appl. Crystallogr.* **38,** 1004–1011 (2005).

85. Terech, P. Structural Study of Cholesteryl Anthraquinone-2-carboxylate (CAQ) Physical Organogels by Neutron and X-ray Small Angle Scattering. *J. Phys. Chem.* **100,** 3759–3766 (1996).
86. Teixeira, J. Small-Angle Scattering by Fractal Systems. *J. Appl. Crystallogr.* **21,** 781–785 (1988).
87. Hammouda, B. & Horkay, F. Clustering and Solvation in Poly(acrylic acid) Polyelectrolyte Solutions. *Macromolecules* **38,** 2019–2021 (2005).
88. Dowling, M. B. *et al.* Biomaterials A self-assembling hydrophobically modi fi ed chitosan capable of reversible hemostatic action. *Biomaterials* **32,** 3351–3357 (2011).
89. Laudano, A. P. & Doolittle, R. F. Studies on synthetic peptides that bind to fibrinogen and prevent fibrin polymerization. Structural requirements, number of binding sites, and species differences. *Biochemistry* **19,** 1013–1019 (1980).
90. Lukyanov, A. N. & Torchilin, V. P. Micelles from lipid derivatives of water-soluble polymers as delivery systems for poorly soluble drugs. **56,** 1273–1289 (2004).
91. Rizvi, S. A. A. & Saleh, A. M. Applications of nanoparticle systems in drug delivery technology. *Saudi Pharm. J.* **26,** 64–70 (2018).
92. Kieler-ferguson, H. M. & Fr, J. M. J. Clinical developments of chemotherapeutic nanomedicines : polymers and liposomes for delivery of camptothecins and platinum (II). **5,** (2013).
93. Press, D. Effective use of nanocarriers as drug delivery systems for the treatment of selected tumors. 7291–7309 (2017).
94. Langer, R. Drug delivery and targeting. **392,** 5–10 (1998).
95. Montet, X., Funovics, M., Montet-abou, K., Weissleder, R. & Josephson, L. Multivalent Effects of RGD Peptides Obtained by Nanoparticle Display. 6087–6093 (2006). doi:10.1021/jm060515m
96. Lee, H., Fonge, H., Hoang, B., Reilly, R. M. & Allen, C. articles The Effects of Particle Size and Molecular Targeting on the Intratumoral and Subcellular Distribution of Polymeric Nanoparticles. **7,** 1195–1208 (2010).
97. Lamm, R. J. *et al.* Peptide valency plays an important role in the activity of a synthetic fibrin-crosslinking polymer. *Biomaterials* **132,** 96–104 (2017).
98. Devlin, J., Panganiban, L. & Devlin, P. Random peptide libraries: a sourse of specific

protein binding molecules. *Science (80-.).* **249,** 404–406 (1990).

99. Fan, S. *et al.* Curcumin-loaded PLGA-PEG nanoparticles conjugated with B6 peptide for potential use in Alzheimer ' s disease. *Drug Deliv.* **25,** 1044–1055 (2018).
100. Duvall, C. L., Convertine, A. J., Benoit, D. S. W., Hoffman, A. S. & Stayton, P. S. articles Intracellular Delivery of a Proapoptotic Peptide via Conjugation to a RAFT Synthesized Endosomolytic Polymer. (2010).
101. Chu, D. S. *et al.* As featured in : Biomaterials Science. (2015). doi:10.1039/c4bm00259h
102. Johnson, R. N. *et al.* Synthesis of Statistical Copolymers Containing Multiple Functional Peptides for Nucleic Acid Delivery. *Biomacromolecules* **11,** 3007–13 (2010).
103. Chu, D. S. H., Schellinger, J. G., Bocek, M. J., Johnson, R. N. & Pun, S. H. Optimization of Tet1 ligand density in HPMA-co-oligolysine copolymers for targeted neuronal gene delivery. *Biomaterials* **34,** 9632–9637 (2013).
104. Schellinger, J. G. *et al.* Melittin-grafted HPMA-oligolysine based copolymers for gene delivery. *Biomaterials* **34,** 2318–2326 (2013).
105. Kanaide, H. & Shainoff, J. R. Cross-linking of fibrinogen and fibrin by fibrin-stabilizing factor (factor XIIIa). *Transl. Res.* **85,** 574–597 (1975).
106. O'Brien-Simpson, N. M., Ede, N. J., Brown, L. E., Swan, J. & Jackson, D. C. Polymerization of unprotected synthetic peptides: A view toward synthetic peptide vaccines. *J. Am. Chem. Soc.* **119,** 1183–1188 (1997).
107. Hasson, C. J., Caldwell, G. E. & Emmerik, R. E. A. Van. NIH Public Access. *Motor Control* **27,** 590–609 (2009).
108. Studenovská, H., Šlouf, M. & Rypáček, F. Poly(HEMA) hydrogels with controlled pore architecture for tissue regeneration applications. *J. Mater. Sci. Mater. Med.* **19,** 615–621 (2008).
109. Kopeckova, P. Water soluble polymers in tumor targeted delivery. *J. Control. Release* **74,** 147–158 (2001).
110. Cunningham, V. J. *et al.* Poly(glycerol monomethacrylate) − Poly(benzyl methacrylate) Diblock Copolymer Nanoparticles via RAFT Emulsion Polymerization: Synthesis, Characterization, and Interfacial Activity. (2014). doi:10.1021/ma501140h
111. Save, M., Weaver, J. V. M., Armes, S. P. & Mckenna, P. Atom Transfer Radical Polymerization of Hydroxy-Functional Methacrylates at Ambient Temperature:

Comparison of Glycerol Monomethacrylate with 2-Hydroxypropyl Methacrylate. 1152–1159 (2002). doi:10.1021/ma011541r

112. Das, D. *et al.* RAFT polymerization of ciprofloxacin prodrug monomers for the controlled intracellular delivery of antibiotics. *Polym. Chem* **7,** 826–837 (2016).
113. Shin, H. C., Alani, A. W. G., Rao, D. A., Rockich, N. C. & Kwon, G. S. Multi-drug loaded polymeric micelles for simultaneous delivery of poorly soluble anticancer drugs. *J. Control. Release* **140,** 294–300 (2009).
114. Hughes, H. C. Swine in cardiovascular research. *Lab Anim. Sci.* **36,** 348–350 (1986).
115. Swindle, M. M., Makin, A., Herron, A. J., Clubb, F. J. & Frazier, K. S. Swine as Models in Biomedical Research and Toxicology Testing. *Vet. Pathol.* **49,** 344–356 (2012).
116. Pusateri, A. E. *et al.* Effect of a Chitosan-Based Hemostatic Dressing on Blood Loss and Survival in a Model of Severe Venous Hemorrhage and Hepatic Injury in Swine. *J trauma* **54,** 177–182 (2003).
117. Pusateri, A. E. *et al.* Advanced Hemostatic Dressing Development Program : Animal Model Selection Criteria and Results of a Study of Nine Hemostatic Dressings in a Model of Severe Large Venous Hemorrhage and Hepatic Injury in Swine. *J Trauma* **55,** 518–526 (2003).
118. Stern, S. *et al.* RESUSCITATION WITH THE HEMOGLOBIN-BASED OXYGEN CARRIER , HBOC-201 , IN A SWINE MODEL OF SEVERE UNCONTROLLED HEMORRHAGE AND TRAUMATIC BRAIN INJURY. *Shock* **31,** 64–79 (2009).
119. White, N. J., Wang, X., Liles, W. C. & Stern, S. Fibrinogen Concentrate Improves Survival During Limited Resuscitation of Uncontrolled Hemorrhagic Shock in a Swine Model. *Shock* **42,** 456–463 (2014).
120. Szebeni, J., Bed, P. & Rozsnyay, Z. Liposome-induced complement activation and related cardiopulmonary distress in pigs : factors promoting reactogenicity of Doxil and AmBisome. **8,** 176–184 (2012).
121. Szebeni, J. *et al.* A porcine model of complement-mediated infusion reactions to drug carrier nanosystems and other medicines ☆. **64,** 1706–1716 (2012).
122. Bertram, J. P. *et al.* Intravenous Hemostat : Nanotechnology to Halt Bleeding. (2009).
123. Boldt, J., Haisch, G., Suttner, S., Kumle, B. & Schellhaass, A. Effects of a new modifed, balanced hydroxyethyl starch preparation (Hextend). *Br. J. Anaesth.* **89,** 722–728 (2002).

124. Landskroner, K., Olson, N. & Jesmok, G. Cross-species pharmacologic evaluation of plasmin as a direct-acting thrombolytic agent: Ex vivo evaluation for large animal model development. *J. Vasc. Interv. Radiol.* **16,** 369–377 (2005).
125. Mitterlechner, T. *et al.* Prothrombin complex concentrate and recombinant prothrombin alone or in combination with recombinant factor X and FVIIa in dilutional coagulopathy: A porcine model. *J. Thromb. Haemost.* **9,** 729–737 (2011).
126. R. Baylis, J. *et al.* Rapid hemostasis in a sheep model using particles that propel thrombin and tranexamic acid. *Laryngoscope* **127,** 787–793 (2017).
127. Ngambenjawong, C., Gustafson, H. H., Sylvestre, M. & Pun, S. H. A Facile Cyclization Method Improves Peptide Serum Stability and Confers Intrinsic Fluorescence. *ChemBioChem* **18,** 2395–2398 (2017).
128. Von Maltzahn, G. *et al.* Nanoparticles that communicate in vivo to amplify tumour targeting. *Nat. Mater.* **10,** 545–552 (2011).
129. Liu, G. W. *et al.* Glomerular disease augments kidney accumulation of synthetic anionic polymers. *Biomaterials* **178,** 317–325 (2018).
130. Tabata, Y. & Ikada, Y. Effect of the size and surface charge of polymer microspheres on their phagocytosis by macrophage. *Biomaterials* **9,** 356–362 (1988).
131. Caliceti, P. & Veronese, F. P harmacokinetic and biodistribution properties of poly(ethylene glycol)–protein conjugates Paolo. *Adv. Drug Deliv. Rev.* **55,** 1261–1277 (2003).
132. Beier, J. I. *et al.* Fibrin accumulation plays a critical role in the sensitization to lipopolyccharide-induced liver injury caused by ethanol in mice. *Hepatology* **49,** 1545–1553 (2009).
133. Imokawa, S. *et al.* Tissue factor expression and fibrin deposition in the lungs of patients with idiopathic pulmonary fibrosis and systemic sclerosis. *Am. J. Respir. Crit. Care Med.* **156,** 631–636 (1997).
134. Brown, L. F., Dvorak, A. M. & Dvorak, H. F. Leaky vessels, fibrin deposition, and fibrosis: a sequence of events common to solid tumors and to many other types of disease. *Am. Rev. Respir. Dis.* **140,** 1104–7 (1989).
135. Hiramoto, R., Bernecky, J., Jurandowski, J. & Pressman, D. Fibrin in Human Tumors. *Cancer Res.* **20,** 592–593 (1960).

136. Fernandez, P. M., Patierno, S. R. & Rickles, F. R. Tissue factor and fibrin in tumor angiogenesis. *Semin. Thromb. Hemost.* **30,** 31–44 (2004).
137. Wallace, A. C. Demonstration of Fibrin in Early Stages of Experimental Metastases. *Cancer Res.* **36,** 1904–1909 (1976).
138. Dirix, L. Y. *et al.* Plasma fibrin D-dimer levels correlate with tumour volume, progression rate and survival in patients with metastatic breast cancer. *Br. J. Cancer* **86,** 389–395 (2002).
139. Chu, D. S. *et al.* MMP9-sensitive polymers mediate environmentally-responsive bivalirudin release and thrombin inhibition. *Biomater. Sci.* **3,** 41–45 (2015).
140. Warkentin, T. E., Greinacher, A. & Koster, A. Bivalirudin. *Thromb. Haemost.* **99,** 830–839 (2008).
141. Hejna, M., Raderer, M. & Zielinski, C. C. Inhibition of metastases by anticoagulants. *J. Natl. Cancer Inst.* **91,** 22–36 (1999).
142. Amirkhosravi, A. *et al.* Tissue factor pathway inhibitor reduces experimental lung metastasis of B16 melanoma. *Thromb. Haemost.* **87,** 930–936 (2002).
143. Kondapaka, S. B., Fridman, R. & Reddy, K. B. Epidermal growth factor and amphiregulin up-regulate matrix metalloproteinase-9 (MMP-9) in human breast cancer cells. *Int. J. Cancer* **70,** 722–726 (1997).
144. Svendsen, L., Blombäck, B., Blombäck, M. & Olsson, P. I. Synthetic chromogenic substrates for determination of trypsin, thrombin and thrombin-like enzymes. *Thromb. Res.* **1,** 267–278 (1972).
145. Reinhard, J., Brösicke, N., Theocharidis, U. & Faissner, A. The extracellular matrix niche microenvironment of neural and cancer stem cells in the brain. *Int. J. Biochem. Cell Biol.* **81,** 174–183 (2016).
146. Palumbo, J. S. *et al.* Platelets and fibrin(ogen) increase metastatic potential by impeding natural killer cell-mediated elimination of tumor cells. *Blood* **105,** 178–185 (2005).
147. Ogston, A. OGSTON, M.D., Surgeon. *J. Anat.* **16,** 526–567 (1882).
148. Lowry, F. D. Staphylococcus aureus Infections. *N. Engl. J. Med.* **339,** 520–532 (1998).
149. Lake, J. G. *et al.* Pathogen distribution and antimicrobial resistance among pediatric healthcare-associated infections reported to the National Healthcare Safety Network, 2011-2014. *Infect. Control Hosp. Epidemiol.* **39,** 1–11 (2018).

150. Weiner, L. M. *et al.* Antimicrobial-Resistant Pathogens Associated with Healthcare-Associated Infections: Summary of Data Reported to the National Healthcare Safety Network at the Centers for Disease Control and Prevention, 2011-2014. *Infect. Control Hosp. Epidemiol.* **37,** 1288–1301 (2016).
151. Lee, A. S. *et al.* Methicillin-resistant Staphylococcus aureus. *Nat. Rev. Dis. Prim.* **4,** (2018).
152. Jevons, P. M. 'Celbenin'-resistant Staphylococci. *Br. Med. J.* **1,** 124–125 (1961).
153. Hiramatsu, K. *et al.* Methicillin-resistant Staphylococcus aureus clinical strani with reduced vancomycin susceptibility. *J. Antimicrob. Chemother.* **40,** 135–146 (1997).
154. Huh, A. J. & Kwon, Y. J. 'Nanoantibiotics': A new paradigm for treating infectious diseases using nanomaterials in the antibiotics resistant era. *J. Control. Release* **156,** 128–145 (2011).
155. Loughman, A. *et al.* Roles for fibrinogen, immunoglobulin and complement in platelet activation promoted by Staphylococcus aureus clumping factor A. *Mol. Microbiol.* **57,** 804–818 (2005).
156. Mcdevitt, D. *et al.* Characterization of the interaction between the Staphylococcus aureus clumping factor (ClfA) and fibrinogen. *Eur. J. Biochem.* **247,** 416–424 (1997).
157. Que, Y. *et al.* Reassessing the Role of Staphylococcus aureus Clumping Factor and Fibronectin-Binding Protein by Expression in Lactococcus. *Infect. Immun.* **69,** 6296–6302 (2001).
158. Patti, J. M. A humanized monoclonal antibody targeting Staphylococcus aureus. *Vaccine* **22,** (2004).
159. Takeoka, S. *et al.* Function of fibrinogen gamma-chain dodecapeptide-conjugated latex beads under flow. *Biochem. Biophys. Res. Commun.* **312,** 773–9 (2003).
160. Okamura, Y. *et al.* Hemostatic effects of fibrinogen gamma-chain dodecapeptide-conjugated polymerized albumin particles in vitro and in vivo. *Transfusion* **45,** 1221–8 (2005).
161. Okamura, Y., Maekawa, I., Teramura, Y., Maruyama, H. & Handa, M. Hemostatic Effects of Phospholipid Vesicles Carrying Fibrinogen γ Chain Dodecapeptide in Vitro and in Vivo. 30–33 (2005).
162. Pease, D. C. An Electron Microscopy Study of Red Bone Marrow. *Blood* **11,** 501–526

(1956).

163. Wagner, B. C. L. *et al.* Analysis of GPIIb/IIIa Receptor Number by Quantification of 7E3 Binding to Human Platelets. (2015).
164. Nilsson, I. M., Patti, J. M., Bremell, T., Höök, M. & Tarkowski, A. Vaccination with a recombinant fragment of collagen adhesin provides protection against Staphylococcus aureus-mediated septic death. *J. Clin. Invest.* **101,** 2640–2649 (1998).
165. Stevens, K. A., Sheldon, B. W., Klapes, N. A. & Klaenhammer, T. R. Nisin treatment for inactivation of Salmonella species and other gram- negative bacteria. *Appl. Environ. Microbiol.* **57,** 3613–3615 (1991).
166. Millette, M., Le Tien, C., Smoragiewicz, W. & Lacroix, M. Inhibition of Staphylococcus aureus on beef by nisin-containing modified alginate films and beads. *Food Control* **18,** 878–884 (2007).
167. Hancock, R. E. W. Peptide antibiotics. *Lancet* **349,** 418–422 (1997).
168. Biscola, V. *et al.* Isolation and characterization of a nisin-like bacteriocin produced by a Lactococcus lactis strain isolated from charqui, a Brazilian fermented, salted and dried meat product. *Meat Sci.* **93,** 607–613 (2013).
169. Miao, J. *et al.* Membrane disruption and DNA binding of Staphylococcus aureus cell induced by a novel antimicrobial peptide produced by Lactobacillus paracasei subsp. tolerans FX-6. *Food Control* **59,** 609–613 (2016).

3.8 SUPPLEMENTAL

Table 3.S2. Peptide valency is controlled by molar ratio of peptide to NHS-groups during conjugation

Batch No.	Peptide:NHS Molar Feed	Peptide Valency (mean + S.D.)
1	1.5	10.29 ± 0.11
1	1.0	7.89 ± 0.48
2	1.0	8.8 ± 0.61
1	0.5	4.19 ± 0.13
2	0.5	4.1 ± 0.15
1	0.25	2.9 ± 0.09
1	0.1	1.43 ± 0.09
1	0.0	0.27 ± 0.04

Table 3.S3. Concentrations of PolySTAT in SANS experiments

Condition	Concentration in clot (mg/mL)
PS-0	0.833
PS-2	1.57
PS-4	1.52
PS-7	1.11

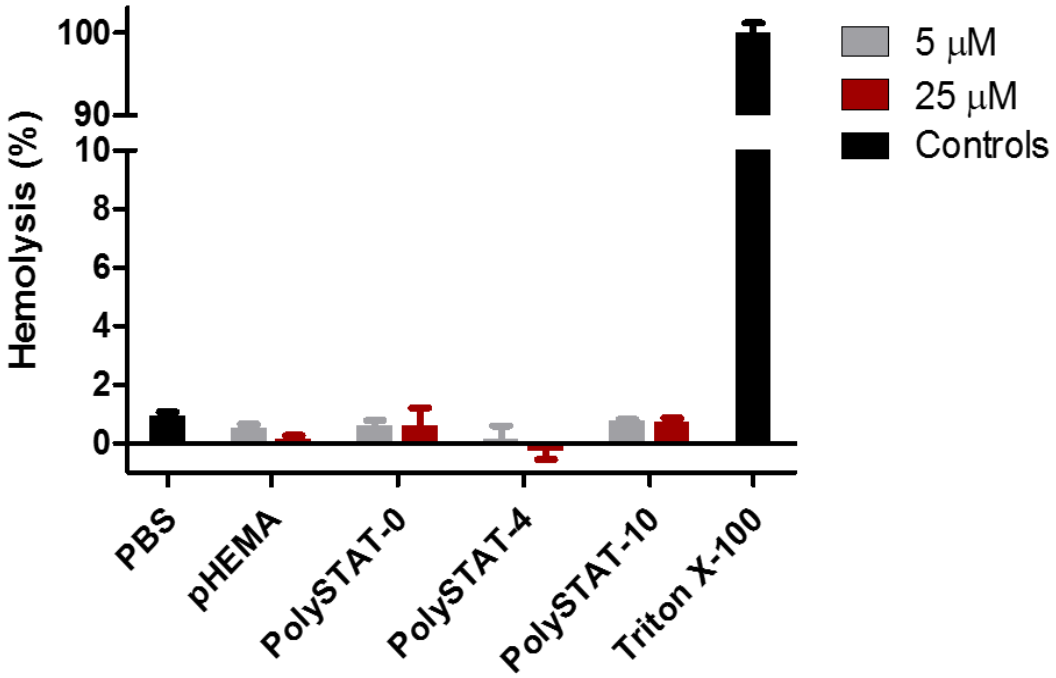

Figure 3.S1. Hemolysis activity of PolySTAT. The polymer backbone as well as PolySTAT with a range of peptide valencies were found to be non-lytic to blood cells, suggesting hemocompatibility. The concentrations were chosen to reflect the *in vivo* dose of 15 mg/kg (5.2 μM) as well as an excess concentration nearly 5-times greater than the *in vivo* dose (25μM). Red blood cells were incubated for 1 h at 37 °C and lysis was determined by absorbance at 451 nm. PBS was included as a negative control and Triton X-100 as a positive control. Values are presented as mean and standard deviation.

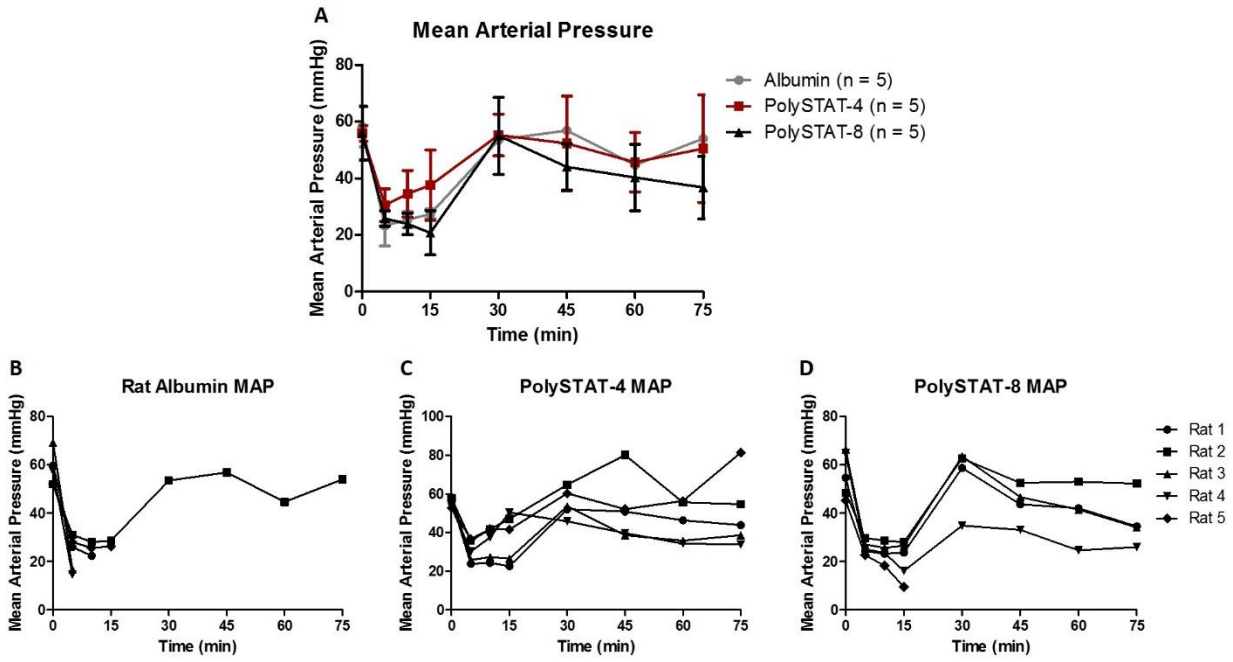

Figure 3.S2. Mean arterial pressures of animals during femoral artery injury and resuscitation model. (A) All treatments. Values are presented as mean and standard deviation for surviving animals at each time point. **(B-D)** Mean arterial pressure lactate for individual animals treated with rat albumin **(B)**, PolySTAT-4 **(C)**, and PolySTAT-8 **(D)**.

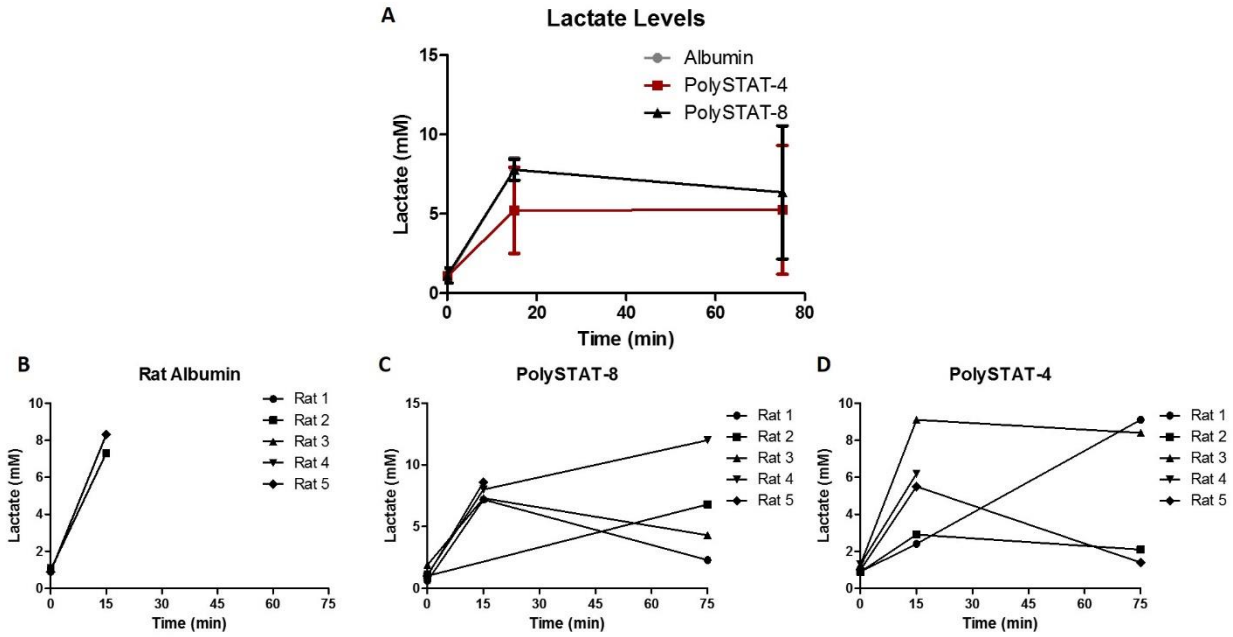

Figure 3.S3. Blood lactate concentrations of animals during femoral artery injury and resuscitation model. **(A)** All treatments. Values are presented as mean and standard deviation for surviving animals at each time point. **(B-D)** Blood lactate for individual animals treated with rat albumin **(B)**, PolySTAT-4 **(C)**, and PolySTAT-8 **(D)**.

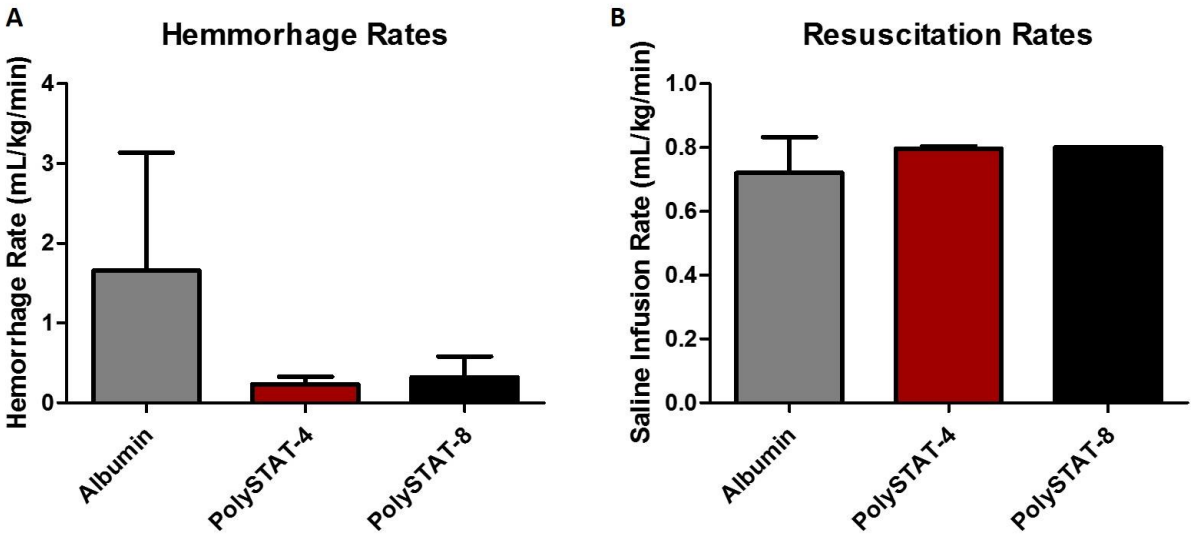

Figure 3.S4. Hemorrhage (A) and resuscitation (B) rates of animals during femoral artery injury and resuscitation model.

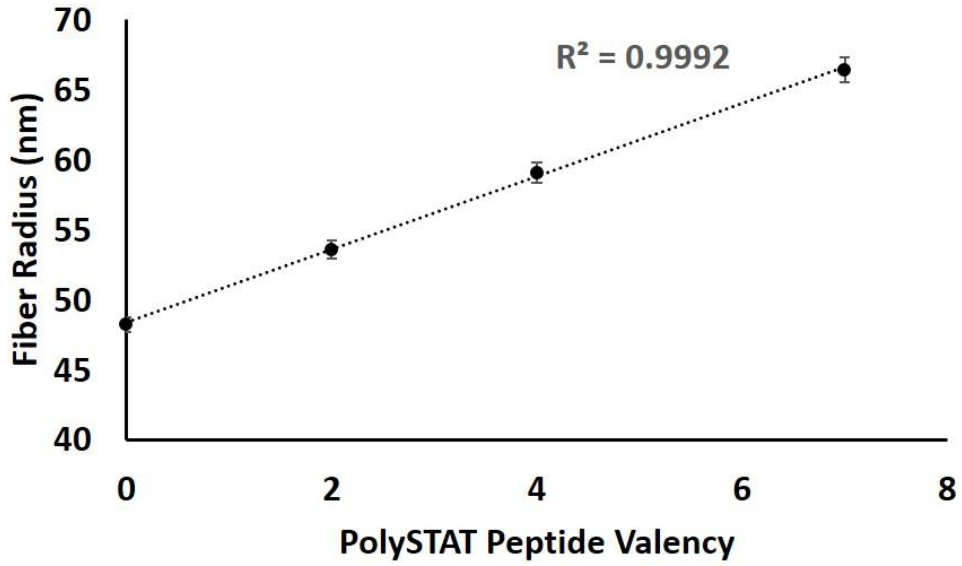

Figure 3.S5. Fibrin fiber radius from Guinier fits. Radius trends with strong correlation to PolySTAT peptide valency.

CHAPTER 4: IMPROVED WATER SOLUBILITY AND SYNTHETIC EFFICIENCY OF A FIBRIN-CROSSLINKING POLYMER

Robert J. Lamm, Frederick Huyan, Alexander N. Prossnitz, Karl Manner,

Nathan J. White, Suzie H. Pun

4.1 INTRODUCTION

Two chief goals of drug delivery systems are to confer water solubility to drugs and multivalency to targeting components. For example, researchers in nanotechnology improved the formulation of poorly soluble chemotherapeutics for treatment by encapsulating such molecules in micelles[90], nanoparticles[91], polymersomes[92], and liposomes[92,93]. In addition, delivery systems can be functionalized for active cell targeting by attaching moieties with high affinities for a receptor of interest[94]. Some targeting ligands, such as antibodies, have extremely high affinities for their target; lower affinity targeting ligands, such as peptides, can benefit from the display of multiple copies of the ligand, or multivalency, which results in an effective increase in the association of the nanocarrier to the target[95]. Modulation of multivalency not only changes the avidity of the carrier to a target, but can lead to changes in the function of nanocarriers[46,96,97]. A current downside to active targeting is that targeting ligands add complexity and additional steps in the synthesis of nanocarriers.

Polymeric drug delivery systems have proven highly promising for their ability to confer water solubility and valency via a synthetic backbone. Synthetic materials have the benefit of prolonged storage conditions and stability. With controlled radical polymerization, synthetic polymers can be made with desired molecular weights and monodisperse populations[67,68]. Polymers may improve biodistribution due to prolonged circulation properties over nanoparticles when of the correct size and composition[69], making them attractive for use in biomedical applications.

Peptides provide complementary attributes to polymers in drug delivery systems. Peptides retain much of the chemical and functional diversity of proteins, notably in their ability to bind proteins[98]. Peptides can be synthesized easily by solid-phase Fmoc peptide synthesis, and their incorporation into materials yields functionality while not greatly affecting base material characteristics conferred by larger polymers. Thus, peptide-polymer conjugates are fully synthetic materials that can be easily engineered for the delivery of a wide array of therapeutics including small molecules[99], peptides[100,101], and nucleic acids[102–104].

We have previously reported the use of a therapeutic peptide-polymer conjugate, deemed PolySTAT, as a potential treatment for hemorrhage, or uncontrolled bleeding[66]. PolySTAT consists of a poly(hydroxylethyl methacrylate) (pHEMA) backbone decorated with fibrin-binding

peptides (FBPs). This simple design is effective in promoting hemostasis by crosslinking fibrin at the wound site in a fashion similar to that of factor XIIIa (FXIIIa); fibrin clots are naturally crosslinked in the body via covalent bonds catalyzed by FXIIIa's transglutaminase activity[105]. PolySTAT enhances hemostasis similar to recombinant factor VIIa, commercially known as NovoSeven® and exhibits similar antifibrinolytic capabilities as tranexamic acid, a drug that is currently widely investigated in clinical trials[71]. FBP is the active component of PolySTAT, and the valency of FBP must be high enough to confer activity to the material[97]. This is important not only for understanding how material structure affects the material, but also for the cost associated with the treatment. As FBP is the most expensive component of the material, efforts to improve the yield of the peptide incorporated into the material will improve the likelihood of translation for PolySTAT. The direct polymerization of peptides into polymer backbones was a large technological advancement since conjugations can lead to extra protecting/deprotecting steps, or alter the residues of the desired peptide[106]. The use of this strategy has been utilized in drug delivery and yielded high levels of incorporation; our lab, specifically, has incorporated multiple peptides with HPMA for varied uses[104,107]. Here we describe the synthesis of polymerizable FBP monomers and the subsequent direct polymerization approach (Fig 4.1).

While an inactive component in PolySTAT, the HEMA backbone adds complexity to PolySTAT. HEMA is a material commonly used for its hydrophilic and biocompatible nature, however its solubility in water is not very high, reflected by the fact that it forms hydrogels with minimal cross-linking in water[70,108]. This is exacerbated by FBP, which contains many hydrophobic residues and which we have observed to have very poor water solubility without a polymer backbone. Thus, pHEMA is not adequately upholding one of the two chief goals of a drug delivery system, water solubility. To improve solubility in water, peptide monomers were polymerized with comonomers well known to yield hydrophilic, water-soluble polymers. N-(2-Hydroxypropyl) methacrylamide (HPMA) and glycerol monomethacrylate (GmMA) have been utilized in drug delivery systems and were specifically chosen for their water-solubility and hydrophilicity[102–104,109–111].

In this work, we demonstrate improvements in the water solubility of PolySTAT via alternative comonomers and improved synthetic yield both through improved water solubility and a direct polymerization synthesis strategy which decreases synthetic complexity while improving peptide yield.

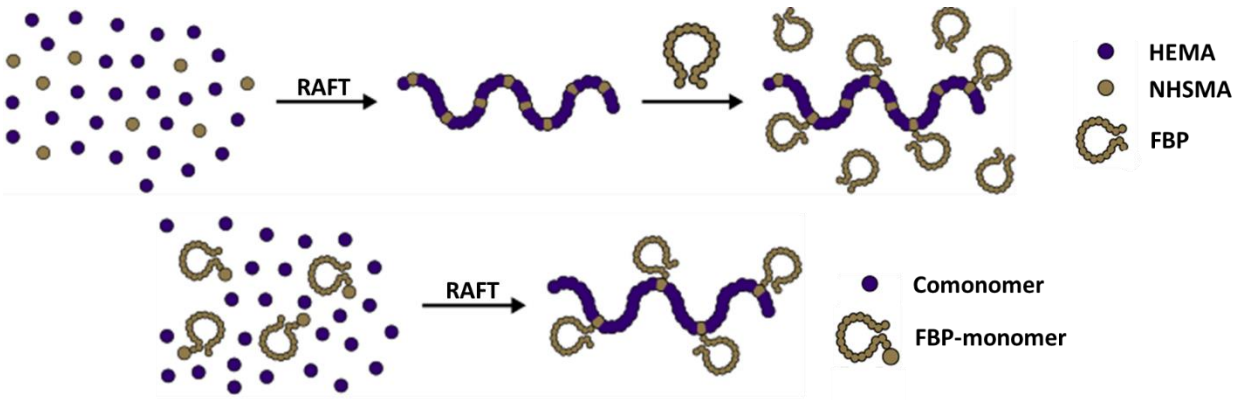

Figure 4.1 Diagram of PolySTAT synthesis strategies. Above, the current approach to synthesizing PolySTAT, which leads to low efficiency of peptide attachment. Below, a new approach to synthesis which utilizes a peptide monomer for direct polymerization of FBP into the backbone.

4.2 Materials and Methods

4.2.1 *Materials*

2,2′-Azobis(2-methylpropionitrile) (AIBN), 4-cyanopentanoic acid dithiobenzoate (CTP), 2-hydroxyethyl methacrylate (HEMA), glycidyl methacrylate (GMA) and all other reagents were purchased from Sigma-Aldrich (Saint Louis, MO) unless noted otherwise. 4-Cyano-4-(ethylsulfanylthiocarbonyl) sulfanyl pentanoic acid (ECT) was a gift from Prof. Tony Convertine (University of Washington, Bioengineering), N-hydroxysuccinimide methacrylate (NHSMA) was purchased from TCI America (Portland, OR). The fibrin binding peptide (FBP; Sequence: Ac-Y(DGl)C(HPr)YGLCYIQGK),[64] developed by the Caravan group, was purchased from GL Biochem (Shanghai, China) as a custom order. Thrombin (Fibri-Prest Automate 5) was purchased from Stago (Asnières sur Seine, France). Fibrinogen and plasmin were purchased from Enzyme Research Laboratories (South Bend, IN).

4.2.2 *Hydrolysis of Glycidyl methacrylate to Glycerol monomethacrylate*

Glycerol monomethacrylate (GmMA) was synthesized via hydrolysis of glycidyl methacrylate (GMA) as described previously for poly(GMA)[110]. GMA (11.4 mL)

was added to DI water (68.6 mL) at a mass ratio of 15% in a two-necked round bottom flask with one neck sealed and a vigreux column in the other. The mixture was sparged with air and stirred at 80 °C for 16 h. The solution was subsequently cooled, and sodium chloride added to a final concentration of 300 mg/mL. GmMA was extracted into an organic phase via 3x washes with 30 mL ethyl acetate. GmMA was isolated by removal of ethyl acetate via rotavap and stored at -20 °C.

4.2.3 *Synthesis of pHEMA and pGmMA*

pHEMA and pGmMA were synthesized via reversible addition-fragmentation chain transfer (RAFT) polymerization as described previously[66]. Briefly, monomer (HEMA or GmMA) was combined with CTP and AIBN at 200:1:0.333 ratio in dimethylacetamide at a monomer concentration of 0.6 M. This mixture was allowed to react for 24 h at 70 °C. PHEMA polymers were subsequently precipitated 2x in diethyl ether with dimethylacetamide as the intermediate solvent. Precipitated polymer was collected by centrifugation at 4500 x g. PGmMA polymers were precipitated in diethyl ether followed by dissolution in dimethylsulfoxide and a second precipitation in acetone. PGmMA polymers were collected by the same method as the pHEMA polymers. Dithiobenzoate groups were removed via an end-capping reaction with 20x molar excess AIBN at 70 °C for 24 hours. Polymers were characterized via gel permeation chromatography (GPC) with static light scattering and refractive index detectors (MiniDawn Treos and OptilabRex, respectively, both Wyatt Technology, Santa Barbara, CA) to determine molecular weight and polydispersity index (PDI). ^{1}H nuclear magnetic resonance (NMR) was utilized to determine conversion of the polymer prior to purification, and composition afterward.

4.2.4 *Polymerization kinetics of p(HEMA-co-NHSMA) and p(GmMA-co-NHSMA)*

Backbone polymers were synthesized as described previously[66,97], where HEMA or GmMA and NHSMA were synthesized as described above with a 40:160:1:0.333 NHSMA:comonomer:CTP:AIBN ratio. A large scale reaction was split into multiple reaction vessels and reactinos were stopped at 2 h, 4 h, 8 h, 12 h, and 24 h. 10 µL

samples of each reaction was combined with 700 µL of deuterated DMSO, and subsequently measured via NMR. Percent conversion was calculated by comparing the ratio of comonomer protons to vinyls at t_0 to the ratio at later time points.

4.2.5 *Synthesis of PolySTAT via conjugation*

PolySTAT was synthesized as described previously[66,97]. Backbones containing HEMA or GmMA and amine-reactive NHSMA were synthesized as described above with a 40:160:1:0.333 NHSMA:comonomer:CTP:AIBN ratio. Polymers were precipitated, end-capped, and characterized as described above. Backbone polymers were decorated with FBP via reaction of the C-terminal lysine in the peptide under organic basic conditions in DMSO at a varying ratios of peptide:NHS with N.N-diisopropylethylamine added at a 5:1 ratio base:peptide[79]. This was allowed to react for 24 h at 50 °C after which unreacted NHSMA groups were capped with 10x molar ratio of 1-amino-2-propanol. Peptide-polymer conjugates were purified by extensive dialysis as follows. First, the product was dialyzed against phosphate-buffered saline (PBS) for 24 h (3 buffer changes, 4 L of buffer) during which a precipitate formed. Contents of the dialysis bag were collected and centrifuged at 4500 x g for 8 min to remove unreacted peptide; the supernatant was collected and moved to a fresh dialysis bag. Dialysis continued for 24 h (3 buffer changes), followed by water for 48 h (6 dialysate changes) to remove PBS salts. Peptide content of materials was determined using the extinction coefficient of FBP and the materials' absorbance at a wavelength of 280 nm using a NanoDrop 2000 UV-Vis spectrophotometer (Thermo Fisher Scientific, Waltham, MA).

4.2.6 *Synthesis of FBP-containing methacrylamide monomer, FBP-methacrylamide*

FBP-methacrylamide was synthesized via reaction of the C-terminal lysine in FBP with NHSMA under organic basic conditions in DMSO at a 1:2 ratio with base added at a 5:1 ratio base:peptide[79]. A common reaction contained 96 mg FBP (100 mg/mL) dissolved in DMSO, 21 mg NHSMA, and 51 µL N,N-diisopropylethylamine. This was reacted for 24 h at 50° C and subsequently precipitated in diethyl ether to remove unreacted NHSMA. Free amines were determined to be not present via ninhydrin

assay. Molecular weight was confirmed via MALDI-ToF (Bruker Autoflex Max, Billerica, Massachusetts). After a proof of concept synthesis, FBP-methacrylamide was subsequently ordered from GL Biochem (Shanghai, China) as a custom order.

4.2.7 *Synthesis of PolySTAT via FBP-methacrylamide*

To first determine optimum chain transfer agent (CTA) and CTA:Intitiator ratio, a degree of polymerization of 200 was targeted by combining HPMA and CTA at a 200:1 ratio in dimethyl sulfoxide (DMSO) and adding AIBN at varying amounts under nitrogen for 24 h at 70 °C. The desired product was purified from unreacted monomer by 2x precipitation in acetone, with DMSO as the intermediate solvent. Precipitated polymer was collected by centrifugation at 4500 x g. Dithiobenzoate and trithiocarbonate groups were removed via an end capping reaction with 20x molar excess AIBN at 70 °C for 24 hours. Polymers were characterized via gel permeation chromatography (GPC) with static light scattering and refractive index detectors (MiniDawn Treos and OptilabRex, respectively, both Wyatt Technology, Santa Barbara, CA) to determine molecular weight and polydispersity index (PDI). ^{1}H nuclear magnetic resonance (NMR) was utilized to determine conversion of the polymer prior to purification, and composition afterward. FBPMA-containing copolymers were synthesized as above, but with a target composition of 8% FBPMA by combining FBPMA and HPMA at a ratio of 16:184:1:0.333 FBPMA:HPMA:CTP:AIBN.

4.2.8 *Synthesis of FBP-containing methacrylate monomer, FBP-methacrylate*

Synthesis of FBP-methacrylate was preceded by synthesis of an NHS-activated mono-2-(Methacryloyloxy)ethyl succinate (SMA) as described previously[112]. 5.95 g SMA Mono-2-(methacryloyloxy)ethyl succinate (26 mmol) was dissolved in 97 mL dichloromethane and cooled on ice, NHS (27 mmol) and DCC (28 mmol) were each added and the mixture reacted under stirring for 16 h at room temperature. The resulting solution was filtered to remove dicyclohexylurea, and the purified NHS-activated SMA (NHS-SMA) was isolated via rotary evaporation.

FBP-methacrylate was synthesized via reaction of the C-terminal lysine in FBP with NHS-SMA under organic basic conditions in DMSO at a 1:2 ratio with base added at a 5:1 ratio base:peptide[79]. A common reaction contained 176 mg FBP (100 mg/mL) dissolved in DMSO, 67 mg NHS-SMA, 94 µL N,N-diisopropylethylamine. This was reacted for 24 h at 50° C and subsequently precipitated in diethyl ether to remove unreacted NHS-SMA. Free amines were determined to be not present via ninhydrin assay.

4.2.9 *Synthesis of PolySTAT via FBP-methacrylate*

Copolymers containing FBP-methacrylate were synthesized similarly to pHEMA and pGmMA. A composition of 5% FBP-methacrylate was targeted by combining FBP-methacrylate and HEMA or GmMA at a ratio of 10:190:1:0.333 FBP-methacrylate:comonomer:CTP:AIBN. Polymers were precipitated, end-capped, and characterized as above.

4.2.10 *Solubility testing*

Solubility of polymers was determined by the absorbance at a wavelength of 650 nm. Polymers were weighed out into a 96 well plate and water or PBS added at a final concentration of 100 mg/mL. Immediately after addition of solvent, the plate was placed in a Tecan Infinite M1000 plate reader (Tecan, Männedorf, Switzerland) and measurements were taken every minute over 2 h.

4.2.11 *ROTEM Characterization of PolySTATs from various synthesis strategies*

ROTEM experiments consisted of 300 µL of clotting solution in a standard ROTEM cup placed in a ROTEM whole blood hemostasis analyzer (ROTEM, Basel, Switzerland). Final concentrations in the ROTEM were 1.5 mg/mL fibrinogen, 0.5 IU/mL thrombin, 4 µg/mL plasmin, 0.1 mmol/L $CaCl_2$, and 5 or 20 µmol/L PolySTAT. Measured parameters in ROTEM included: (i) the clotting time (CT), measured as the time between reagent addition to clot formation; (ii) α-angle, which reflects the rate of clot formation, (iii) the maximum clot firmness (MCF), the highest strength observed for the clot, (iv) the lysis index-30 minutes (LI-30), the percentage

of MCF retained 30 minutes after initiation of clot formation, and (v) maximum lysis (ML), the percentage of clot strength lost compared to the MCF at the end of analysis.

4.3 RESULTS

4.3.1 *Monomer Synthesis*

FBP-methacrylamide monomers were successfully synthesized as confirmed by MALDI-ToF with a MW of 1,692 Da. Methacrylamide-containing monomers were purified to > 95% by high performance liquid chromatography. FBP-methacrylate was successfully synthesized with a MW of 1,836 Da by MALDI-ToF. NMR confirmed presence of vinyl peaks for both molecules.

4.3.2 *Methacrylamide Polymer Synthesis*

FBP-methacrylamide was found to polymerize slowly in organic solvents (Fig. 4.2). Purely methacrylamide polymers showed greatest conversion with ECT as the chain transfer agent (CTA); however, low CTA:initiator ratios were necessary to achieve > 80% conversion. 48 h polymerizations with CTP as the CTA improved conversion, however there are concerns of control of such reactions due to increased opportunities for termination events. Notably, a copolymerization of HEMA and FBP-methacrylamide yielded conversion > 90%.

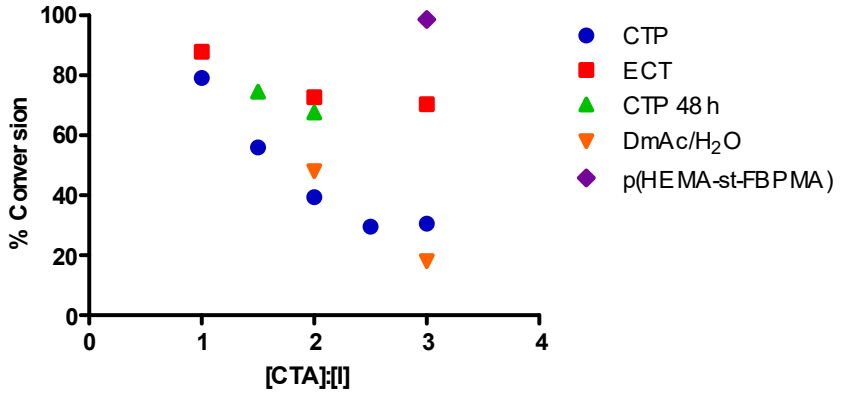

Figure 4.2 Polymer conversion at different CTA:initiator ratios of FBP-methacrylamide in organic solvents. Kinetics measurement were taken by NMR for FBP-methacrylamide polymerizations with HPMA p(HPMA-st-FBPMA). Polymerizations were performed in DMSO for optimal FBP solubility.

Table 4.1 Reaction conditions for FBP-methacrylamide synthesis.

Monomer	CTA	Initiator	Solvent	Concentration (M)	CTA:I	Time (h)	Conversion (%)	Control	FBP/polymer
HPMA	CTP	AIBN	DMSO	2	1	24	80	Poor	-
HPMA	CTP	AIBN	DMSO	2	1.5	24	56	-	-
HPMA	CTP	AIBN	DMSO	2	1.5	48	74	-	-
HPMA	CTP	AIBN	DMSO	2	2	24	39	-	-
HPMA	CTP	AIBN	DMSO	2	2	48	67	-	-
HPMA	CTP	AIBN	DMSO	2	2.5	24	29	-	-
HPMA	CTP	AIBN	DMSO	2	3	24	30	-	-
HPMA	CTP	AIBN	$DmAc/H_2O$	2	2	24	18	-	-
HPMA	CTP	AIBN	$DmAc/H_2O$	2	3	24	48	-	-
HPMA	ECT	AIBN	DMSO	2	1	24	70	Okay	-
HPMA	ECT	AIBN	DMSO	2	2	24	75	Good	-
HPMA	ECT	AIBN	DMSO	2	3	24	87	Good	-
HEMA-st-FBPMA	CTP	AIBN	DmAc	2	3	24	98	-	TBD
HPMA-st-FBPMA	CTP	AIBN	DMSO	2	1	24	80	Poor	13

4.3.3 *Methacrylate Polymer Synthesis*

Copolymers of HEMA and FBP-methacrylate resulted in polymers poorly soluble in DMSO. Copolymers of GmMA and FBP-methacrylate were synthesized successfully. These reactions achieved >90% conversion by NMR with 4.6 peptides per polymer achieved from a target of 5 s determined by UV-Vis. MW by MALDI-ToF shows a median m/z of 43,821.

4.3.4 *Solubility of pHEMA, pGmMA, p(HEMA-co-FBP) and p(GmMA-co-FBP)*

Turbidity, assessed by absorbance at 650 nm, was used to observe the solubility of polymers in phosphate buffered saline (PBS) and water[113]. Homopolymers of HEMA and GmMA showed a large difference in solubility; after 40 minutes absorbance was greater than 0.4 arbitrary units for HEMA polymers in both aqueous solvents, whereas pGmMA absorbance was less than 0.2 arbitrary units by 20 minutes in both solvents (Fig. 4.3). This difference was decreased for peptide-conjugated polymers. However, there was a statistically significant difference in absorbance between HEMA-based material and GmMA-based material ($p < 0.001$). The difference between GmMA-based PolySTAT and pure PBS was also significant ($p < 0.01$).

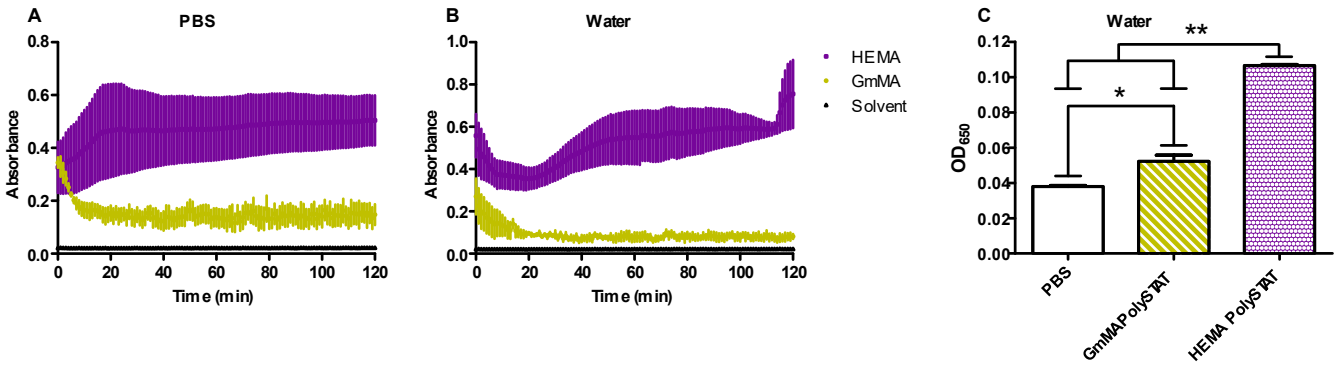

Figure 4.3 Solubility of HEMA and GmMA polymers. Absorbance measurements at a wavelength of 650 nm were taken to measure solubility of polymers in water and pH 7.4 PBS. A, solubility kinetics of pHEMA (purple squares) and pGmMMA (gold circles) over 2 hours in PBS. Black triangles indicate solvent only measurement. B, solubility kinetics of pHEMA (purple squares) and pGmMA (gold circles). C, Absorbance at 650 nm for GmMA-based and HEMA-based PolySTAT after 1 h in water. Differences determined by one-way ANOVA with Tukey Post-Hoc (*, $p < 0.01$; **, $p < 0.001$).

4.3.5 *Polymerization kinetics of p(HEMA-co-NHSMA) and p(GmMA-co-NHSMA) for peptide-grafted polymers*

Copolymers containing NHSMA and either HEMA or GmMA polymerized to >80% conversion over 24 h at a CTA:I ratio of 3:1. P(GmMA-co-NHSMA) polymerized slightly slower than p(HEMA-co-NHSMA) and NHSMA was used up slightly faster when polymerizing with GmMA than HEMA. These backbone polymers were used to synthesize PolySTAT containing FBP at two different peptide valencies, HEMA-based materials had 13 peptides per polymer and GmMA-based materials had about 36 peptides per polymer.

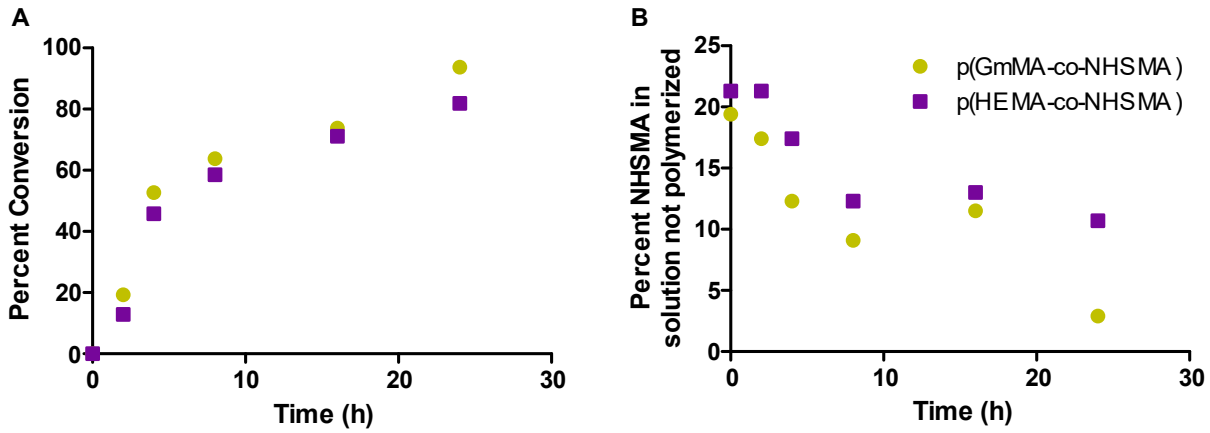

Figure 4.4 Polymerization kinetics of p(GmMA-co-NHSMA) and p(HEMA-co-NHSMA). A, percent conversion over time of p(HEMA-co-NHSMA) (purple squares) and p(GmMMA-co-NHSMA) (gold circles) over 24 hours. B, amount of NHSMA remaining unpolymerized in solution at each timepoint.

4.3.6 *ROTEM Characterization of PolySTATs from various synthesis strategies*

PolySTATs synthesized by all strategies enhanced clotting in ROTEM studies.

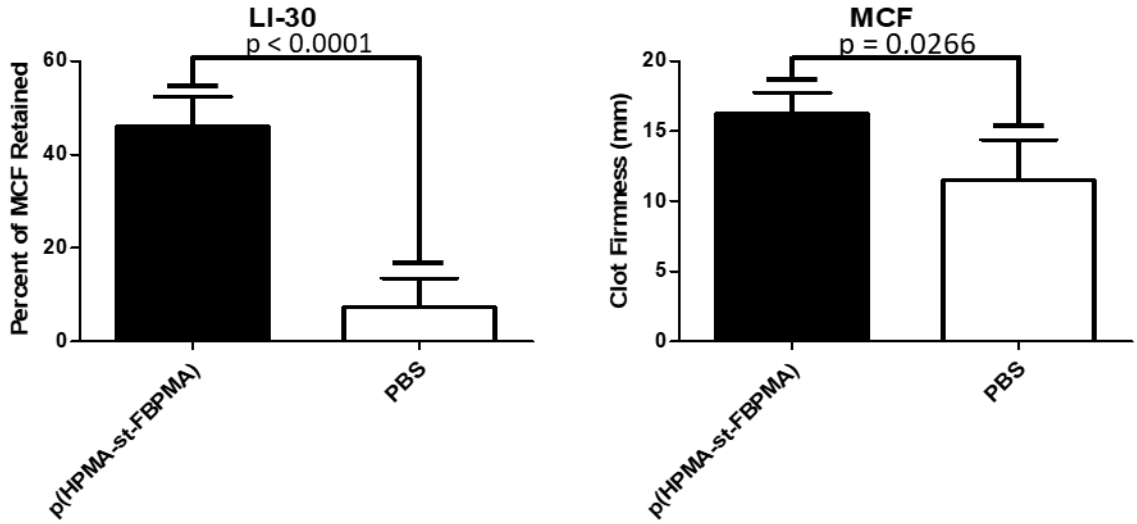

Figure 4.5 ROTEM Characterization of PolySTAT synthesized via FBP-methacrylamide. ROTEM shows decreased lysis, and increased clot strength of clots formed under hyperfibrinolytic conditions.

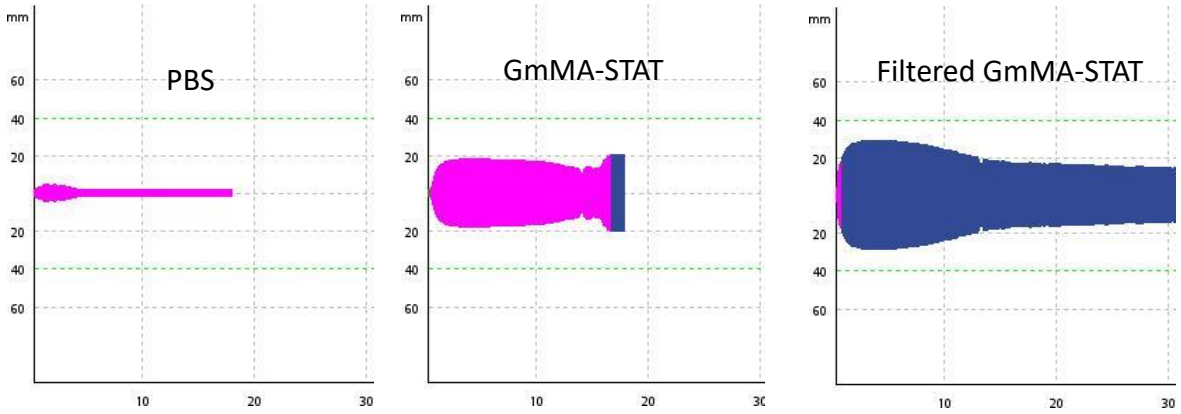

Figure 4.6 ROTEM Characterization of GmMA-based PolySTAT synthesized via FBP conjugation. ROTEM shows PolySTATs decrease lysis and increase clot strength of clots formed under hyperfibrinolytic conditions.

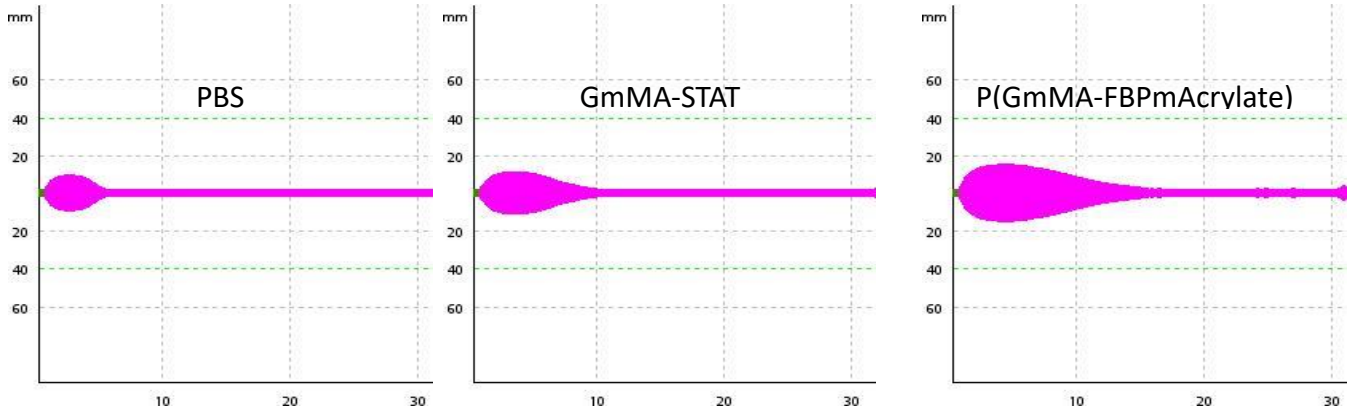

Figure 4.7 ROTEM Characterization of GmMA-based PolySTAT synthesized via FBP conjugation. ROTEM shows PolySTATs decrease lysis and increase clot strength of clots formed under hyperfibrinolytic conditions.

4.4 Discussion and Conclusions

Synthetic strategies of nanotechnology need be reproducible and efficient for the ultimate translation. Designs of nanotechnology range widely and even simple designs can pose challenges. In the case of PolySTAT, the active ingredient, FBP is poorly soluble in aqueous solutions and requires a polymer backbone not only to enable its crosslinking action via multivalency, but also to improve solubility in physiologically relevant vehicles.

All synthesis strategies yielded PolySTATs that are active by ROTEM. Our previous studies have shown strong indication that ROTEM is predictive of success in our rat model of traumatic injury and fluid resuscitation[66,97]. It is encouraging that PolySTAT activity is robust to varied comonomers and synthesis strategies. This allows us to focus on synthetic efficiency and ease. The methacrylamide polymerization requires synthesis of monomer types that are not ideal in organic solvent. In addition to this, poor control of homopolymers at the necessary CTA:I ratios suggest this is not the ideal synthesis route. The FBP-methacrylate synthesis is inefficient in purification of the peptide monomer. About 60% yield is achieved when collecting FBP-methacrylate via precipitation. Further optimization of this strategy may make this the best option in the future, especially since this strategy removes the need for anhydrous solvents and simplifies purification post-polymerization. However, conjugation to p(GmMA-st-NHSMA) yields a highly efficient reaction with nearly 100% conjugation in some cases. This increase in conjugation efficicency is due to improved solubility of the product during dialysis. We have observed that increased peptide valency decreases solubility and understand that purification by dialysis in PBS acted as a challenge of solubility against the population of polymers, culling those with the highest grafting. This removes the necessity of end-capping unreacted NHSMA with aminopropanol. In the future, purification may be streamlined without dialysis against PBS due to the increased solubility of pGmMA in comparison to pHEMA. There is ongoing work to perform unbiased head-to-head reactions and comparisons to confirm true peptide efficiencies that account for

synthesis, purification, conjugation or polymerization, and purification of the final product to determine the optimal synthesis strategy.

4.5 REFERENCES

1. WISQARS: Leading Causes of Death Reports. *Centers for Disease Control and Prevention* (2015).
2. WISQARS: Years of Potential Life Lost. *Centers for Disease Control and Prevention* (2015).
3. Murray, C. J. L., Lopez, A. D., Mathers, C. D. & Stein, C. *The Global Burden of Disease 2000 project: aims, methods and data sources*. (2001).
4. World Health Organization: The top 10 causes of death. (2017). Available at: http://www.who.int/mediacentre/factsheets/fs310/en/.
5. Sauaia, A. *et al.* Epidemiology of Trauma Deaths: A Reassessment. *J. Trauma* **38,** 185–193 (1995).
6. Lerner, E. B. & Moscati, R. M. The Golden Hour : Scientific Fact or Medical 'Urban Legend'. *Am. Emerg. Med.* **8,** 758–760 (2001).
7. Kauvar, D. S., Lefering, R. & Wade, C. E. Impact of Hemorrhage on Trauma Outcome : An Overview of Epidemiology, Clinical Presentations, and Therapeutic Considerations. *J. Trauma* **60,** 3–11 (2006).
8. Champion, H. R. *et al.* A Profile of Combat Injury. *J. Trauma* **54,** 513–519 (2003).
9. Holcomb, J. B. *et al.* Causes of Death in U . S . Special Operations Forces in the Global War on Terrorism. **245,** 986–991 (2007).
10. Chan, L. W., White, N. J. & Pun, S. H. Synthetic Strategies for Engineering Intravenous Hemostats. *Bioconjug. Chem.* **26,** 1224–1236 (2015).
11. Chen, H., Locke, D., Liu, Y., Liu, C. & Kahn, M. L. The Platelet Receptor GPVI Mediates Both Adhesion and Signaling Responses to Collagen in a Receptor Density-dependent Fashion*. **277,** 3011–3019 (2002).
12. Daniel, J. L. *et al.* Molecular Basis for ADP-induced Platelet Activation. **273,** 2024–2029 (1998).
13. Klinik, M. *et al.* Molecular Mechanisms of Platelet Activation. *Pharm. Rev.* **69,** 58–141 (1989).

14. Shattil, S. J., Hoxie, J. A., Cunningham, M. & Brass, L. F. Changes in the Platelet Membrane Glycoprotein IIb * IIIa Complex during Platelet Activation *. **260,** (1985).
15. Takeoka, S. *et al.* Function of fibrinogen. **312,** 773–779 (2003).
16. Tomiyama, Y., Tsubakio, T. & Kurata, Y. The Arg-Gly-Asp (RGD) recognition site of platelet glycoprotein IIb- IIIa on nonactivated platelets is accessible to high-affinity macromolecules. *Blood* **79,** 2303–2312 (2011).
17. Davie, E. W., Fujikawa, K. & Kisiel, W. The Coagulation Cascade: Initiation, Maintenance, and Regulation. *Biochemistry* **30,** 10363–10370 (1991).
18. Morrison, D. C. & Cochrane, C. G. Direct Evidence For Hageman Factor (Factor XII) Activation by Bacterial Lipopolysaccharides. *J. Exp. Med.* **140,** 797–811 (1974).
19. Bouma, B. N. & Griffin, J. H. Human blood coagulation factor XI . Purification , properties , and mechanism of activation by activated factor XII. *J. Biol. Chem.* **252,** 6432–6437 (1977).
20. Hoffman, M., Monroe, D. M. & Roberts, H. R. Activated factor VII activates factors IX and X on the surface of activated platelets : thoughts on the mechanism of action of ... *Blood Coagul. Fibrinolysis* **9,** S61–S65 (1998).
21. Mann, K. G., Brummel, K. & Butenas, S. What is all that thrombin for? *J Thromb Haemost* **1,** 1504–1514 (2003).
22. White, N. J. Mechanisms of trauma-induced coagulopathy. *Haematology* 660–663 (2013).
23. Kushimoto, S., Kudo, D. & Kawazoe, Y. Acute traumatic coagulopathy and trauma-induced coagulopathy : an overview. *J. Intensive Care* 1–7 (2017). doi:10.1186/s40560-016-0196-6
24. Brohi, K., Singh, J., Heron, M. & Coats, T. Acute traumatic coagulopathy. *J. Trauma* **54,** 1127–1130 (2003).
25. Kaafarani, H. M. a & Velmahos, G. C. Damage control resuscitation in trauma. *Scand. J. Surg.* **103,** 81–88 (2014).
26. Mikhail, J. The trauma triad of death: hypothermia, acidosis, and coagulopathy. *AACN clinical issues* **10,** 85–94 (1999).
27. Niles, S. E. *et al.* Increased Mortality Associated With the Early Coagulopathy of Trauma in Combat Casualties. *J. Trauma Inj. Infect. Crit. Care* **64,** 1459–1465 (2008).
28. Standbury, L. G. & Hess, J. R. Blood Transfusion in World War I : The Roles of

Lawrence Bruce. *Transfus. Med. Rev.* **23,** 232–236 (2009).

29. Boyle, R., Willis, T. & Wren, C. The History of Blood Transfusion. *Br. J. Haemotology* **110,** 758–767 (2000).
30. Duchesne, J. C., Hunt, J. P., Wahl, G. & Marr, A. B. Review of Current Blood Transfusions Strategies in a Mature Level I Trauma Center : Were We Wrong for the Last 60. *J. Trauma* **65,** 272–278 (2008).
31. Repine, T. B., Perkins, J. G., Kauvar, D. S. & Blackborne, L. The Use of Fresh Whole Blood in Massive Transfusion. **60,** (2005).
32. Sihler, K. C. & Napolitano, L. M. Complications of Massive Transfusion. *Chest* **137,** 209–220 (2010).
33. Riou, B. *et al.* Recombinant factor VIIa (Novoseven) as adjunctive therapy for bleeding contorl in trauma - a randomized. placebo-controlled trial. in *Shock* 228 (2004).
34. Rizoli, S. B. *et al.* Recombinant activated factor VII as an adjunctive therapy for bleeding control in severe trauma patients with coagulopathy : subgroup analysis from two randomized trials. *Crit. Care* **10,** 1–11 (2006).
35. Raza, I. *et al.* The incidence and magnitude of fibrinolytic activation in trauma patients. *J. Thromb. Haemost.* **11,** 307–314 (2013).
36. Williams-johnson, J. A., Mcdonald, A. H., Strachan, G. G. & Williams, E. W. Effects of Tranexamic Acid on Death, Vascular Occlusive Events, and Blood Transfusion in Trauma Patients with Significant Haemorrhage (CRASH-2) A Randomised, Placebo-Controlled Trial. *West Indian Med J* **59,** 612–624 (2010).
37. Houston, F. S. Military Application of Tranexamic Acid in Trauma Emergency Resuscitation (MATTERs) Study. **147,** 113–119 (2012).
38. Search Results: tranexamic acid. *ClinicalTrials.gov* (2018).
39. Coller, B. S. Interaction of normal, thrombathemis, and Bernard-Soulier platelets with immobilized fibrinogen: defective platelet-fibrinogen interaction in thrombastatin. *Blood* **55,** 169–179 (1980).
40. Coller, B. S. *et al.* Thromboerythrocytes In Vitro Studies of a Potential Autologous , Semi-artificial Alternative to Platelet Transfusions. *J Clin Invest* **98,** 546–555 (1992).
41. Ten, O. Fibrinogen-coated albumin microcapsules reduce bleeding in severely thrombocytopenic rabbits. **9,** 107–111 (1999).

42. Illum, L. *et al.* Blood clearance and organ deposition of intravenously administered colloidal particles . The effects of particle size , nature and shape. **12,** 135–146 (1982).
43. Okamura, Y. *et al.* Hemostatic effects of phospholipid vesicles carrying fibrinogen gamma chain dodecapeptide in vitro and in vivo. *Bioconjug. Chem.* **16,** 1589–96 (2005).
44. Okamura, Y. *et al.* Development of fibrinogen gamma-chain peptide-coated, adenosine diphosphate-encapsulated liposomes as a synthetic platelet substitute. *J. Thromb. Haemost.* **7,** 470–7 (2009).
45. Bertram, J. P. *et al.* Intravenous Hemostat : Nanotechnology to Halt Bleeding. *Sci. Transl. Med.* **1,** 11–22 (2009).
46. Shoffstall, A. J. *et al.* Tuning ligand density on intravenous hemostatic nanoparticles dramatically increases survival following blunt trauma. *Biomacromolecules* **14,** 2790–2797 (2013).
47. Lashof-sullivan, M. *et al.* Hemostatic Nanoparticles Improve Survival Following Blunt Trauma Even after 1 Week Incubation at 50 °C. *ACS Biomater. Sci. Eng.* **2,** 385–392 (2016).
48. Shoffstall, A. J. *et al.* Intravenous hemostatic nanoparticles increase survival following blunt trauma injury. *Biomacromolecules* **13,** 3850–3857 (2012).
49. Hubbard, W. B., Lashof-Sullivan, M. M., Lavik, E. B. & Vandevord, P. J. Steroid-loaded hemostatic nanoparticles combat lung injury after blast trauma. *ACS Macro Lett.* **4,** 387–391 (2015).
50. Onwukwe, C. *et al.* Engineering Intravenously Administered Nanoparticles to Reduce Infusion Reaction and Stop Bleeding in a Large Animal Model of Trauma. (2018). doi:10.1021/acs.bioconjchem.8b00335
51. Gupta, A. Sen, Huang, G., Lestini, B. J., Sagnella, S. & Kottke-marchant, K. RGD-modified liposomes targeted to activated platelets as a potential vascular drug delivery system RGD-modified liposomes targeted to activated platelets as a potential vascular drug delivery system. *Thromb Haemost* **93,** 106–114 (2005).
52. Ravikumar, M., Modery, C. L., Wong, T. L. & Gupta, A. Sen. Peptide-Decorated Liposomes Promote Arrest and Aggregation of Activated Platelets under Flow on Vascular Injury Relevant Protein Surfaces in Vitro. *Biomacromolecules* **13,** 1495–1502 (2012).

53. Ravikumar, M. *et al.* Mimicking Adhesive Functionalities of Blood Platelets using Ligand- Decorated Liposomes. *Bioconjug. Chem.* **23,** 1266–1275 (2012).
54. Modery-Pawlowski, C. L., Tian, L. L., Ravikumar, M., Wong, T. L. & Gupta, A. Sen. In vitro and in vivo hemostatic capabilities of a functionally integrated platelet-mimetic liposomal nanoconstruct. *Biomaterials* **34,** 3031–3041 (2013).
55. Hickman, D. A. *et al.* Intravenous synthetic platelet (SynthoPlate) nanoconstructs reduce bleeding and improve ‘ golden hour ’ survival in a porcine model of traumatic arterial hemorrhage. *Sci. Rep.* 1–14 (2018). doi:10.1038/s41598-018-21384-z
56. Shukla, M., Sekhon, U. D. S., Li, W. & Hickman, D. A. In vitro characterization of SynthoPlate (synthetic platelet) technology and its in vivo evaluation in severely thrombocytopenic mice. *J Thromb Haemost* **15,** 375–387 (2016).
57. Lashof-sullivan, M., Sho, A. & Lavik, E. Intravenous hemostats : challenges in translation to patients. *Nanoscale* **5,** 10719–10728 (2013).
58. Szebeni, J. *et al.* Prevention of infusion reactions to PEGylated liposomal doxorubicin via tachyphylaxis induction by placebo vesicles: A porcine model. *J. Control. Release* **160,** 382–387 (2012).
59. Brown, A. C. *et al.* Ultrasoft microgels displaying emergent platelet-like behaviours. *Nat. Mater.* **13,** 1–7 (2014).
60. Niewlarowski, S., Regoeczi, E., Stewart, G. J., Senyi, A. F. & Mustard, J. F. Platelet Interaction with Polymerizing Fibrin. **51,** 685–700 (1972).
61. Welsch, N., Brown, A. C., Barker, T. H. & Lyon, L. A. Colloids and Surfaces B : Biointerfaces Enhancing clot properties through fibrin-specific self-cross-linked PEG side-chain microgels. *Colloids Surfaces B Biointerfaces* **166,** 89–97 (2018).
62. Lorand, L. A double-headed Gly-Pro-Arg-Pro ligand mimics the functions of the E domain of fibrin for promoting the end-to-end crosslinking of □ chains by factor XIII a. **95,** 537–541 (1998).
63. Soon, A. S. C., Lee, C. S. & Barker, T. H. Modulation of fibrin matrix properties via knob:hole affinity interactions using peptide-PEG conjugates. *Biomaterials* **32,** 4406–4414 (2011).
64. Kolodziej, A. F. *et al.* Fibrin Specific Peptides Derived by Phage Display: Characterization of Peptides and Conjugates for Imaging. *Bioconjug. Chem.* **23,** 548–556

(2012).

65. Kolodziej, A. F., Zhang, Z., Overoye-chan, K., Jacques, V. & Caravan, P. Peptide Optimization and Conjugation Strategies Magnetic Resonance Imaging Contrast Agents. **1088,** 185–211
66. Chan, L. W. *et al.* A synthetic fibrin cross-linking polymer for modulating clot properties and inducing hemostasis. *Sci. Transl. Med.* **7,** (2015).
67. Chiefari, J. *et al.* Living Free-Radical Polymerization by Reversible Addition - Fragmentation Chain Transfer : The RAFT Process We wish to report a new living free-radical polymer- ization of exceptional effectiveness and versatility . 1 The living character is conferred by . **9297,** 5559–5562 (1998).
68. Chu, D. S. H. *et al.* Application of living free radical polymerization for nucleic acid delivery. *Acc. Chem. Res.* **45,** 1089–1099 (2012).
69. Kopeček, J., Kopečková, P., Minko, T., Lu, Z. R. & Peterson, C. M. Water soluble polymers in tumor targeted delivery. *J. Control. Release* **74,** 147–158 (2001).
70. Barrett, G. D., Constable, I. J. & Stewart, A. D. Clinical results of hydrogel lens implantation. *J. Cataract Refract. Surg.* **12,** 623–631 (1986).
71. Chan, L. W., White, N. J. & Pun, S. H. A Fibrin Cross-linking Polymer Enhances Clot Formation Similar to Factor Concentrates and Tranexamic Acid in an in Vitro Model of Coagulopathy. *ACS Biomater. Sci. Eng.* (2016). doi:10.1021/acsbiomaterials.5b00536
72. Maegele, M. *et al.* Early coagulopathy in multiple injury: An analysis from the German Trauma Registry on 8724 patients. *Injury* **38,** 298–304 (2007).
73. 6 Factor VIII Concentrates, Factor VIII/von Willebrand Factor Concentrates, Factor IX Concentrates, Activated Prothrombin Complex Concentrates. *Transfus. Med. Hemotherapy* **36,** 409–418 (2009).
74. Okamura, Y. *et al.* Development of fibrinogen c-chain peptide-coated, adenosine diphosphate-encapsulated liposomes as a synthetic platelet substitute. *J Thromb Haemost* **7,** 470–477 (2009).
75. Fasting, C. *et al.* Multivalency as a Chemical Organization and Action Principle. *Angew. Rev.* **51,** 10472–10498 (2012).
76. Spain, S. G. & Cameron, N. R. A spoonful of sugar : the application of glycopolymers in therapeutics. *Polym. Chem.* **2,** 60–68 (2011).

77. Weigandt, K. M., Pozzo, D. C. & Porcar, L. Structure of high density fibrin networks probed with neutron scattering and rheology. *Soft Matter* **5,** 4321–4330 (2009).
78. Weigandt, K. M., Porcar, L. & Pozzo, D. C. In situ neutron scattering study of structural transitions in fibrin networks under shear deformation. *Soft Matter* **7,** 9992–10000 (2011).
79. Yanjarappa, M. J., Gujraty, K. V, Joshi, A., Saraph, A. & Kane, R. S. Synthesis of Copolymers Containing an Active Ester of Methacrylic Acid by RAFT : Controlled Molecular Weight Scaffolds for Biofunctionalization. *Biomacromolecules* **7,** 1665–1670 (2006).
80. Kirby, N. M. *et al.* research papers A low-background-intensity focusing small-angle X-ray scattering undulator beamline. 1670–1680 (2013). doi:10.1107/S002188981302774X
81. Hammouda, B., Ho, D. L. & Kline, S. Insight into Clustering in Poly (ethylene oxide) Solutions. *Macromolecules* **37,** 6932–6937 (2004).
82. Glinka, C. J. *et al.* The 30 m Small-Angle Neutron Scattering Instruments at the National Institute of Standards and Technology. *J. Appl. Crystallogr.* **31,** 430–445 (1998).
83. Kline, S. R. Reduction and analysis of SANS and USANS data using IGOR Pro. *J. Appl. Crystallogr.* **39,** 895–900 (2006).
84. Barker, J. G. *et al.* Design and performance of a thermal-neutron double-crystal diffractometer for USANS at NIST. *J. Appl. Crystallogr.* **38,** 1004–1011 (2005).
85. Terech, P. Structural Study of Cholesteryl Anthraquinone-2-carboxylate (CAQ) Physical Organogels by Neutron and X-ray Small Angle Scattering. *J. Phys. Chem.* **100,** 3759–3766 (1996).
86. Teixeira, J. Small-Angle Scattering by Fractal Systems. *J. Appl. Crystallogr.* **21,** 781–785 (1988).
87. Hammouda, B. & Horkay, F. Clustering and Solvation in Poly(acrylic acid) Polyelectrolyte Solutions. *Macromolecules* **38,** 2019–2021 (2005).
88. Dowling, M. B. *et al.* Biomaterials A self-assembling hydrophobically modi fi ed chitosan capable of reversible hemostatic action. *Biomaterials* **32,** 3351–3357 (2011).
89. Laudano, A. P. & Doolittle, R. F. Studies on synthetic peptides that bind to fibrinogen and prevent fibrin polymerization. Structural requirements, number of binding sites, and species differences. *Biochemistry* **19,** 1013–1019 (1980).
90. Lukyanov, A. N. & Torchilin, V. P. Micelles from lipid derivatives of water-soluble

polymers as delivery systems for poorly soluble drugs. **56,** 1273–1289 (2004).

91. Rizvi, S. A. A. & Saleh, A. M. Applications of nanoparticle systems in drug delivery technology. *Saudi Pharm. J.* **26,** 64–70 (2018).
92. Kieler-ferguson, H. M. & Fr, J. M. J. Clinical developments of chemotherapeutic nanomedicines : polymers and liposomes for delivery of camptothecins and platinum (II). **5,** (2013).
93. Press, D. Effective use of nanocarriers as drug delivery systems for the treatment of selected tumors. 7291–7309 (2017).
94. Langer, R. Drug delivery and targeting. **392,** 5–10 (1998).
95. Montet, X., Funovics, M., Montet-abou, K., Weissleder, R. & Josephson, L. Multivalent Effects of RGD Peptides Obtained by Nanoparticle Display. 6087–6093 (2006). doi:10.1021/jm060515m
96. Lee, H., Fonge, H., Hoang, B., Reilly, R. M. & Allen, C. articles The Effects of Particle Size and Molecular Targeting on the Intratumoral and Subcellular Distribution of Polymeric Nanoparticles. **7,** 1195–1208 (2010).
97. Lamm, R. J. *et al.* Peptide valency plays an important role in the activity of a synthetic fibrin-crosslinking polymer. *Biomaterials* **132,** 96–104 (2017).
98. Devlin, J., Panganiban, L. & Devlin, P. Random peptide libraries: a sourse of specific protein binding molecules. *Science (80-.).* **249,** 404–406 (1990).
99. Fan, S. *et al.* Curcumin-loaded PLGA-PEG nanoparticles conjugated with B6 peptide for potential use in Alzheimer ' s disease. *Drug Deliv.* **25,** 1044–1055 (2018).
100. Duvall, C. L., Convertine, A. J., Benoit, D. S. W., Hoffman, A. S. & Stayton, P. S. articles Intracellular Delivery of a Proapoptotic Peptide via Conjugation to a RAFT Synthesized Endosomolytic Polymer. (2010).
101. Chu, D. S. *et al.* As featured in : Biomaterials Science. (2015). doi:10.1039/c4bm00259h
102. Johnson, R. N. *et al.* Synthesis of Statistical Copolymers Containing Multiple Functional Peptides for Nucleic Acid Delivery. *Biomacromolecules* **11,** 3007–13 (2010).
103. Chu, D. S. H., Schellinger, J. G., Bocek, M. J., Johnson, R. N. & Pun, S. H. Optimization of Tet1 ligand density in HPMA-co-oligolysine copolymers for targeted neuronal gene delivery. *Biomaterials* **34,** 9632–9637 (2013).
104. Schellinger, J. G. *et al.* Melittin-grafted HPMA-oligolysine based copolymers for gene

delivery. *Biomaterials* **34,** 2318–2326 (2013).

105. Kanaide, H. & Shainoff, J. R. Cross-linking of fibrinogen and fibrin by fibrin-stabilizing factor (factor XIIIa). *Transl. Res.* **85,** 574–597 (1975).
106. O'Brien-Simpson, N. M., Ede, N. J., Brown, L. E., Swan, J. & Jackson, D. C. Polymerization of unprotected synthetic peptides: A view toward synthetic peptide vaccines. *J. Am. Chem. Soc.* **119,** 1183–1188 (1997).
107. Hasson, C. J., Caldwell, G. E. & Emmerik, R. E. A. Van. NIH Public Access. *Motor Control* **27,** 590–609 (2009).
108. Studenovská, H., Šlouf, M. & Rypáček, F. Poly(HEMA) hydrogels with controlled pore architecture for tissue regeneration applications. *J. Mater. Sci. Mater. Med.* **19,** 615–621 (2008).
109. Kopeckova, P. Water soluble polymers in tumor targeted delivery. *J. Control. Release* **74,** 147–158 (2001).
110. Cunningham, V. J. *et al.* Poly(glycerol monomethacrylate) − Poly(benzyl methacrylate) Diblock Copolymer Nanoparticles via RAFT Emulsion Polymerization: Synthesis, Characterization, and Interfacial Activity. (2014). doi:10.1021/ma501140h
111. Save, M., Weaver, J. V. M., Armes, S. P. & Mckenna, P. Atom Transfer Radical Polymerization of Hydroxy-Functional Methacrylates at Ambient Temperature: Comparison of Glycerol Monomethacrylate with 2-Hydroxypropyl Methacrylate. 1152–1159 (2002). doi:10.1021/ma011541r
112. Das, D. *et al.* RAFT polymerization of ciprofloxacin prodrug monomers for the controlled intracellular delivery of antibiotics. *Polym. Chem* **7,** 826–837 (2016).
113. Shin, H. C., Alani, A. W. G., Rao, D. A., Rockich, N. C. & Kwon, G. S. Multi-drug loaded polymeric micelles for simultaneous delivery of poorly soluble anticancer drugs. *J. Control. Release* **140,** 294–300 (2009).
114. Hughes, H. C. Swine in cardiovascular research. *Lab Anim. Sci.* **36,** 348–350 (1986).
115. Swindle, M. M., Makin, A., Herron, A. J., Clubb, F. J. & Frazier, K. S. Swine as Models in Biomedical Research and Toxicology Testing. *Vet. Pathol.* **49,** 344–356 (2012).
116. Pusateri, A. E. *et al.* Effect of a Chitosan-Based Hemostatic Dressing on Blood Loss and Survival in a Model of Severe Venous Hemorrhage and Hepatic Injury in Swine. *J trauma* **54,** 177–182 (2003).

117. Pusateri, A. E. *et al.* Advanced Hemostatic Dressing Development Program : Animal Model Selection Criteria and Results of a Study of Nine Hemostatic Dressings in a Model of Severe Large Venous Hemorrhage and Hepatic Injury in Swine. *J Trauma* **55,** 518–526 (2003).
118. Stern, S. *et al.* RESUSCITATION WITH THE HEMOGLOBIN-BASED OXYGEN CARRIER , HBOC-201 , IN A SWINE MODEL OF SEVERE UNCONTROLLED HEMORRHAGE AND TRAUMATIC BRAIN INJURY. *Shock* **31,** 64–79 (2009).
119. White, N. J., Wang, X., Liles, W. C. & Stern, S. Fibrinogen Concentrate Improves Survival During Limited Resuscitation of Uncontrolled Hemorrhagic Shock in a Swine Model. *Shock* **42,** 456–463 (2014).
120. Szebeni, J., Bed, P. & Rozsnyay, Z. Liposome-induced complement activation and related cardiopulmonary distress in pigs : factors promoting reactogenicity of Doxil and AmBisome. **8,** 176–184 (2012).
121. Szebeni, J. *et al.* A porcine model of complement-mediated infusion reactions to drug carrier nanosystems and other medicines ☆. **64,** 1706–1716 (2012).
122. Bertram, J. P. *et al.* Intravenous Hemostat : Nanotechnology to Halt Bleeding. (2009).
123. Boldt, J., Haisch, G., Suttner, S., Kumle, B. & Schellhaass, A. Effects of a new modifed, balanced hydroxyethyl starch preparation (Hextend). *Br. J. Anaesth.* **89,** 722–728 (2002).
124. Landskroner, K., Olson, N. & Jesmok, G. Cross-species pharmacologic evaluation of plasmin as a direct-acting thrombolytic agent: Ex vivo evaluation for large animal model development. *J. Vasc. Interv. Radiol.* **16,** 369–377 (2005).
125. Mitterlechner, T. *et al.* Prothrombin complex concentrate and recombinant prothrombin alone or in combination with recombinant factor X and FVIIa in dilutional coagulopathy: A porcine model. *J. Thromb. Haemost.* **9,** 729–737 (2011).
126. R. Baylis, J. *et al.* Rapid hemostasis in a sheep model using particles that propel thrombin and tranexamic acid. *Laryngoscope* **127,** 787–793 (2017).
127. Ngambenjawong, C., Gustafson, H. H., Sylvestre, M. & Pun, S. H. A Facile Cyclization Method Improves Peptide Serum Stability and Confers Intrinsic Fluorescence. *ChemBioChem* **18,** 2395–2398 (2017).
128. Von Maltzahn, G. *et al.* Nanoparticles that communicate in vivo to amplify tumour targeting. *Nat. Mater.* **10,** 545–552 (2011).

129. Liu, G. W. *et al.* Glomerular disease augments kidney accumulation of synthetic anionic polymers. *Biomaterials* **178,** 317–325 (2018).
130. Tabata, Y. & Ikada, Y. Effect of the size and surface charge of polymer microspheres on their phagocytosis by macrophage. *Biomaterials* **9,** 356–362 (1988).
131. Caliceti, P. & Veronese, F. P harmacokinetic and biodistribution properties of poly(ethylene glycol)–protein conjugates Paolo. *Adv. Drug Deliv. Rev.* **55,** 1261–1277 (2003).
132. Beier, J. I. *et al.* Fibrin accumulation plays a critical role in the sensitization to lipopolyccharide-induced liver injury caused by ethanol in mice. *Hepatology* **49,** 1545–1553 (2009).
133. Imokawa, S. *et al.* Tissue factor expression and fibrin deposition in the lungs of patients with idiopathic pulmonary fibrosis and systemic sclerosis. *Am. J. Respir. Crit. Care Med.* **156,** 631–636 (1997).
134. Brown, L. F., Dvorak, A. M. & Dvorak, H. F. Leaky vessels, fibrin deposition, and fibrosis: a sequence of events common to solid tumors and to many other types of disease. *Am. Rev. Respir. Dis.* **140,** 1104–7 (1989).
135. Hiramoto, R., Bernecky, J., Jurandowski, J. & Pressman, D. Fibrin in Human Tumors. *Cancer Res.* **20,** 592–593 (1960).
136. Fernandez, P. M., Patierno, S. R. & Rickles, F. R. Tissue factor and fibrin in tumor angiogenesis. *Semin. Thromb. Hemost.* **30,** 31–44 (2004).
137. Wallace, A. C. Demonstration of Fibrin in Early Stages of Experimental Metastases. *Cancer Res.* **36,** 1904–1909 (1976).
138. Dirix, L. Y. *et al.* Plasma fibrin D-dimer levels correlate with tumour volume, progression rate and survival in patients with metastatic breast cancer. *Br. J. Cancer* **86,** 389–395 (2002).
139. Chu, D. S. *et al.* MMP9-sensitive polymers mediate environmentally-responsive bivalirudin release and thrombin inhibition. *Biomater. Sci.* **3,** 41–45 (2015).
140. Warkentin, T. E., Greinacher, A. & Koster, A. Bivalirudin. *Thromb. Haemost.* **99,** 830–839 (2008).
141. Hejna, M., Raderer, M. & Zielinski, C. C. Inhibition of metastases by anticoagulants. *J. Natl. Cancer Inst.* **91,** 22–36 (1999).

142. Amirkhosravi, A. *et al.* Tissue factor pathway inhibitor reduces experimental lung metastasis of B16 melanoma. *Thromb. Haemost.* **87,** 930–936 (2002).
143. Kondapaka, S. B., Fridman, R. & Reddy, K. B. Epidermal growth factor and amphiregulin up-regulate matrix metalloproteinase-9 (MMP-9) in human breast cancer cells. *Int. J. Cancer* **70,** 722–726 (1997).
144. Svendsen, L., Blombäck, B., Blombäck, M. & Olsson, P. I. Synthetic chromogenic substrates for determination of trypsin, thrombin and thrombin-like enzymes. *Thromb. Res.* **1,** 267–278 (1972).
145. Reinhard, J., Brösicke, N., Theocharidis, U. & Faissner, A. The extracellular matrix niche microenvironment of neural and cancer stem cells in the brain. *Int. J. Biochem. Cell Biol.* **81,** 174–183 (2016).
146. Palumbo, J. S. *et al.* Platelets and fibrin(ogen) increase metastatic potential by impeding natural killer cell-mediated elimination of tumor cells. *Blood* **105,** 178–185 (2005).
147. Ogston, A. OGSTON, M.D., Surgeon. *J. Anat.* **16,** 526–567 (1882).
148. Lowry, F. D. Staphylococcus aureus Infections. *N. Engl. J. Med.* **339,** 520–532 (1998).
149. Lake, J. G. *et al.* Pathogen distribution and antimicrobial resistance among pediatric healthcare-associated infections reported to the National Healthcare Safety Network, 2011-2014. *Infect. Control Hosp. Epidemiol.* **39,** 1–11 (2018).
150. Weiner, L. M. *et al.* Antimicrobial-Resistant Pathogens Associated with Healthcare-Associated Infections: Summary of Data Reported to the National Healthcare Safety Network at the Centers for Disease Control and Prevention, 2011-2014. *Infect. Control Hosp. Epidemiol.* **37,** 1288–1301 (2016).
151. Lee, A. S. *et al.* Methicillin-resistant Staphylococcus aureus. *Nat. Rev. Dis. Prim.* **4,** (2018).
152. Jevons, P. M. 'Celbenin'-resistant Staphylococci. *Br. Med. J.* **1,** 124–125 (1961).
153. Hiramatsu, K. *et al.* Methicillin-resistant Staphylococcus aureus clinical strani with reduced vancomycin susceptibility. *J. Antimicrob. Chemother.* **40,** 135–146 (1997).
154. Huh, A. J. & Kwon, Y. J. 'Nanoantibiotics': A new paradigm for treating infectious diseases using nanomaterials in the antibiotics resistant era. *J. Control. Release* **156,** 128–145 (2011).
155. Loughman, A. *et al.* Roles for fibrinogen, immunoglobulin and complement in platelet

activation promoted by Staphylococcus aureus clumping factor A. *Mol. Microbiol.* **57,** 804–818 (2005).

156. Mcdevitt, D. *et al.* Characterization of the interaction between the Staphylococcus aureus clumping factor (ClfA) and fibrinogen. *Eur. J. Biochem.* **247,** 416–424 (1997).
157. Que, Y. *et al.* Reassessing the Role of Staphylococcus aureus Clumping Factor and Fibronectin-Binding Protein by Expression in Lactococcus. *Infect. Immun.* **69,** 6296–6302 (2001).
158. Patti, J. M. A humanized monoclonal antibody targeting Staphylococcus aureus. *Vaccine* **22,** (2004).
159. Takeoka, S. *et al.* Function of fibrinogen gamma-chain dodecapeptide-conjugated latex beads under flow. *Biochem. Biophys. Res. Commun.* **312,** 773–9 (2003).
160. Okamura, Y. *et al.* Hemostatic effects of fibrinogen gamma-chain dodecapeptide-conjugated polymerized albumin particles in vitro and in vivo. *Transfusion* **45,** 1221–8 (2005).
161. Okamura, Y., Maekawa, I., Teramura, Y., Maruyama, H. & Handa, M. Hemostatic Effects of Phospholipid Vesicles Carrying Fibrinogen γ Chain Dodecapeptide in Vitro and in Vivo. 30–33 (2005).
162. Pease, D. C. An Electron Microscopy Study of Red Bone Marrow. *Blood* **11,** 501–526 (1956).
163. Wagner, B. C. L. *et al.* Analysis of GPIIb/IIIa Receptor Number by Quantification of 7E3 Binding to Human Platelets. (2015).
164. Nilsson, I. M., Patti, J. M., Bremell, T., Höök, M. & Tarkowski, A. Vaccination with a recombinant fragment of collagen adhesin provides protection against Staphylococcus aureus-mediated septic death. *J. Clin. Invest.* **101,** 2640–2649 (1998).
165. Stevens, K. A., Sheldon, B. W., Klapes, N. A. & Klaenhammer, T. R. Nisin treatment for inactivation of Salmonella species and other gram- negative bacteria. *Appl. Environ. Microbiol.* **57,** 3613–3615 (1991).
166. Millette, M., Le Tien, C., Smoragiewicz, W. & Lacroix, M. Inhibition of Staphylococcus aureus on beef by nisin-containing modified alginate films and beads. *Food Control* **18,** 878–884 (2007).
167. Hancock, R. E. W. Peptide antibiotics. *Lancet* **349,** 418–422 (1997).

168. Biscola, V. *et al.* Isolation and characterization of a nisin-like bacteriocin produced by a Lactococcus lactis strain isolated from charqui, a Brazilian fermented, salted and dried meat product. *Meat Sci.* **93,** 607–613 (2013).
169. Miao, J. *et al.* Membrane disruption and DNA binding of Staphylococcus aureus cell induced by a novel antimicrobial peptide produced by Lactobacillus paracasei subsp. tolerans FX-6. *Food Control* **59,** 609–613 (2016).

PART 3: EVALUATE POLYSTAT IN A LARGE ANIMAL MODEL

CHAPTER 5: POLYSTAT ADMINISTRATION IS SAFE IN A SWINE MODEL OF AORTIC TEAR.

Robert J. Lamm, Xu Wang, Tianyong Zheng, Krystyn Ringgold,

Suzie H. Pun, Nathan J. White

5.1 INTRODUCTION

Swine are a commonly used model for cardiovascular research for their unique similarities to humans, including their size, anatomy, and cardiovascular physiology[114,115]. In addition to these benefits, swine have large volumes of blood which allows researchers to perform blood draws to perform extensive testing throughout the course of experiments. This makes swine an excellent model for the evaluation of hemostatic materials, and such models have been useful in determining the ability of hemorrhage interventions to slow bleeding and improve survival[116–119]. Earlier this year, two synthetic platelets demonstrated decreased blood loss in a model of traumatic injury in swine[50,55]. In each of these cases, the researchers paid close attention to the potential for their nanoparticle formulation to elicit a strong immune response known as complement-related psuedoallergy (CARPA).

CARPA is a complement response to infused nanomaterials that is observed in pigs and humans[120,121]. Notably, CARPA is observed in response to two commercially-available therapies, Doxil (liposomal Doxorubicin) and Ambisome (liposomal amphotericin B) in both species[58,122]. At its most severe, CARPA can be fatal in swine as described by massive exsanguination experienced by animals in the Lavik's group investigation of their synthetic platelets[50]. This was ameliorated through a redesign of material components to decrease complement activation. While this reaction is not expected to be as severe in humans, it precludes the use of swine as a model for evaluation of a synthetic hemostat, making such design considerations imperative.

In this work, we evaluate the safety and observe the effectiveness of PolySTAT in a swine model of trauma via aortic tear. We observe the effects of the material on uninjured animals as well as observe animals who have undergone an aortic tear. Throughout each experiment, we measured the mean arterial pressure and pulmonary arterial pressure of the animals as well as recorded blood gas and metabolite values. Through these studies, we concluded that PolySTAT does not elicit a CARPA response in swine and therefore evaluation of PolySTAT in pigs is feasible. Unfortunately, there was no benefit to PolySTAT treatment in this model and further development is required.

Upon future completion of a large-scale efficacy study, the data will be used to confirm results previously seen in rat models of trauma which showed PolySTAT is capable of improving survival after lethal traumatic injury[66,97]. The Food and Drug Administration (FDA) requires

efficacy testing in at least two different animal species for IND applications, with a preference for one of the species. Efficacy in swine will put PolySTAT in a good position to translate from the benchtop to first responders.

5.2 MATERIALS AND METHODS

5.2.1 *Materials*

2,2′-Azobis(2-methylpropionitrile) (AIBN), 4-cyanopentanoic acid dithiobenzoate (CTP), 2-hydroxyethyl methacrylate (HEMA), and all other reagents were purchased from Sigma-Aldrich (Saint Louis, MO) unless noted otherwise. N-hydroxysuccinimide methacrylate (NHSMA) was purchased from TCI America (Portland, OR). The fibrin binding peptide (FBP; Sequence: Ac-Y(DGl)C(HPr)YGLCYIQGK),[64] developed by the Caravan group, was purchased from GL Biochem (Shanghai, China) as a custom peptide.

5.2.2 *Synthesis of HEMA backbone polymer*

Poly(hydroxyethyl methacrylate) (pHEMA) backbone polymers were synthesized by reversible addition-fragmentation chain transfer (RAFT) polymerization as described previously[66]. HEMA, NHSMA, CTP, and AIBN were combined at a 160:40:1:0.333 ratio in dimethylacetamide (DmAc) and stirred for 24 h at 70° C. The resulting p(HEMA-st-NHSMA) polymers were isolated by 2x precipitation in diethyl ether with DmAc as the intermediate solvent. Dithiobenzoate groups were removed via an end capping reaction with 20x molar excess AIBN at 70 °C for 24 hours. Polymers were characterized via gel permeation chromatography (GPC) with static light scattering and refractive index detectors (MiniDawn Treos and OptilabRex, respectively, both Wyatt Technology, Santa Barbara, CA) to determine molecular weight and polydispersity index (PDI). ^{1}H Nuclear magnetic resonance (NMR) was utilized to determine composition of the polymers and confirm removal of dithiobenzoate groups. Polymers were then dissolved at 100 mg/mL in DMSO and with 10:1 1-amino-2-propanol:NHS and 5:1 N,N-diisopropylethylamine (DIPEA) to

cap NHS groups. Polymers were isolated by 48 h dialysis (3,500 MWCO) against DI water and subsequently lyophilized.

5.2.3 *PolySTAT Synthesis*

PolySTAT was synthesized as described previously[66]. Poly(HEMA-st-NHSMA) was reacted with FBP via the primary amine present in the peptide's lysine residue at the C-terminus under organic basic conditions described by Yanjarappa *et al*[79]. Briefly, polymer and peptide were combined at a 1.5:1 ratio of peptide:NHS with DIPEA in DMSO and allowed to react at 50 °C for 24 hours. Unreacted NHS groups were then capped with a 10x molar feed of 1-amino-2-propanol. Polymers were purified by dialysis against phosphate-buffered saline (PBS) for 24 h (3 buffer changes, 4 L of buffer) followed by dialysis against DI water for 48 h (6 dialysate changes) to remove PBS salts. Peptide content of materials was determined using the extinction coefficient of FBP and the materials' absorbance at a wavelength of 280 nm using a NanoDrop 2000 UV-Vis spectrophotometer (Thermo Fisher Scientific, Waltham, MA).

5.2.4 *Evaluation of PolySTAT Administration in Uninjured Swine*

Animal use was carried out in accordance with protocols approved by the University of Washington Institutional Animal Care and Use Committee. Domestic swine were sedated via intramuscular injection of Ketamine followed by subcutaneous buprenorphine injection. Anesthesia was maintained by continuous delivery of isoflurane via endotracheal tube. Body temperature was monitored continuously via a rectal temperature probe. After anesthesia, pigs were catheterized in the femoral artery and vein for blood pressure measurements and drug and fluid infusion, respectively. Swine were infused with varying doses of PolySTAT over 10 minutes. One animal each received 1.0, 3.0, or 9.0 mg/kg doses of PolySTAT. Pigs were subsequently administered a bolus of 2 mL/kg Hextend® (6% hetastarch in lactated electrolyte) over two minutes and observed for 30 minutes total.

5.2.5 *Evaluation of PolySTAT Administration in a Swine Model of Trauma via Aortic Tear*

Animals were prepared including anesthesia and catheterization as described above and the animals prepped for an aortic tear model as described previously[119]. After baseline blood gas and metabolites were confirmed appropriate, a midline incision was made through the abdominal skin and underlying muscle layers. A splenectomy was performed to prevent auto-transfusion, which is common in pigs in response to blood loss but does not occur in humans. The infrarenal aorta was identified and a curved needle used to place a thin wire longitudinally through 4-5 mm of the anterior wall of the aorta. The wire was exteriorized through the midline incision and secured in place. The abdomen was subsequently closed with sutures. Prior to injury, catheter hemorrhage was performed to a mean blood pressure $\leq$ 30 mm Hg. Injury was induced by pulling on the wire to create a 4-5 mm aortic tear injury. Hypotensive blood pressure was maintained with additional catheter bleeding until adequate shock is achieved defined as a blood lactate concentration of 2 mmol/L. After 15-30 minutes of shock, treatment was administered to the vein at 15 mg/kg 10 minutes. Animals received either 15 mg/kg PolySTAT (n = 3) or 15 mg/kg pHEMA backbone (n = 3). Fluid resuscitation with Ringers Lactate buffered saline solution was infused at 1-3 ml/kg/min as needed to achieve mean arterial pressure of 60 mm Hg up to 90 min. If blood pressure dropped below 20 mm Hg for at least 1 minute, and arterial pressure waveform was lost, indicating cardiac arrest, pigs were deemed a clinical death and euthanized by a pentobarbital overdose. The abdomen was reopened and shed blood collected and measured using pre-weighed gauze.

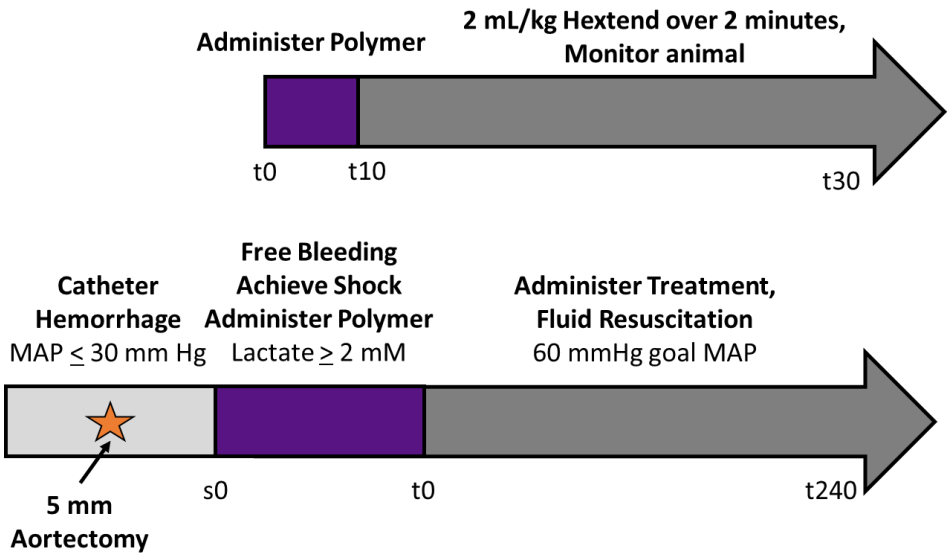

Figure 4.1 Schematic of animal protocols used in this chapter. Swine administered 3.0 mg/kg (purple circles), 5.5 mg/kg (gold squares), or 9.0 mg/kg (black triangles) were observed for 30 minutes. Above, Pulmonary Arterial Pressure (PAP) showed no large spike (> 30 mm Hg) over the course of infusion. Below, mean arterial pressure (MAP) suggests that animals receiving 9.0mg/kg of PolySTAT experience a resuscitative response. C, MAP-normalized PAP values allow for observation of variations in PAP that is not accounted for in variations of systemic blood pressure.

5.3 RESULTS

5.3.1 *PolySTAT Synthesis*

PHEMA backbones and PolySTAT were synthesized to parameters described previously[97]. PHEMA backbone was 28.8 kDa by GPC and p(HEMA-st-NHSMA) was 29.1 kDa, both with PDIs below 1.3. PolySTATs had 10.6 peptides per polymer.

5.3.2 *Evaluation of PolySTAT Administration in Uninjured Swine*

Uninjured swine received 3 different doses of PolySTAT: 1.0 mg/kg, to mimic a lower dose reflective of a surface area dose equivalency to rats; 3.0 mg/kg, an intermediate dose; and 9.0 mg/kg, an intermediate high dose. These animals tolerated

preparation and treatment well with no signs of metabolic distress before, during, or after treatment.

The pulmonary arterial pressure (PAP) in all animals stayed stable and below 20 mm Hg (Fig. 4.2A). The mean arterial pressure was stable for animals receiving 1.0 and 3.0 mg/kg doses, however the animal that received 9.0 mg/kg exhibited an increase in MAP (Fig. 4.2B). All animals survived through the treatment without adverse effects.

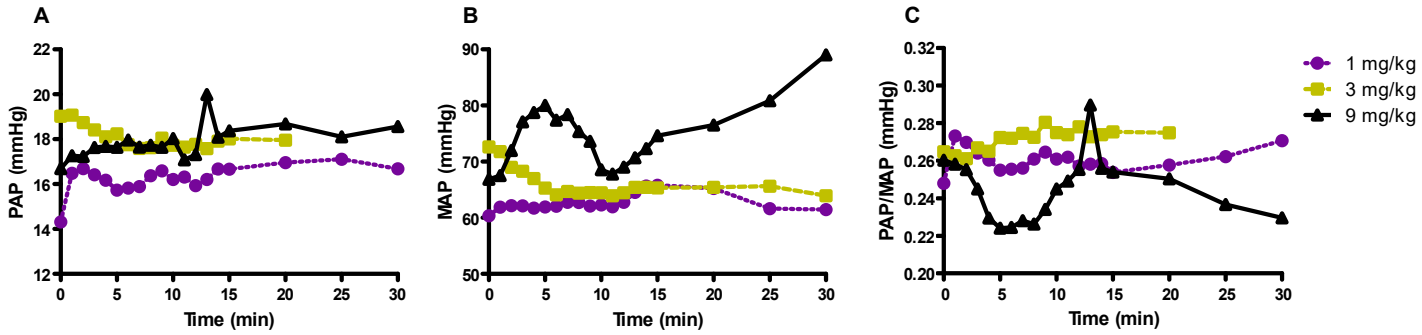

Figure 4.2 Arterial pressures during PolySTAT infusion of non-injured animals suggests the material does not elicit CARPA. Swine administered 1.0 mg/kg (purple circles), 3.0 mg/kg (gold squares), or 9.0 mg/kg (black triangles) were observed for 30 minutes. A, pulmonary Arterial Pressure (PAP) showed no large spike (> 30 mm Hg) over the course of infusion. B, mean arterial pressure (MAP) suggests that animals receiving 9.0mg/kg of PolySTAT experience a resuscitative response. C, MAP-normalized PAP values allow for observation of variations in PAP that is not accounted for in variations of systemic blood pressure.

5.3.3 *Evaluation of PolySTAT Administration in a Swine Model of Trauma via Aortic Tear*

All pigs tolerated experimental preparation. PolySTAT and backbone infusions were well tolerated with no spike in PAP during infusion (Fig. 4.3A). Additionally, there was no PAP spike observed after bolus Hextend infution (Fig. 4.3D). The PAP/MAP is moderately increased in PolySTAT animals, suggesting a MAP-independent increase in PAP (Fig. 4.3C & F).

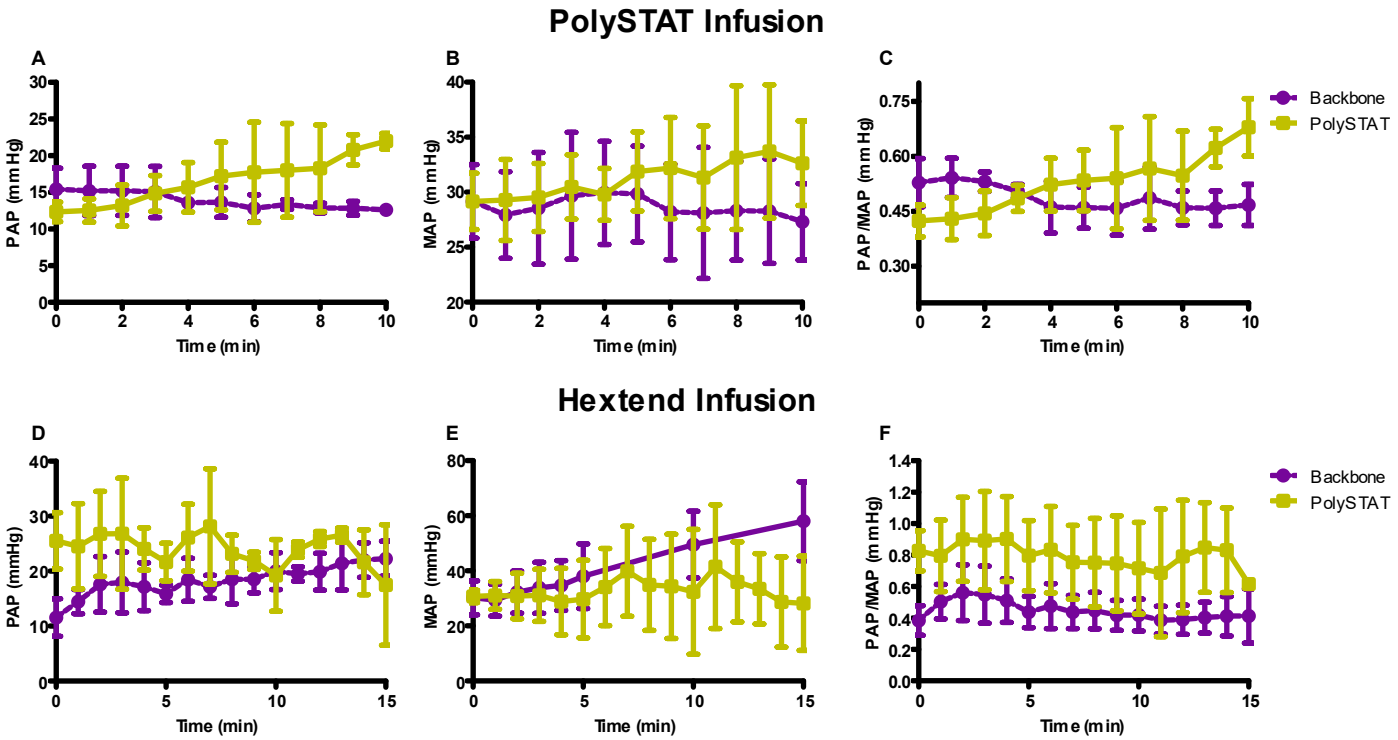

Figure 4.3 Arterial pressures during PolySTAT infusion of injured animals suggests the material does not elicit CARPA. Swine administered 15.0 mg/kg of pHEMA backbone or PolySTAT were observed for 240 minutes. A, Pulmonary Arterial Pressure (PAP) showed no large spike (≥ 40 mm Hg) over the course of PolySTAT infusion. B, mean arterial pressure (MAP) suggests that animals receiving 15.0 mg/kg of PolySTAT experience a resuscitative response. C, MAP-normalized PAP values allow for observation of variations in PAP that is not accounted for in variations of systemic blood pressure, suggesting mild increases in PAP. D, PAP over Hextend infusion. E, MAP over Hextend infusion. F, PAP/MAP over Hextend infusion.

There was no significant difference in survival or hemorrhage volume between animals treated with PolySTAT or the control backbone (Fig 4.4). In fact, normalizing by survival time reveals animals receiving PolySTAT tended to bleed more than animals treated with the pHEMA backbone (Fig 4.4C).

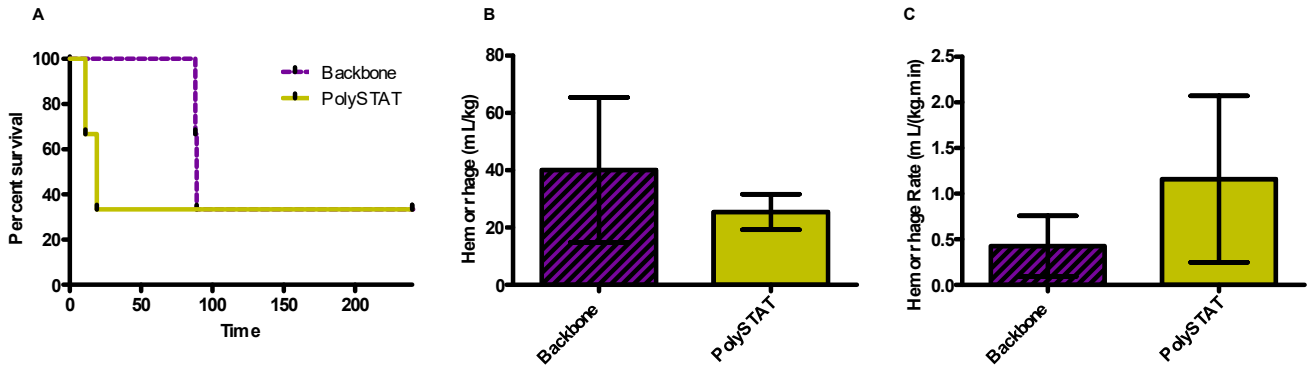

Figure 4.4 Efficacy of PolySTAT in a swine model of traumatic injury via aortic tear. Swine administered 15.0 mg/kg of pHEMA backbone or PolySTAT were observed for 240 minutes. A, survival over the course of observation for PolySTAT (solid gold) and pHEMA backbone (dashed purple). B, hemorrhage normalized to body mass. C, survival time-normalized hemorrhage rates.

During out studies observed that animals treated with PolySTAT in the aortic tear model experienced resuscitative effects which resulted in an average increase in MAP above 30 mm Hg during the shock period at which the method calls for catheter hemorrhage with a goal of 30 mm Hg (Fig. 4.5A). Under such conditions, we consistently withdraw blood from animals that are becoming healthier. Observing data from animals with a maximum catheter hemorrhage volume of 10 mL/kg, we reveal a modest trend of improvement with PolySTAT treatment, though no differences are significant (Fig 4.5 B-D).

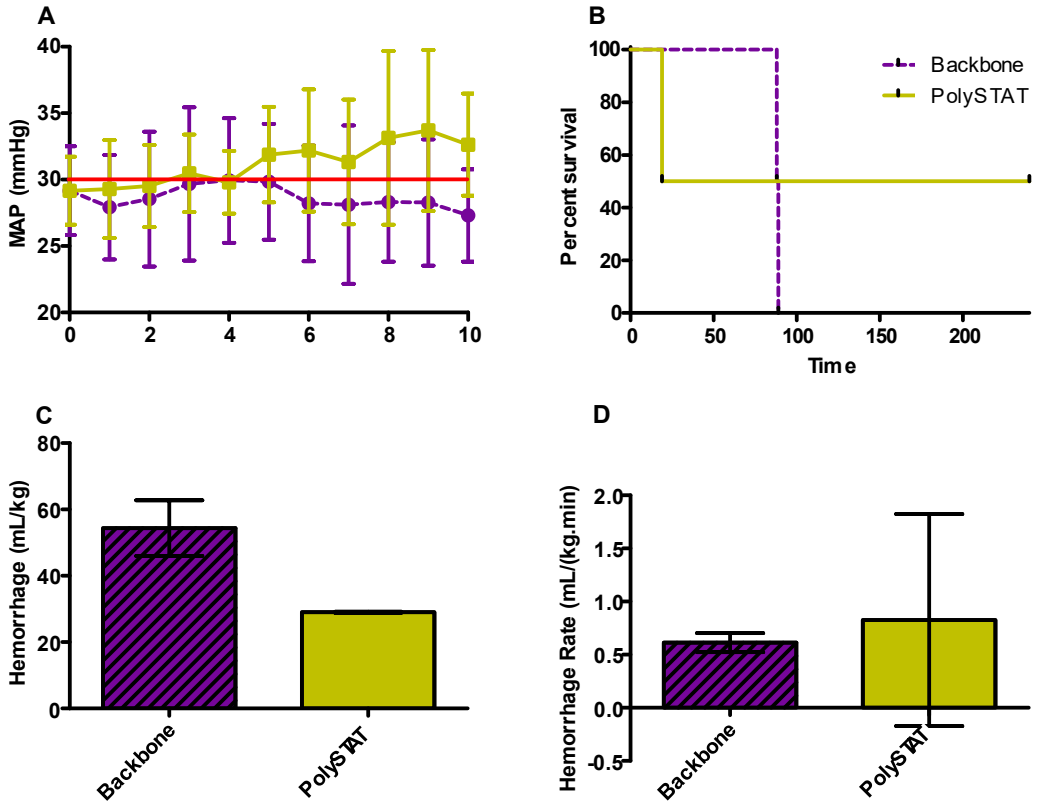

Figure 4.5 Catheter Hemorrhage with a shock goal counteracts PolySTAT benefits. Swine administered 15.0 mg/kg of pHEMA backbone or PolySTAT were observed for 240 minutes. A, MAP of all animals receiving PolySTAT infusion. The red line indicates the goal MAP of 30 mm Hg above which pigs receive catheter hemorrhage. B, Survival of animals with a maimum Survival over the course of observation for PolySTAT (solid gold) and pHEMA backbone (dashed purple). B, hemorrhage normalized to body mass. C, survival time-normalized hemorrhage rates.

5.4 Discussion and Conclusions

PolySTAT is a promising therapeutic which, with strong results in rat models of traumatic injury[66,97], requires evaluation in a large animal model to next determine its fit for translation. In this work, we evaluated the safety of PolySTAT in pigs to determine feasibility of swine models of traumatic injury. We paid close attention to PAP due to previous observations suggesting that nanotechnology, synthetic hemostats and otherwise, can be fatal in pigs when they elicit CARPA[50,57,121]. We also examined the efficacy of PolySTAT in injured pigs to inform model development for a large-scale large animal study in the future.

PolySTAT treatment did not lead to a spike in PAP when administered to animals with or without injury. This is important for the feasibility of future evaluation in swine. Notably, significant engineering was required to ensure that synthetic platelets developed by the Lavik group did not elicit CARPA which led to massive exsanguination through a significant immune response[50]. A spike in PAP, while not fatal, is also triggered by fibrinogen concentrate when administered as an hemorrhage intervention as demonstrated by White *et al*[119]. Our findings not only suggest that PolySTAT is feasible for use swine and is unlikely to elicit CARPA responses in humans, but also that peptide-polymer conjugates may be an advantageous platform for nanotechnology since CARPA has plagued many classes of nanocarriers.

In our current model of traumatic injury via aortic tear, PolySTAT administration did not improve survival nor did it decrease bleeding. Our results were important nonetheless as between we confirmed a resuscitative effect with PolySTAT administered at doses of 9mg/kg or greater in injured and non-injuted swine. This is important for model development as we will necessarily alter our catheter hemorrhage protocol so as to not punish material-induced resuscitation with upper goal MAPs during shock phases. Knowledge of resuscitative effects also has larger impact in the context of PolySTAT as a therapeutic. Resuscitation is an important aspect of emergency medicine and must be tightly regulated such that pressures are great enough to keep a patient out of shock, but not so great that nascent clots are disrupted and hemorrhage is exacerbated[22,25,26]. Patients, porcine and otherwise, receiving PolySTAT in the future may require smaller volumes of resuscitation fluids due to the material's resuscitative effects. Alternatively, these resuscitative effects may be found to be too strong too early in hemostasis and cause pressures at which a clot

cannot sufficiently form. In this case, we know from our non-injury pigs that doses of 5.5 mg/kg and lower do not induce resuscitation. Future work may also aim to engineer our tunable material to further enable resuscitation – larger and more hydrophilic molecules can act as stronger volume expanders[56,123].

Moving forward, greater model development is required to evaluate PolySTAT as a treatment for traumatic injury in swine. PolySTAT acts very strongly as an antifibrinolytic, highlighted by a low recurrence of bleeding in rats treated PolySTAT after femoral artery injury[66]. Swine, however, form fibrin clots which are highly robust against plasmin degradation[124]. Landskroner *et al* demonstrated that porcine clots formed with 12 mL serum experienced < 10% lysis after 1 h of incubation with 1 mg of plasmin, whereas human, sheep, and cow serum experienced ≥ 25% lysis. Pig plasma's inherent strength against fibrinolysis may result in a small opportunity for PolySTAT to show an effect in swine models. Moving forward, we will develop a coagulopathic model which more closes mimics the state of a trauma patient as described by Mittlechner *et al*[125]. Finally, we can explore other large animal species that have been used for hemorrhage models[44,57,124,126].

Overall, this work demonstrates that PolySTAT does not elicit CARPA at a dose of 15 mg/kg or lower. This establishes feasibility in swine for future studies as well as shows the promise of polymer drug delivery platforms as safe alternatives to nanoparticles and other larger molecular structures.

5.5 *REFERENCES*

1. WISQARS: Leading Causes of Death Reports. *Centers for Disease Control and Prevention* (2015).
2. WISQARS: Years of Potential Life Lost. *Centers for Disease Control and Prevention* (2015).
3. Murray, C. J. L., Lopez, A. D., Mathers, C. D. & Stein, C. *The Global Burden of Disease 2000 project: aims, methods and data sources*. (2001).
4. World Health Organization: The top 10 causes of death. (2017). Available at: http://www.who.int/mediacentre/factsheets/fs310/en/.
5. Sauaia, A. *et al.* Epidemiology of Trauma Deaths: A Reassessment. *J. Trauma* **38,** 185–193 (1995).

6. Lerner, E. B. & Moscati, R. M. The Golden Hour : Scientific Fact or Medical ‘Urban Legend’. *Am. Emerg. Med.* **8,** 758–760 (2001).
7. Kauvar, D. S., Lefering, R. & Wade, C. E. Impact of Hemorrhage on Trauma Outcome : An Overview of Epidemiology, Clinical Presentations, and Therapeutic Considerations. *J. Trauma* **60,** 3–11 (2006).
8. Champion, H. R. *et al.* A Profile of Combat Injury. *J. Trauma* **54,** 513–519 (2003).
9. Holcomb, J. B. *et al.* Causes of Death in U . S . Special Operations Forces in the Global War on Terrorism. **245,** 986–991 (2007).
10. Chan, L. W., White, N. J. & Pun, S. H. Synthetic Strategies for Engineering Intravenous Hemostats. *Bioconjug. Chem.* **26,** 1224–1236 (2015).
11. Chen, H., Locke, D., Liu, Y., Liu, C. & Kahn, M. L. The Platelet Receptor GPVI Mediates Both Adhesion and Signaling Responses to Collagen in a Receptor Density-dependent Fashion*. **277,** 3011–3019 (2002).
12. Daniel, J. L. *et al.* Molecular Basis for ADP-induced Platelet Activation. **273,** 2024–2029 (1998).
13. Klinik, M. *et al.* Molecular Mechanisms of Platelet Activation. *Pharm. Rev.* **69,** 58–141 (1989).
14. Shattil, S. J., Hoxie, J. A., Cunningham, M. & Brass, L. F. Changes in the Platelet Membrane Glycoprotein IIb * IIIa Complex during Platelet Activation *. **260,** (1985).
15. Takeoka, S. *et al.* Function of fibrinogen. **312,** 773–779 (2003).
16. Tomiyama, Y., Tsubakio, T. & Kurata, Y. The Arg-Gly-Asp (RGD) recognition site of platelet glycoprotein IIb- IIIa on nonactivated platelets is accessible to high-affinity macromolecules. *Blood* **79,** 2303–2312 (2011).
17. Davie, E. W., Fujikawa, K. & Kisiel, W. The Coagulation Cascade: Initiation, Maintenance, and Regulation. *Biochemistry* **30,** 10363–10370 (1991).
18. Morrison, D. C. & Cochrane, C. G. Direct Evidence For Hageman Factor (Factor XII) Activation by Bacterial Lipopolysaccharides. *J. Exp. Med.* **140,** 797–811 (1974).
19. Bouma, B. N. & Griffin, J. H. Human blood coagulation factor XI . Purification , properties , and mechanism of activation by activated factor XII. *J. Biol. Chem.* **252,** 6432–6437 (1977).
20. Hoffman, M., Monroe, D. M. & Roberts, H. R. Activated factor VII activates factors IX

and X on the surface of activated platelets : thoughts on the mechanism of action of ... *Blood Coagul. Fibrinolysis* **9,** S61–S65 (1998).

21. Mann, K. G., Brummel, K. & Butenas, S. What is all that thrombin for? *J Thromb Haemost* **1,** 1504–1514 (2003).
22. White, N. J. Mechanisms of trauma-induced coagulopathy. *Haematology* 660–663 (2013).
23. Kushimoto, S., Kudo, D. & Kawazoe, Y. Acute traumatic coagulopathy and trauma-induced coagulopathy : an overview. *J. Intensive Care* 1–7 (2017). doi:10.1186/s40560-016-0196-6
24. Brohi, K., Singh, J., Heron, M. & Coats, T. Acute traumatic coagulopathy. *J. Trauma* **54,** 1127–1130 (2003).
25. Kaafarani, H. M. a & Velmahos, G. C. Damage control resuscitation in trauma. *Scand. J. Surg.* **103,** 81–88 (2014).
26. Mikhail, J. The trauma triad of death: hypothermia, acidosis, and coagulopathy. *AACN clinical issues* **10,** 85–94 (1999).
27. Niles, S. E. *et al.* Increased Mortality Associated With the Early Coagulopathy of Trauma in Combat Casualties. *J. Trauma Inj. Infect. Crit. Care* **64,** 1459–1465 (2008).
28. Standbury, L. G. & Hess, J. R. Blood Transfusion in World War I : The Roles of Lawrence Bruce. *Transfus. Med. Rev.* **23,** 232–236 (2009).
29. Boyle, R., Willis, T. & Wren, C. The History of Blood Transfusion. *Br. J. Haemotology* **110,** 758–767 (2000).
30. Duchesne, J. C., Hunt, J. P., Wahl, G. & Marr, A. B. Review of Current Blood Transfusions Strategies in a Mature Level I Trauma Center : Were We Wrong for the Last 60. *J. Trauma* **65,** 272–278 (2008).
31. Repine, T. B., Perkins, J. G., Kauvar, D. S. & Blackborne, L. The Use of Fresh Whole Blood in Massive Transfusion. **60,** (2005).
32. Sihler, K. C. & Napolitano, L. M. Complications of Massive Transfusion. *Chest* **137,** 209–220 (2010).
33. Riou, B. *et al.* Recombinant factor VIIa (Novoseven) as adjunctive therapy for bleeding contorl in trauma - a randomized. placebo-controlled trial. in *Shock* 228 (2004).
34. Rizoli, S. B. *et al.* Recombinant activated factor VII as an adjunctive therapy for bleeding control in severe trauma patients with coagulopathy : subgroup analysis from two

randomized trials. *Crit. Care* **10,** 1–11 (2006).

35. Raza, I. *et al.* The incidence and magnitude of fibrinolytic activation in trauma patients. *J. Thromb. Haemost.* **11,** 307–314 (2013).
36. Williams-johnson, J. A., Mcdonald, A. H., Strachan, G. G. & Williams, E. W. Effects of Tranexamic Acid on Death, Vascular Occlusive Events, and Blood Transfusion in Trauma Patients with Significant Haemorrhage (CRASH-2) A Randomised, Placebo-Controlled Trial. *West Indian Med J* **59,** 612–624 (2010).
37. Houston, F. S. Military Application of Tranexamic Acid in Trauma Emergency Resuscitation (MATTERs) Study. **147,** 113–119 (2012).
38. Search Results: tranexamic acid. *ClinicalTrials.gov* (2018).
39. Coller, B. S. Interaction of normal, thrombathemis, and Bernard-Soulier platelets with immobilized fibrinogen: defective platelet-fibrinogen interaction in thrombastatin. *Blood* **55,** 169–179 (1980).
40. Coller, B. S. *et al.* Thromboerythrocytes In Vitro Studies of a Potential Autologous , Semi-artificial Alternative to Platelet Transfusions. *J Clin Invest* **98,** 546–555 (1992).
41. Ten, O. Fibrinogen-coated albumin microcapsules reduce bleeding in severely thrombocytopenic rabbits. **9,** 107–111 (1999).
42. Illum, L. *et al.* Blood clearance and organ deposition of intravenously administered colloidal particles . The effects of particle size , nature and shape. **12,** 135–146 (1982).
43. Okamura, Y. *et al.* Hemostatic effects of phospholipid vesicles carrying fibrinogen gamma chain dodecapeptide in vitro and in vivo. *Bioconjug. Chem.* **16,** 1589–96 (2005).
44. Okamura, Y. *et al.* Development of fibrinogen gamma-chain peptide-coated, adenosine diphosphate-encapsulated liposomes as a synthetic platelet substitute. *J. Thromb. Haemost.* **7,** 470–7 (2009).
45. Bertram, J. P. *et al.* Intravenous Hemostat : Nanotechnology to Halt Bleeding. *Sci. Transl. Med.* **1,** 11–22 (2009).
46. Shoffstall, A. J. *et al.* Tuning ligand density on intravenous hemostatic nanoparticles dramatically increases survival following blunt trauma. *Biomacromolecules* **14,** 2790–2797 (2013).
47. Lashof-sullivan, M. *et al.* Hemostatic Nanoparticles Improve Survival Following Blunt Trauma Even after 1 Week Incubation at 50 °C. *ACS Biomater. Sci. Eng.* **2,** 385–392

(2016).

48. Shoffstall, A. J. *et al.* Intravenous hemostatic nanoparticles increase survival following blunt trauma injury. *Biomacromolecules* **13,** 3850–3857 (2012).
49. Hubbard, W. B., Lashof-Sullivan, M. M., Lavik, E. B. & Vandevord, P. J. Steroid-loaded hemostatic nanoparticles combat lung injury after blast trauma. *ACS Macro Lett.* **4,** 387–391 (2015).
50. Onwukwe, C. *et al.* Engineering Intravenously Administered Nanoparticles to Reduce Infusion Reaction and Stop Bleeding in a Large Animal Model of Trauma. (2018). doi:10.1021/acs.bioconjchem.8b00335
51. Gupta, A. Sen, Huang, G., Lestini, B. J., Sagnella, S. & Kottke-marchant, K. RGD-modified liposomes targeted to activated platelets as a potential vascular drug delivery system RGD-modified liposomes targeted to activated platelets as a potential vascular drug delivery system. *Thromb Haemost* **93,** 106–114 (2005).
52. Ravikumar, M., Modery, C. L., Wong, T. L. & Gupta, A. Sen. Peptide-Decorated Liposomes Promote Arrest and Aggregation of Activated Platelets under Flow on Vascular Injury Relevant Protein Surfaces in Vitro. *Biomacromolecules* **13,** 1495–1502 (2012).
53. Ravikumar, M. *et al.* Mimicking Adhesive Functionalities of Blood Platelets using Ligand- Decorated Liposomes. *Bioconjug. Chem.* **23,** 1266–1275 (2012).
54. Modery-Pawlowski, C. L., Tian, L. L., Ravikumar, M., Wong, T. L. & Gupta, A. Sen. In vitro and in vivo hemostatic capabilities of a functionally integrated platelet-mimetic liposomal nanoconstruct. *Biomaterials* **34,** 3031–3041 (2013).
55. Hickman, D. A. *et al.* Intravenous synthetic platelet (SynthoPlate) nanoconstructs reduce bleeding and improve ‘ golden hour ’ survival in a porcine model of traumatic arterial hemorrhage. *Sci. Rep.* 1–14 (2018). doi:10.1038/s41598-018-21384-z
56. Shukla, M., Sekhon, U. D. S., Li, W. & Hickman, D. A. In vitro characterization of SynthoPlate (synthetic platelet) technology and its in vivo evaluation in severely thrombocytopenic mice. *J Thromb Haemost* **15,** 375–387 (2016).
57. Lashof-sullivan, M., Sho, A. & Lavik, E. Intravenous hemostats : challenges in translation to patients. *Nanoscale* **5,** 10719–10728 (2013).
58. Szebeni, J. *et al.* Prevention of infusion reactions to PEGylated liposomal doxorubicin via

tachyphylaxis induction by placebo vesicles: A porcine model. *J. Control. Release* **160,** 382–387 (2012).

59. Brown, A. C. *et al.* Ultrasoft microgels displaying emergent platelet-like behaviours. *Nat. Mater.* **13,** 1–7 (2014).
60. Niewlarowski, S., Regoeczi, E., Stewart, G. J., Senyi, A. F. & Mustard, J. F. Platelet Interaction with Polymerizing Fibrin. **51,** 685–700 (1972).
61. Welsch, N., Brown, A. C., Barker, T. H. & Lyon, L. A. Colloids and Surfaces B : Biointerfaces Enhancing clot properties through fibrin-specific self-cross-linked PEG side-chain microgels. *Colloids Surfaces B Biointerfaces* **166,** 89–97 (2018).
62. Lorand, L. A double-headed Gly-Pro-Arg-Pro ligand mimics the functions of the E domain of fibrin for promoting the end-to-end crosslinking of chains by factor XIII a. **95,** 537–541 (1998).
63. Soon, A. S. C., Lee, C. S. & Barker, T. H. Modulation of fibrin matrix properties via knob:hole affinity interactions using peptide-PEG conjugates. *Biomaterials* **32,** 4406–4414 (2011).
64. Kolodziej, A. F. *et al.* Fibrin Specific Peptides Derived by Phage Display: Characterization of Peptides and Conjugates for Imaging. *Bioconjug. Chem.* **23,** 548–556 (2012).
65. Kolodziej, A. F., Zhang, Z., Overoye-chan, K., Jacques, V. & Caravan, P. Peptide Optimization and Conjugation Strategies Magnetic Resonance Imaging Contrast Agents. **1088,** 185–211
66. Chan, L. W. *et al.* A synthetic fibrin cross-linking polymer for modulating clot properties and inducing hemostasis. *Sci. Transl. Med.* **7,** (2015).
67. Chiefari, J. *et al.* Living Free-Radical Polymerization by Reversible Addition - Fragmentation Chain Transfer : The RAFT Process We wish to report a new living free-radical polymer- ization of exceptional effectiveness and versatility . 1 The living character is conferred by . **9297,** 5559–5562 (1998).
68. Chu, D. S. H. *et al.* Application of living free radical polymerization for nucleic acid delivery. *Acc. Chem. Res.* **45,** 1089–1099 (2012).
69. Kopeček, J., Kopečková, P., Minko, T., Lu, Z. R. & Peterson, C. M. Water soluble polymers in tumor targeted delivery. *J. Control. Release* **74,** 147–158 (2001).

70. Barrett, G. D., Constable, I. J. & Stewart, A. D. Clinical results of hydrogel lens implantation. *J. Cataract Refract. Surg.* **12,** 623–631 (1986).
71. Chan, L. W., White, N. J. & Pun, S. H. A Fibrin Cross-linking Polymer Enhances Clot Formation Similar to Factor Concentrates and Tranexamic Acid in an in Vitro Model of Coagulopathy. *ACS Biomater. Sci. Eng.* (2016). doi:10.1021/acsbiomaterials.5b00536
72. Maegele, M. *et al.* Early coagulopathy in multiple injury: An analysis from the German Trauma Registry on 8724 patients. *Injury* **38,** 298–304 (2007).
73. 6 Factor VIII Concentrates, Factor VIII/von Willebrand Factor Concentrates, Factor IX Concentrates, Activated Prothrombin Complex Concentrates. *Transfus. Med. Hemotherapy* **36,** 409–418 (2009).
74. Okamura, Y. *et al.* Development of fibrinogen c-chain peptide-coated, adenosine diphosphate-encapsulated liposomes as a synthetic platelet substitute. *J Thromb Haemost* **7,** 470–477 (2009).
75. Fasting, C. *et al.* Multivalency as a Chemical Organization and Action Principle. *Angew. Rev.* **51,** 10472–10498 (2012).
76. Spain, S. G. & Cameron, N. R. A spoonful of sugar : the application of glycopolymers in therapeutics. *Polym. Chem.* **2,** 60–68 (2011).
77. Weigandt, K. M., Pozzo, D. C. & Porcar, L. Structure of high density fibrin networks probed with neutron scattering and rheology. *Soft Matter* **5,** 4321–4330 (2009).
78. Weigandt, K. M., Porcar, L. & Pozzo, D. C. In situ neutron scattering study of structural transitions in fibrin networks under shear deformation. *Soft Matter* **7,** 9992–10000 (2011).
79. Yanjarappa, M. J., Gujraty, K. V, Joshi, A., Saraph, A. & Kane, R. S. Synthesis of Copolymers Containing an Active Ester of Methacrylic Acid by RAFT : Controlled Molecular Weight Scaffolds for Biofunctionalization. *Biomacromolecules* **7,** 1665–1670 (2006).
80. Kirby, N. M. *et al.* research papers A low-background-intensity focusing small-angle X-ray scattering undulator beamline. 1670–1680 (2013). doi:10.1107/S002188981302774X
81. Hammouda, B., Ho, D. L. & Kline, S. Insight into Clustering in Poly (ethylene oxide) Solutions. *Macromolecules* **37,** 6932–6937 (2004).
82. Glinka, C. J. *et al.* The 30 m Small-Angle Neutron Scattering Instruments at the National Institute of Standards and Technology. *J. Appl. Crystallogr.* **31,** 430–445 (1998).

83. Kline, S. R. Reduction and analysis of SANS and USANS data using IGOR Pro. *J. Appl. Crystallogr.* **39,** 895–900 (2006).
84. Barker, J. G. *et al.* Design and performance of a thermal-neutron double-crystal diffractometer for USANS at NIST. *J. Appl. Crystallogr.* **38,** 1004–1011 (2005).
85. Terech, P. Structural Study of Cholesteryl Anthraquinone-2-carboxylate (CAQ) Physical Organogels by Neutron and X-ray Small Angle Scattering. *J. Phys. Chem.* **100,** 3759–3766 (1996).
86. Teixeira, J. Small-Angle Scattering by Fractal Systems. *J. Appl. Crystallogr.* **21,** 781–785 (1988).
87. Hammouda, B. & Horkay, F. Clustering and Solvation in Poly(acrylic acid) Polyelectrolyte Solutions. *Macromolecules* **38,** 2019–2021 (2005).
88. Dowling, M. B. *et al.* Biomaterials A self-assembling hydrophobically modi fi ed chitosan capable of reversible hemostatic action. *Biomaterials* **32,** 3351–3357 (2011).
89. Laudano, A. P. & Doolittle, R. F. Studies on synthetic peptides that bind to fibrinogen and prevent fibrin polymerization. Structural requirements, number of binding sites, and species differences. *Biochemistry* **19,** 1013–1019 (1980).
90. Lukyanov, A. N. & Torchilin, V. P. Micelles from lipid derivatives of water-soluble polymers as delivery systems for poorly soluble drugs. **56,** 1273–1289 (2004).
91. Rizvi, S. A. A. & Saleh, A. M. Applications of nanoparticle systems in drug delivery technology. *Saudi Pharm. J.* **26,** 64–70 (2018).
92. Kieler-ferguson, H. M. & Fr, J. M. J. Clinical developments of chemotherapeutic nanomedicines : polymers and liposomes for delivery of camptothecins and platinum (II). **5,** (2013).
93. Press, D. Effective use of nanocarriers as drug delivery systems for the treatment of selected tumors. 7291–7309 (2017).
94. Langer, R. Drug delivery and targeting. **392,** 5–10 (1998).
95. Montet, X., Funovics, M., Montet-abou, K., Weissleder, R. & Josephson, L. Multivalent Effects of RGD Peptides Obtained by Nanoparticle Display. 6087–6093 (2006). doi:10.1021/jm060515m
96. Lee, H., Fonge, H., Hoang, B., Reilly, R. M. & Allen, C. articles The Effects of Particle Size and Molecular Targeting on the Intratumoral and Subcellular Distribution of

Polymeric Nanoparticles. **7,** 1195–1208 (2010).

97. Lamm, R. J. *et al.* Peptide valency plays an important role in the activity of a synthetic fibrin-crosslinking polymer. *Biomaterials* **132,** 96–104 (2017).
98. Devlin, J., Panganiban, L. & Devlin, P. Random peptide libraries: a sourse of specific protein binding molecules. *Science (80-.).* **249,** 404–406 (1990).
99. Fan, S. *et al.* Curcumin-loaded PLGA-PEG nanoparticles conjugated with B6 peptide for potential use in Alzheimer ' s disease. *Drug Deliv.* **25,** 1044–1055 (2018).
100. Duvall, C. L., Convertine, A. J., Benoit, D. S. W., Hoffman, A. S. & Stayton, P. S. articles Intracellular Delivery of a Proapoptotic Peptide via Conjugation to a RAFT Synthesized Endosomolytic Polymer. (2010).
101. Chu, D. S. *et al.* As featured in : Biomaterials Science. (2015). doi:10.1039/c4bm00259h
102. Johnson, R. N. *et al.* Synthesis of Statistical Copolymers Containing Multiple Functional Peptides for Nucleic Acid Delivery. *Biomacromolecules* **11,** 3007–13 (2010).
103. Chu, D. S. H., Schellinger, J. G., Bocek, M. J., Johnson, R. N. & Pun, S. H. Optimization of Tet1 ligand density in HPMA-co-oligolysine copolymers for targeted neuronal gene delivery. *Biomaterials* **34,** 9632–9637 (2013).
104. Schellinger, J. G. *et al.* Melittin-grafted HPMA-oligolysine based copolymers for gene delivery. *Biomaterials* **34,** 2318–2326 (2013).
105. Kanaide, H. & Shainoff, J. R. Cross-linking of fibrinogen and fibrin by fibrin-stabilizing factor (factor XIIIa). *Transl. Res.* **85,** 574–597 (1975).
106. O'Brien-Simpson, N. M., Ede, N. J., Brown, L. E., Swan, J. & Jackson, D. C. Polymerization of unprotected synthetic peptides: A view toward synthetic peptide vaccines. *J. Am. Chem. Soc.* **119,** 1183–1188 (1997).
107. Hasson, C. J., Caldwell, G. E. & Emmerik, R. E. A. Van. NIH Public Access. *Motor Control* **27,** 590–609 (2009).
108. Studenovská, H., Šlouf, M. & Rypáček, F. Poly(HEMA) hydrogels with controlled pore architecture for tissue regeneration applications. *J. Mater. Sci. Mater. Med.* **19,** 615–621 (2008).
109. Kopeckova, P. Water soluble polymers in tumor targeted delivery. *J. Control. Release* **74,** 147–158 (2001).
110. Cunningham, V. J. *et al.* Poly(glycerol monomethacrylate) − Poly(benzyl methacrylate)

Diblock Copolymer Nanoparticles via RAFT Emulsion Polymerization: Synthesis, Characterization, and Interfacial Activity. (2014). doi:10.1021/ma501140h

111. Save, M., Weaver, J. V. M., Armes, S. P. & Mckenna, P. Atom Transfer Radical Polymerization of Hydroxy-Functional Methacrylates at Ambient Temperature: Comparison of Glycerol Monomethacrylate with 2-Hydroxypropyl Methacrylate. 1152–1159 (2002). doi:10.1021/ma011541r
112. Das, D. *et al.* RAFT polymerization of ciprofloxacin prodrug monomers for the controlled intracellular delivery of antibiotics. *Polym. Chem* **7,** 826–837 (2016).
113. Shin, H. C., Alani, A. W. G., Rao, D. A., Rockich, N. C. & Kwon, G. S. Multi-drug loaded polymeric micelles for simultaneous delivery of poorly soluble anticancer drugs. *J. Control. Release* **140,** 294–300 (2009).
114. Hughes, H. C. Swine in cardiovascular research. *Lab Anim. Sci.* **36,** 348–350 (1986).
115. Swindle, M. M., Makin, A., Herron, A. J., Clubb, F. J. & Frazier, K. S. Swine as Models in Biomedical Research and Toxicology Testing. *Vet. Pathol.* **49,** 344–356 (2012).
116. Pusateri, A. E. *et al.* Effect of a Chitosan-Based Hemostatic Dressing on Blood Loss and Survival in a Model of Severe Venous Hemorrhage and Hepatic Injury in Swine. *J trauma* **54,** 177–182 (2003).
117. Pusateri, A. E. *et al.* Advanced Hemostatic Dressing Development Program : Animal Model Selection Criteria and Results of a Study of Nine Hemostatic Dressings in a Model of Severe Large Venous Hemorrhage and Hepatic Injury in Swine. *J Trauma* **55,** 518–526 (2003).
118. Stern, S. *et al.* RESUSCITATION WITH THE HEMOGLOBIN-BASED OXYGEN CARRIER , HBOC-201 , IN A SWINE MODEL OF SEVERE UNCONTROLLED HEMORRHAGE AND TRAUMATIC BRAIN INJURY. *Shock* **31,** 64–79 (2009).
119. White, N. J., Wang, X., Liles, W. C. & Stern, S. Fibrinogen Concentrate Improves Survival During Limited Resuscitation of Uncontrolled Hemorrhagic Shock in a Swine Model. *Shock* **42,** 456–463 (2014).
120. Szebeni, J., Bed, P. & Rozsnyay, Z. Liposome-induced complement activation and related cardiopulmonary distress in pigs : factors promoting reactogenicity of Doxil and AmBisome. **8,** 176–184 (2012).
121. Szebeni, J. *et al.* A porcine model of complement-mediated infusion reactions to drug

carrier nanosystems and other medicines ☆. **64,** 1706–1716 (2012).

122. Bertram, J. P. *et al.* Intravenous Hemostat : Nanotechnology to Halt Bleeding. (2009).
123. Boldt, J., Haisch, G., Suttner, S., Kumle, B. & Schellhaass, A. Effects of a new modifed, balanced hydroxyethyl starch preparation (Hextend). *Br. J. Anaesth.* **89,** 722–728 (2002).
124. Landskroner, K., Olson, N. & Jesmok, G. Cross-species pharmacologic evaluation of plasmin as a direct-acting thrombolytic agent: Ex vivo evaluation for large animal model development. *J. Vasc. Interv. Radiol.* **16,** 369–377 (2005).
125. Mitterlechner, T. *et al.* Prothrombin complex concentrate and recombinant prothrombin alone or in combination with recombinant factor X and FVIIa in dilutional coagulopathy: A porcine model. *J. Thromb. Haemost.* **9,** 729–737 (2011).
126. R. Baylis, J. *et al.* Rapid hemostasis in a sheep model using particles that propel thrombin and tranexamic acid. *Laryngoscope* **127,** 787–793 (2017).
127. Ngambenjawong, C., Gustafson, H. H., Sylvestre, M. & Pun, S. H. A Facile Cyclization Method Improves Peptide Serum Stability and Confers Intrinsic Fluorescence. *ChemBioChem* **18,** 2395–2398 (2017).
128. Von Maltzahn, G. *et al.* Nanoparticles that communicate in vivo to amplify tumour targeting. *Nat. Mater.* **10,** 545–552 (2011).
129. Liu, G. W. *et al.* Glomerular disease augments kidney accumulation of synthetic anionic polymers. *Biomaterials* **178,** 317–325 (2018).
130. Tabata, Y. & Ikada, Y. Effect of the size and surface charge of polymer microspheres on their phagocytosis by macrophage. *Biomaterials* **9,** 356–362 (1988).
131. Caliceti, P. & Veronese, F. P harmacokinetic and biodistribution properties of poly(ethylene glycol)–protein conjugates Paolo. *Adv. Drug Deliv. Rev.* **55,** 1261–1277 (2003).
132. Beier, J. I. *et al.* Fibrin accumulation plays a critical role in the sensitization to lipopolyccharide-induced liver injury caused by ethanol in mice. *Hepatology* **49,** 1545–1553 (2009).
133. Imokawa, S. *et al.* Tissue factor expression and fibrin deposition in the lungs of patients with idiopathic pulmonary fibrosis and systemic sclerosis. *Am. J. Respir. Crit. Care Med.* **156,** 631–636 (1997).
134. Brown, L. F., Dvorak, A. M. & Dvorak, H. F. Leaky vessels, fibrin deposition, and

fibrosis: a sequence of events common to solid tumors and to many other types of disease. *Am. Rev. Respir. Dis.* **140,** 1104–7 (1989).

135. Hiramoto, R., Bernecky, J., Jurandowski, J. & Pressman, D. Fibrin in Human Tumors. *Cancer Res.* **20,** 592–593 (1960).
136. Fernandez, P. M., Patierno, S. R. & Rickles, F. R. Tissue factor and fibrin in tumor angiogenesis. *Semin. Thromb. Hemost.* **30,** 31–44 (2004).
137. Wallace, A. C. Demonstration of Fibrin in Early Stages of Experimental Metastases. *Cancer Res.* **36,** 1904–1909 (1976).
138. Dirix, L. Y. *et al.* Plasma fibrin D-dimer levels correlate with tumour volume, progression rate and survival in patients with metastatic breast cancer. *Br. J. Cancer* **86,** 389–395 (2002).
139. Chu, D. S. *et al.* MMP9-sensitive polymers mediate environmentally-responsive bivalirudin release and thrombin inhibition. *Biomater. Sci.* **3,** 41–45 (2015).
140. Warkentin, T. E., Greinacher, A. & Koster, A. Bivalirudin. *Thromb. Haemost.* **99,** 830–839 (2008).
141. Hejna, M., Raderer, M. & Zielinski, C. C. Inhibition of metastases by anticoagulants. *J. Natl. Cancer Inst.* **91,** 22–36 (1999).
142. Amirkhosravi, A. *et al.* Tissue factor pathway inhibitor reduces experimental lung metastasis of B16 melanoma. *Thromb. Haemost.* **87,** 930–936 (2002).
143. Kondapaka, S. B., Fridman, R. & Reddy, K. B. Epidermal growth factor and amphiregulin up-regulate matrix metalloproteinase-9 (MMP-9) in human breast cancer cells. *Int. J. Cancer* **70,** 722–726 (1997).
144. Svendsen, L., Blombäck, B., Blombäck, M. & Olsson, P. I. Synthetic chromogenic substrates for determination of trypsin, thrombin and thrombin-like enzymes. *Thromb. Res.* **1,** 267–278 (1972).
145. Reinhard, J., Brösicke, N., Theocharidis, U. & Faissner, A. The extracellular matrix niche microenvironment of neural and cancer stem cells in the brain. *Int. J. Biochem. Cell Biol.* **81,** 174–183 (2016).
146. Palumbo, J. S. *et al.* Platelets and fibrin(ogen) increase metastatic potential by impeding natural killer cell-mediated elimination of tumor cells. *Blood* **105,** 178–185 (2005).
147. Ogston, A. OGSTON, M.D., Surgeon. *J. Anat.* **16,** 526–567 (1882).

148. Lowry, F. D. Staphylococcus aureus Infections. *N. Engl. J. Med.* **339,** 520–532 (1998).
149. Lake, J. G. *et al.* Pathogen distribution and antimicrobial resistance among pediatric healthcare-associated infections reported to the National Healthcare Safety Network, 2011-2014. *Infect. Control Hosp. Epidemiol.* **39,** 1–11 (2018).
150. Weiner, L. M. *et al.* Antimicrobial-Resistant Pathogens Associated with Healthcare-Associated Infections: Summary of Data Reported to the National Healthcare Safety Network at the Centers for Disease Control and Prevention, 2011-2014. *Infect. Control Hosp. Epidemiol.* **37,** 1288–1301 (2016).
151. Lee, A. S. *et al.* Methicillin-resistant Staphylococcus aureus. *Nat. Rev. Dis. Prim.* **4,** (2018).
152. Jevons, P. M. 'Celbenin'-resistant Staphylococci. *Br. Med. J.* **1,** 124–125 (1961).
153. Hiramatsu, K. *et al.* Methicillin-resistant Staphylococcus aureus clinical strani with reduced vancomycin susceptibility. *J. Antimicrob. Chemother.* **40,** 135–146 (1997).
154. Huh, A. J. & Kwon, Y. J. 'Nanoantibiotics': A new paradigm for treating infectious diseases using nanomaterials in the antibiotics resistant era. *J. Control. Release* **156,** 128–145 (2011).
155. Loughman, A. *et al.* Roles for fibrinogen, immunoglobulin and complement in platelet activation promoted by Staphylococcus aureus clumping factor A. *Mol. Microbiol.* **57,** 804–818 (2005).
156. Mcdevitt, D. *et al.* Characterization of the interaction between the Staphylococcus aureus clumping factor (ClfA) and fibrinogen. *Eur. J. Biochem.* **247,** 416–424 (1997).
157. Que, Y. *et al.* Reassessing the Role of Staphylococcus aureus Clumping Factor and Fibronectin-Binding Protein by Expression in Lactococcus. *Infect. Immun.* **69,** 6296–6302 (2001).
158. Patti, J. M. A humanized monoclonal antibody targeting Staphylococcus aureus. *Vaccine* **22,** (2004).
159. Takeoka, S. *et al.* Function of fibrinogen gamma-chain dodecapeptide-conjugated latex beads under flow. *Biochem. Biophys. Res. Commun.* **312,** 773–9 (2003).
160. Okamura, Y. *et al.* Hemostatic effects of fibrinogen gamma-chain dodecapeptide-conjugated polymerized albumin particles in vitro and in vivo. *Transfusion* **45,** 1221–8 (2005).

161. Okamura, Y., Maekawa, I., Teramura, Y., Maruyama, H. & Handa, M. Hemostatic Effects of Phospholipid Vesicles Carrying Fibrinogen γ Chain Dodecapeptide in Vitro and in Vivo. 30–33 (2005).
162. Pease, D. C. An Electron Microscopy Study of Red Bone Marrow. *Blood* **11,** 501–526 (1956).
163. Wagner, B. C. L. *et al.* Analysis of GPIIb/IIIa Receptor Number by Quantification of 7E3 Binding to Human Platelets. (2015).
164. Nilsson, I. M., Patti, J. M., Bremell, T., Höök, M. & Tarkowski, A. Vaccination with a recombinant fragment of collagen adhesin provides protection against Staphylococcus aureus-mediated septic death. *J. Clin. Invest.* **101,** 2640–2649 (1998).
165. Stevens, K. A., Sheldon, B. W., Klapes, N. A. & Klaenhammer, T. R. Nisin treatment for inactivation of Salmonella species and other gram- negative bacteria. *Appl. Environ. Microbiol.* **57,** 3613–3615 (1991).
166. Millette, M., Le Tien, C., Smoragiewicz, W. & Lacroix, M. Inhibition of Staphylococcus aureus on beef by nisin-containing modified alginate films and beads. *Food Control* **18,** 878–884 (2007).
167. Hancock, R. E. W. Peptide antibiotics. *Lancet* **349,** 418–422 (1997).
168. Biscola, V. *et al.* Isolation and characterization of a nisin-like bacteriocin produced by a Lactococcus lactis strain isolated from charqui, a Brazilian fermented, salted and dried meat product. *Meat Sci.* **93,** 607–613 (2013).
169. Miao, J. *et al.* Membrane disruption and DNA binding of Staphylococcus aureus cell induced by a novel antimicrobial peptide produced by Lactobacillus paracasei subsp. tolerans FX-6. *Food Control* **59,** 609–613 (2016).

CHAPTER 6: PROPOSED FUTURE WORK

Robert J. Lamm, Suzie H. Pun

6.1 INTRODUCTION

PolySTAT is an exciting biomaterial solution for hemostasis. However, for use in the clinic there are still improvements to be made. Additionally, multivalent display of fibrin-binding peptides is a platform that can be used for multiple applications. In this chapter, we will discuss three proposed projects. The first will pursue a water-soluble version of FBP. This will improve the ability to efficiently synthesize the material and may expand the administration strategies by allowing to deliver more material per injection. The second proposed project will explore the use of multivalent display of FBP as a platform for modulating the tumor metastatic niche to discourage the spread of highly metastatic cancer. Finally, a peptide-polymer platform for targeting *staphylococcus aureas* based on an early suspended project from my time in the Pun Lab.

6.2 PURSUIT OF A WATER-SOLUBLE FIBRIN-BINDING PEPTIDE

The Caravan group at Massachusetts General Hospital discovered multiple families of fibrin-binding peptides via phage display and subsequently optimized these for binding specificity to fibrin and serum stability[64,65]. The current form of fibrin-binding peptide (FBP, sequence: Ac-Y(DGl)C(HPr)(3Cl-Y)GLCYIQGK-Am) used in PolySTAT contains many hydrophobic and aromatic amino acids (7 of 13). In addition to strong hydrophobicity, FBP contains only 2 charges due to modifications at the N- and C-termini; one of these charges is lost post-conjugation via the C-terminal lysine. Thus, FBP in our hands is not soluble in water, yet due to multiple ionic charges it is not soluble in highly non-polar organic solvents; it is only usable in polar organic solvents such as dimethyl sulfoxide. This greatly diminishes the possible synthesis strategies and the solubility of the final product. A water-soluble peptide would provide for aqueous synthesis of methacrylamide-containing monomers and facile synthesis of water-soluble polymers with comonomers such as HPMA[102,109]. As described in Chapter 4, increased solubility of the final PolySTAT product is advantageous from a synthesis perspective.

Work by the Caravan group during their optimization of FBP led to multiple candidates which may have improved solubility in aqueous solvents. Notably, early versions of FBP contain an additional amide-containing glutamine at the N-terminus that may improve solubility. The alanine scan performed by Kolodziej *et al* can be used to inform which amino acids alter the affinity of the peptide to fibrin[65]. From there, peptides can be synthesized with more polar resides. Additionally, polar residues containing charges (D, E, H, K, R) can be incorporated on either side of the sequence. Finally, the disulfide cyclization can be replaced by other methods. Notably, our lab has demonstrated facile cyclization of peptides that helps with stability but also confers fluorescence[127]. This method, or other strategies for cyclization, may not only alter solubility but may also provide functionality.

Another option, however would be to utilize a form of the peptide that has been successfully used in nanotechnology in the past[128]. The Bhatia group previously described liposomes targeted to fibrin via decoration with FBP. The sequence used in this case contains 3 D-aspartic acid residues to confer additional charge and water solubility to the peptide. Utilizing the sequence Ac-dddYeC(HPr)(3Cl-Y)GLCYIQGK-Am, may provide a water-soluble peptide that allows for the use of aqueous polymerization of methacrylamide-containing monomers. This will also confer increased water solubility which will result in more efficient purification of the resulting PolySTAT materials. A concern with this strategy, however, would be the large increase in negative charge of the material. The Lavik group's issues with their synthetic platelets arose from charge-related complement activation; in fact, their solution was to reduce the negative charge present on their targeting peptide[50]. Special care will need be paid to the response to materials containing this peptide.

After synthesis of materials with this alternative peptide, *in vitro* characterization by ROTEM, *in vivo* demonstration of clot enhancement, and *in vivo* evaluation in a model of traumatic injury will be performed. While we do not expect activity of the material to be significantly changed since the modified peptide has been used for fibrin targeting, the biodistribution may be changed. Notably, our lab demonstrated that highly negatively charged polymers have preferential accumulation to the kidneys[129]. Highly negatively charged materials have also been shown to be

sequestered by phagocytes[130]. These more negatively charge PolySTATs will also have to be evaluated for complement reaction. This will be performed mechanistically via complement activation assay as performed by Onwukwe *et al*[50] and Hickman *et al*[55] and functionally by performing infusions of material in swine as described in Chapter 5.

Additional water solubility not only has the potential for improved synthetic efficiency but may allow for increased administration. Increased solubility will allow for a higher dose of material to be delivered in the same volume of vehicle. In this case, not only will this increase the maximum administrable dose of PolySTAT, it may allow for alternative administration techniques. Specifically, intramuscular (IM) injection is an attractive route of administration since it does not require training to dose the patient as seen with EpiPens®. Also, the synthetic nature of PolySTAT lends it well to a stable drug that sit within an IM injecting-pen. IM administration, however, leads to much lower bioavailability and will therefore requires large doses due to the degree of transport necessary to distribute rapidly[131]. Thus, improved water solubility may enable the administration of PoylSATT via IM injection.

6.3 FIBRIN-TARGETED MODULATION OF TUMOR METASTATIC ENVIRONMENT

Fibrin deposition is present in many disease states including liver disease[132], pulmonary fibrosis[133], and cancer[134]. PolySTAT is, therefore, an attractive candidate as a targeting platform for the delivery of therapeutics to the extracellular environment of these diseases. In cancer, extravascular fibrin deposits in the regions around solid tumors[135]. Additionally, fibrin promotes angiogenesis[136] and metastatic outgrowth[137,138]. Our lab has work currently in review describing modulation of metastatic disease using PolySTAT as a fibrin-stabilizing polymer (FSP). When 15 mg/kg FSP was administered every other day for a week to mice in a model of brain metastasis, metastases were more severe, and survival was decreased significantly. In this model, FSP accumulated in the tumor environment, suggesting the potential to deliver therapeutics to hard-to-identify nascent metastases.

The Pun lab, in collaboration with the Horner group, previously reported the use of a thrombin inhibitor, bivalirudin, to enhance healing in spinal cord injury[139]. Bivalirudin is a 20-amino acid peptide inhibitor of thrombin that is FDA-approved for anticoagulation under multiple indications[140]. Limiting coagulation is known to reduce metastasis and in some cases inhibit metastasis formation[141]. In one example, mice seeded with melanoma cells engineered to express tissue factor pathway inhibitor (TFPI) formed 78% fewer lung nodules than animals seeded with melanoma cells not expressing TFPI[142]. While TFPI is a large protein difficult to deliver, bivalirudin is a cargo that our lab has experience delivering that similarly inhibits the coagulation cascade.

A critical first step is to determine whether PolySTAT with 4 peptides or fewer on average still benefits from the targeting of FBP. We previously demonstrated that PolySTAT with 4 peptides or fewer do not enhance clot formation by ROTEM[97]. We will synthesize fluorescently-labeled material with low peptide valency and administer to animals in the metastatic mouse model described above. Ideally, low peptide valency materials will accumulate in tumors and metastases, providing a fibrin-targeting platform that does not affect clotting in the body.

Next, materials with both FBP and bivalirudin (FB Polymers) will be synthesized via post-polymerization conjugation. Backbone polymers will contain thiol-reactive pyridyl disulfide ethyl methacrylate (PDSEMA), amine-reactive n-succinimidyl methacrylate (NHSMA), and glycerol monomethacrylate (GmMA) as an inert, water-soluble comonomer. Note that the bivalirudin peptide attached via cysteine will need to be reacted first as the cysteine could disrupt the disulfide bond in FBP. Also note that bivalirudin contains no lysines, allowing for retention of the activated esters for reaction with FBP once unreacted bivalirudin (and associated thiols) are removed. We will synthesize bivalirudin with and without an enzyme-cleavable peptide linker to ensure optimal activity upon arrival at the metastasis site[139]. Matrix metalloproteinase-9 (MMP9) is a collagenase expressed by various cancers, including breast cancer[143].

FB Polymers will be studied for thrombin inhibition *in vitro*. After material characterization to ensure synthesis, the materials will be tested for direct thrombin

inhibition via a chromogenic thrombin-cleavable substrate[144]. This will be performed with and without the MMP-cleavable linker and with and without MMP9 to ensure activity of the peptide. While previous demonstrated that the peptide is active while retained on the polymer[139], increased diffusion upon arrival at the metastatic site may be beneficial.

Next, ROTEM will be used to evaluate effects on coagulation. In this setting, the balance between clot-enhancing PolySTAT and thrombin-inhibiting bivalirudin can be observed. In this stage, the material will be optimized for bivalirudin that provides a decrease in clotting.

Finally, the fibrin-targeted bivalirudin-containing polymer (FB Polymer) will be administered in the mouse model of metastatic cancer. Mice injected with MDA-MB-231-BR cells will receive material at 15 mg/kg every other day for 1 week to mimic the study that exacerbated metastasis. Additionally, FB Polymer will be evaluated as a prophylactic, administered at 15 mg/kg prior to tumor cell seeding to determine the ability to inhibit metastasis.

This work would provide the basis for a strategy of using the tumor microenvironment to deliver environment-modulating therapeutics. In future designs, materials could target basement membrane proteins present in metastatic lesions such as hyaluronic acid or chondroitin sulfate proteoglycans[145]. This would remove the additional complexity of including the potentially clot-enhancing capability that comes from targeting fibrin in a multivalent fashion. Other therapeutics can also be used; immunomodulation may be a good strategy for treatment beyond thrombin inhibition. Fibrin is known to decrease natural killer (NK) cells' response to tumor cells[146]. Cargo that counteracts the pacification of NK cells via stimulation NK cells may be a promising pathway. Finally, the development of a fibrin-targeting platform that does not enhance clotting would be highly impactful for the treatment of many diseases.

6.4 A TARGETING PLATFORM FOR *STAPHYLOCOCCUS AUREAS*

Staphylococcus aureas is a bacteria with clinical observations dating back to the 1880s[147]. As of 1998, 116 years after the first report, *S. aureus* infections, both in the

hospital and in the community, had increased for 20 years[148]. Today, *S. aureas* is the leading cause of pediatric hospital infection[149], and the second leading cause of hospital infection for all ages in the US[150] as reported by the National Healthcare Safety Network. The prevalence and mortality of *S. aureas* is exacerbated by resistance to antibiotics. Methicillin-resistant *S. aureas* (MRSA) has become increasingly common, especially in the US where in 2005 ~53% of *S. aureas* isolated are methicillin-resistant[151]. Consider that MRSA was first reported in early 1960s[152], and one can appreciate the rapid selection performed on bacteria by antibiotics use. Strains of *S. aureas* resistant to vancomycin, the standard of treatment for MRSA, are now identified worldwide under the title vancomycin intermediate-resistant *S. aureus* (VISA), posing additional concern to clinicians and complicating treatment schedules[153].

Future treatments for multidrug-resistant bacteria will require continuous innovation and multiple platforms for treatment. While there is regular innovation in small molecule antibiotics, this is decreasing with half as many antibiotics approved by the FDA from 2003-2007 as there were from 1983-1987[154]. As such, researchers in nanotechnology have explored the potential of their field for treating infectious disease. Similar to how nanotechnology and drug delivery principles have been applied for the development of synthetic hemostats targeted to platelets and clotting proteins, the delivery of therapeutics and synthetic materials specifically to bacteria in the body has the potential for a new approach to treating this growing public health concern.

S. aureus presents clumping factor A (ClfA) on its surface which binds fibrinogen, allowing for adherence to platelets and immobilized fibrinogen[155]. ClfA binds the C-terminus of the γ-chain of fibrinogen[156], the same region that is bound by GPIIb/IIIa, an integrin on the surface of platelets and the main component by which platelets are crosslinked during primary hemostasis. A synthetic peptide containing the 17 C-terminal amino acids of the fibrinogen γ-chain was shown to inhibit adherence of ClfA to fibrinogen[156]. ClfA is a confirmed strong virulence factor, as *Lactococcus lactis* engineered to express ClfA were 100-fold more infective than the standard strain[157]. Additionally, administration of a monoclonal antibody for ClfA was

protective against IV challenge with MRSA in a mouse septicemia model and a rabbit endocarditis model[158].

The C-terminus of the γ-chain of fibrinogen has caught interest in other fields as well. H12, a 12 amino acid peptide from the C-terminus of the fibrinogen γ-chain, has been thoroughly investigated for its ability to specifically bind the active form of glycoprotein IIb/IIIa (GP IIb/IIIa) on activated platelets[43,44,159,160]. In fact, an previous project in the Pun Lab was to determine if a multivalent H12-polymer conjugate would mimic fibrinogen, crosslinking platelets and improving clot kinetics and strength as a primary hemostasis analog to PolySTAT. For this project, we designed materials and evaluated their ability to enhance clotting.

P(HEMA-st-NHSMA) polymers were synthesized as described previously[66]. Briefly, HEMA, n-succinimidyl methacrylate (NHSMA), 4-cyanopentanoic acid dithiobenzoate (CTP), and azobisisobutyronitrile (AIBN) were combined at an 80:20:1:3 ratio in dimethylacetamide (DMAc) and allowed to react at 70° C for 24 hours. Product was purified by precipitation in ether. Polymers were characterized via gel permeation chromatography (GPC) to determine molecular weight and polydispersity index (PDI). Nuclear magnetic resonance (NMR) was utilized to determine NHSMA content of the polymer.

Propargyl amine was used to incorporate an alkyne functional group for click chemistry. p(HEMA-st-NHSMA) polymers and propargyl amine were combined in DMAc and reacted for 24 hours at 50° C under stirring. The amount of propargyl amine incorporated was determined via NMR.

H12 (HHLGGAKQAGDV) and control peptide, rH12 (VDGAQKAGGLHH) were synthesized on a PS3 peptide synthesizer by solid-phase Fmoc synthesis. The reverse peptide was chosen as a control based on previously reported results[161]. Both peptides were functionalized for click chemistry on-resin with 5-azidopentanoic acid in the presence of HBTU (carboxylic acid activator). Purification was performed via reverse phase high performance liquid chromatography (RP-HPLC).

Azide-functionalized peptides were reacted with alkyne-functionalized polymers through a 1,3-cycloaddition reaction. Briefly, alkyne, azide, CuBr, and PMDETA were combined at a 1:1:1:1 ratio and allowed to react for 24 hours at 60° C. Product

was purified by extensive dialysis against deionized H2O. Peptide content was confirmed qualitatively via amino acid analysis (AAA).

H12 conjugate size and content characterization results are collected in the in Table 5.1. Polymers were synthesized with molecular weights (29 kDa) and NHSMA contents (19 kDa) similar to theoretical values and alkyne-functionalized at ~15%. While peptide presence was confirmed by AAA, pHEMA monomers were not quantifiable, yielding no value for peptide per polymer. As H12 does not contain amino acid residues that absorb at an absorbance of 280 nm, absorbance could not be used.

Table 5.1 Polymer Synthesis Results.

Polymer	DP	Theoretical MW (Da)	Experimental MW (Da)	PDI	Theoretical % NHSMA	Experimental % NHSMA	% Propargyl Amine
pHEMA-*st*-NHSMA (H12 Conj.)	200	28150	29000	1.14	20	18	14.9
pHEMA	200	26000	28500	1.2	0	-	-

Functionalized polymers were tested in blood and platelet-rich plasma (PRP) by thromboelastography (TEG). Under all TEG conditions, the H12 and rH12 conjugates were found to neither increase nor decrease clotting, as shown in Figure 2. TEG measurements were performed in whole blood, PRP, and diluted PRP; some runs contained plasmin for lytic conditions. Since H12 is derived from the C-terminus of fibrinogen, additional peptides were synthesized with a carboxylate at the C-terminus, rather than the original acyl group. Similar results were obtained to those in Figure 5.1.

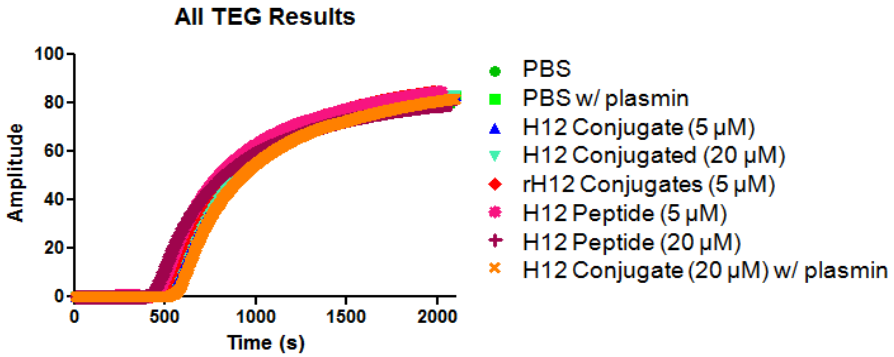

Figure 5.1. H12 Conjugate Thromboelastography. Indicative data from H12 TEG runs. No clot-altering activity observed for any conditions tested.

A likely explanation for the inactivity observed is that the H12 conjugate experiences geometric incompatibilities as a platelet cross-linker. H12 binding can be measured by flow cytometry with fluorescently-labeled peptides. The second possibility is that the H12 conjugate is not a suitable structure for platelet cross-linking. At DP 200, an outstretched conjugate is ~40 nm in length, about two orders of magnitude smaller than the 1-3 μm platelet[162]. As there are ~80,000 GP IIb/IIIa per platelet[163], a single platelet surface may saturate the peptides on the conjugate.

This early work on a platelet crosslinker may be valuable to show that *S. aureas*-targeting polymer would not enhance clotting. Non-specific thrombosis leads to stroke, heart attack, and pulmonary embolism and therefore should be avoided in all treatments.

To develop the *S. aureas*-targeting polymer (PolySTAPH), a proof-of-concept material will be synthesized as above and fluorescently labeled via Cy5-amine. Binding studies will be performed against *S. aureus* by incubating bacteria cells with PolySTAPH and collecting via centrifugation. Fluorescence of the samples will be measured by a plate reader.

PolySTAPH will be evaluated in a mouse model of septicemia described for the ClfA monoclonal antibody[158,164]. Briefly, mice will be inoculated with PolySTAPH and infected with $6x10^6$ CFU per mouse. Mice will be observed for 30 days to determine mortality. As the biodistribution of PolySTAPH will vary significantly from an antibody, a follow up with multiple injections will be performed with mice receiving PolySTAPH every other day starting day -1 to day 4.

The primary mechanism by which the ClfA mAb protects against MRSA infection is believed to be reduced adherence to tissues via immobilized fibrinogen. As such, we expect PolySTAPH alone to improve survival in this *in vivo* model. If this is not the case, bacteriocin peptides may be incorporated into the design. Nisin is an antimicrobial peptide which has shown activity against *S.* aureus[165,166], and similar peptides have been identified and are prime candidates for incorporation into a system to deliver antimicrobial peptides to MRSA[167–169]. Despite the added complexity of design, the fully synthetic nature of these materials provides manufacturing and storage advantages to antibodies.

PolySTAPH may have potential for diagnostic applications. As a diagnostic, PolySTAPH may crosslink or effectively clump *S. aureus* which would allow for an agglutination assay for patient samples. Additional readouts may also be used such as more-costly fluorescence. Finally, additionally functionality could be added to PolySTAPH for isolating and concentrating bacteria for detection. One such option would be to biotinylate PolySTAPH for use in a streptavidin column.

Thus, a material designed in the Pun Lab and initially thought to have failed may see success in a new and impactful field. Concerns of a multivalent material with ligands for platelets are assuaged as an H12-peptide conjugate did not enhance clotting by thromboelastogrpahy. Thus, this GPIIa/IIIa binding polymer may also be used as a *S. aureu*s-binding polymer. This material would likely be therapeutic on its own, however it would also provide a platform for the delivery of drugs to the extremely dangerous MRSA. With the growing list of multidrug resistant *S. aureus*, innovative methods for neutralizing infection will be highly impactful.

6.5 REFERENCES

1. WISQARS: Leading Causes of Death Reports. *Centers for Disease Control and Prevention* (2015).
2. WISQARS: Years of Potential Life Lost. *Centers for Disease Control and Prevention* (2015).
3. Murray, C. J. L., Lopez, A. D., Mathers, C. D. & Stein, C. *The Global Burden of Disease 2000 project: aims, methods and data sources*. (2001).
4. World Health Organization: The top 10 causes of death. (2017). Available at: http://www.who.int/mediacentre/factsheets/fs310/en/.
5. Sauaia, A. *et al.* Epidemiology of Trauma Deaths: A Reassessment. *J. Trauma* **38,** 185–193 (1995).
6. Lerner, E. B. & Moscati, R. M. The Golden Hour : Scientific Fact or Medical 'Urban Legend'. *Am. Emerg. Med.* **8,** 758–760 (2001).
7. Kauvar, D. S., Lefering, R. & Wade, C. E. Impact of Hemorrhage on Trauma Outcome : An Overview of Epidemiology, Clinical Presentations, and Therapeutic Considerations. *J.*

Trauma **60,** 3–11 (2006).

8. Champion, H. R. *et al.* A Profile of Combat Injury. *J. Trauma* **54,** 513–519 (2003).
9. Holcomb, J. B. *et al.* Causes of Death in U . S . Special Operations Forces in the Global War on Terrorism. **245,** 986–991 (2007).
10. Chan, L. W., White, N. J. & Pun, S. H. Synthetic Strategies for Engineering Intravenous Hemostats. *Bioconjug. Chem.* **26,** 1224–1236 (2015).
11. Chen, H., Locke, D., Liu, Y., Liu, C. & Kahn, M. L. The Platelet Receptor GPVI Mediates Both Adhesion and Signaling Responses to Collagen in a Receptor Density-dependent Fashion*. **277,** 3011–3019 (2002).
12. Daniel, J. L. *et al.* Molecular Basis for ADP-induced Platelet Activation. **273,** 2024–2029 (1998).
13. Klinik, M. *et al.* Molecular Mechanisms of Platelet Activation. *Pharm. Rev.* **69,** 58–141 (1989).
14. Shattil, S. J., Hoxie, J. A., Cunningham, M. & Brass, L. F. Changes in the Platelet Membrane Glycoprotein IIb * IIIa Complex during Platelet Activation *. **260,** (1985).
15. Takeoka, S. *et al.* Function of fibrinogen. **312,** 773–779 (2003).
16. Tomiyama, Y., Tsubakio, T. & Kurata, Y. The Arg-Gly-Asp (RGD) recognition site of platelet glycoprotein IIb- IIIa on nonactivated platelets is accessible to high-affinity macromolecules. *Blood* **79,** 2303–2312 (2011).
17. Davie, E. W., Fujikawa, K. & Kisiel, W. The Coagulation Cascade: Initiation, Maintenance, and Regulation. *Biochemistry* **30,** 10363–10370 (1991).
18. Morrison, D. C. & Cochrane, C. G. Direct Evidence For Hageman Factor (Factor XII) Activation by Bacterial Lipopolysaccharides. *J. Exp. Med.* **140,** 797–811 (1974).
19. Bouma, B. N. & Griffin, J. H. Human blood coagulation factor XI . Purification , properties , and mechanism of activation by activated factor XII. *J. Biol. Chem.* **252,** 6432–6437 (1977).
20. Hoffman, M., Monroe, D. M. & Roberts, H. R. Activated factor VII activates factors IX and X on the surface of activated platelets : thoughts on the mechanism of action of ... *Blood Coagul. Fibrinolysis* **9,** S61–S65 (1998).
21. Mann, K. G., Brummel, K. & Butenas, S. What is all that thrombin for? *J Thromb Haemost* **1,** 1504–1514 (2003).

22. White, N. J. Mechanisms of trauma-induced coagulopathy. *Haematology* 660–663 (2013).
23. Kushimoto, S., Kudo, D. & Kawazoe, Y. Acute traumatic coagulopathy and trauma-induced coagulopathy : an overview. *J. Intensive Care* 1–7 (2017). doi:10.1186/s40560-016-0196-6
24. Brohi, K., Singh, J., Heron, M. & Coats, T. Acute traumatic coagulopathy. *J. Trauma* **54,** 1127–1130 (2003).
25. Kaafarani, H. M. a & Velmahos, G. C. Damage control resuscitation in trauma. *Scand. J. Surg.* **103,** 81–88 (2014).
26. Mikhail, J. The trauma triad of death: hypothermia, acidosis, and coagulopathy. *AACN clinical issues* **10,** 85–94 (1999).
27. Niles, S. E. *et al.* Increased Mortality Associated With the Early Coagulopathy of Trauma in Combat Casualties. *J. Trauma Inj. Infect. Crit. Care* **64,** 1459–1465 (2008).
28. Standbury, L. G. & Hess, J. R. Blood Transfusion in World War I : The Roles of Lawrence Bruce. *Transfus. Med. Rev.* **23,** 232–236 (2009).
29. Boyle, R., Willis, T. & Wren, C. The History of Blood Transfusion. *Br. J. Haemotology* **110,** 758–767 (2000).
30. Duchesne, J. C., Hunt, J. P., Wahl, G. & Marr, A. B. Review of Current Blood Transfusions Strategies in a Mature Level I Trauma Center : Were We Wrong for the Last 60. *J. Trauma* **65,** 272–278 (2008).
31. Repine, T. B., Perkins, J. G., Kauvar, D. S. & Blackborne, L. The Use of Fresh Whole Blood in Massive Transfusion. **60,** (2005).
32. Sihler, K. C. & Napolitano, L. M. Complications of Massive Transfusion. *Chest* **137,** 209–220 (2010).
33. Riou, B. *et al.* Recombinant factor VIIa (Novoseven) as adjunctive therapy for bleeding contorl in trauma - a randomized. placebo-controlled trial. in *Shock* 228 (2004).
34. Rizoli, S. B. *et al.* Recombinant activated factor VII as an adjunctive therapy for bleeding control in severe trauma patients with coagulopathy : subgroup analysis from two randomized trials. *Crit. Care* **10,** 1–11 (2006).
35. Raza, I. *et al.* The incidence and magnitude of fibrinolytic activation in trauma patients. *J. Thromb. Haemost.* **11,** 307–314 (2013).
36. Williams-johnson, J. A., Mcdonald, A. H., Strachan, G. G. & Williams, E. W. Effects of

Tranexamic Acid on Death, Vascular Occlusive Events, and Blood Transfusion in Trauma Patients with Significant Haemorrhage (CRASH-2) A Randomised, Placebo-Controlled Trial. *West Indian Med J* **59,** 612–624 (2010).

37. Houston, F. S. Military Application of Tranexamic Acid in Trauma Emergency Resuscitation (MATTERs) Study. **147,** 113–119 (2012).
38. Search Results: tranexamic acid. *ClinicalTrials.gov* (2018).
39. Coller, B. S. Interaction of normal, thrombathemis, and Bernard-Soulier platelets with immobilized fibrinogen: defective platelet-fibrinogen interaction in thrombastatin. *Blood* **55,** 169–179 (1980).
40. Coller, B. S. *et al.* Thromboerythrocytes In Vitro Studies of a Potential Autologous , Semi-artificial Alternative to Platelet Transfusions. *J Clin Invest* **98,** 546–555 (1992).
41. Ten, O. Fibrinogen-coated albumin microcapsules reduce bleeding in severely thrombocytopenic rabbits. **9,** 107–111 (1999).
42. Illum, L. *et al.* Blood clearance and organ deposition of intravenously administered colloidal particles . The effects of particle size , nature and shape. **12,** 135–146 (1982).
43. Okamura, Y. *et al.* Hemostatic effects of phospholipid vesicles carrying fibrinogen gamma chain dodecapeptide in vitro and in vivo. *Bioconjug. Chem.* **16,** 1589–96 (2005).
44. Okamura, Y. *et al.* Development of fibrinogen gamma-chain peptide-coated, adenosine diphosphate-encapsulated liposomes as a synthetic platelet substitute. *J. Thromb. Haemost.* **7,** 470–7 (2009).
45. Bertram, J. P. *et al.* Intravenous Hemostat : Nanotechnology to Halt Bleeding. *Sci. Transl. Med.* **1,** 11–22 (2009).
46. Shoffstall, A. J. *et al.* Tuning ligand density on intravenous hemostatic nanoparticles dramatically increases survival following blunt trauma. *Biomacromolecules* **14,** 2790–2797 (2013).
47. Lashof-sullivan, M. *et al.* Hemostatic Nanoparticles Improve Survival Following Blunt Trauma Even after 1 Week Incubation at 50 °C. *ACS Biomater. Sci. Eng.* **2,** 385–392 (2016).
48. Shoffstall, A. J. *et al.* Intravenous hemostatic nanoparticles increase survival following blunt trauma injury. *Biomacromolecules* **13,** 3850–3857 (2012).
49. Hubbard, W. B., Lashof-Sullivan, M. M., Lavik, E. B. & Vandevord, P. J. Steroid-loaded

hemostatic nanoparticles combat lung injury after blast trauma. *ACS Macro Lett.* **4,** 387–391 (2015).

50. Onwukwe, C. *et al.* Engineering Intravenously Administered Nanoparticles to Reduce Infusion Reaction and Stop Bleeding in a Large Animal Model of Trauma. (2018). doi:10.1021/acs.bioconjchem.8b00335
51. Gupta, A. Sen, Huang, G., Lestini, B. J., Sagnella, S. & Kottke-marchant, K. RGD-modified liposomes targeted to activated platelets as a potential vascular drug delivery system RGD-modified liposomes targeted to activated platelets as a potential vascular drug delivery system. *Thromb Haemost* **93,** 106–114 (2005).
52. Ravikumar, M., Modery, C. L., Wong, T. L. & Gupta, A. Sen. Peptide-Decorated Liposomes Promote Arrest and Aggregation of Activated Platelets under Flow on Vascular Injury Relevant Protein Surfaces in Vitro. *Biomacromolecules* **13,** 1495–1502 (2012).
53. Ravikumar, M. *et al.* Mimicking Adhesive Functionalities of Blood Platelets using Ligand- Decorated Liposomes. *Bioconjug. Chem.* **23,** 1266–1275 (2012).
54. Modery-Pawlowski, C. L., Tian, L. L., Ravikumar, M., Wong, T. L. & Gupta, A. Sen. In vitro and in vivo hemostatic capabilities of a functionally integrated platelet-mimetic liposomal nanoconstruct. *Biomaterials* **34,** 3031–3041 (2013).
55. Hickman, D. A. *et al.* Intravenous synthetic platelet (SynthoPlate) nanoconstructs reduce bleeding and improve ‘ golden hour ’ survival in a porcine model of traumatic arterial hemorrhage. *Sci. Rep.* 1–14 (2018). doi:10.1038/s41598-018-21384-z
56. Shukla, M., Sekhon, U. D. S., Li, W. & Hickman, D. A. In vitro characterization of SynthoPlate (synthetic platelet) technology and its in vivo evaluation in severely thrombocytopenic mice. *J Thromb Haemost* **15,** 375–387 (2016).
57. Lashof-sullivan, M., Sho, A. & Lavik, E. Intravenous hemostats : challenges in translation to patients. *Nanoscale* **5,** 10719–10728 (2013).
58. Szebeni, J. *et al.* Prevention of infusion reactions to PEGylated liposomal doxorubicin via tachyphylaxis induction by placebo vesicles: A porcine model. *J. Control. Release* **160,** 382–387 (2012).
59. Brown, A. C. *et al.* Ultrasoft microgels displaying emergent platelet-like behaviours. *Nat. Mater.* **13,** 1–7 (2014).

60. Niewlarowski, S., Regoeczi, E., Stewart, G. J., Senyi, A. F. & Mustard, J. F. Platelet Interaction with Polymerizing Fibrin. **51,** 685–700 (1972).
61. Welsch, N., Brown, A. C., Barker, T. H. & Lyon, L. A. Colloids and Surfaces B : Biointerfaces Enhancing clot properties through fibrin-specific self-cross-linked PEG side-chain microgels. *Colloids Surfaces B Biointerfaces* **166,** 89–97 (2018).
62. Lorand, L. A double-headed Gly-Pro-Arg-Pro ligand mimics the functions of the E domain of fibrin for promoting the end-to-end crosslinking of chains by factor XIII a. **95,** 537–541 (1998).
63. Soon, A. S. C., Lee, C. S. & Barker, T. H. Modulation of fibrin matrix properties via knob:hole affinity interactions using peptide-PEG conjugates. *Biomaterials* **32,** 4406–4414 (2011).
64. Kolodziej, A. F. *et al.* Fibrin Specific Peptides Derived by Phage Display: Characterization of Peptides and Conjugates for Imaging. *Bioconjug. Chem.* **23,** 548–556 (2012).
65. Kolodziej, A. F., Zhang, Z., Overoye-chan, K., Jacques, V. & Caravan, P. Peptide Optimization and Conjugation Strategies Magnetic Resonance Imaging Contrast Agents. **1088,** 185–211
66. Chan, L. W. *et al.* A synthetic fibrin cross-linking polymer for modulating clot properties and inducing hemostasis. *Sci. Transl. Med.* **7,** (2015).
67. Chiefari, J. *et al.* Living Free-Radical Polymerization by Reversible Addition - Fragmentation Chain Transfer : The RAFT Process We wish to report a new living free-radical polymer- ization of exceptional effectiveness and versatility . 1 The living character is conferred by . **9297,** 5559–5562 (1998).
68. Chu, D. S. H. *et al.* Application of living free radical polymerization for nucleic acid delivery. *Acc. Chem. Res.* **45,** 1089–1099 (2012).
69. Kopeček, J., Kopečková, P., Minko, T., Lu, Z. R. & Peterson, C. M. Water soluble polymers in tumor targeted delivery. *J. Control. Release* **74,** 147–158 (2001).
70. Barrett, G. D., Constable, I. J. & Stewart, A. D. Clinical results of hydrogel lens implantation. *J. Cataract Refract. Surg.* **12,** 623–631 (1986).
71. Chan, L. W., White, N. J. & Pun, S. H. A Fibrin Cross-linking Polymer Enhances Clot Formation Similar to Factor Concentrates and Tranexamic Acid in an in Vitro Model of

Coagulopathy. *ACS Biomater. Sci. Eng.* (2016). doi:10.1021/acsbiomaterials.5b00536

72. Maegele, M. *et al.* Early coagulopathy in multiple injury: An analysis from the German Trauma Registry on 8724 patients. *Injury* **38,** 298–304 (2007).
73. 6 Factor VIII Concentrates, Factor VIII/von Willebrand Factor Concentrates, Factor IX Concentrates, Activated Prothrombin Complex Concentrates. *Transfus. Med. Hemotherapy* **36,** 409–418 (2009).
74. Okamura, Y. *et al.* Development of fibrinogen c-chain peptide-coated, adenosine diphosphate-encapsulated liposomes as a synthetic platelet substitute. *J Thromb Haemost* **7,** 470–477 (2009).
75. Fasting, C. *et al.* Multivalency as a Chemical Organization and Action Principle. *Angew. Rev.* **51,** 10472–10498 (2012).
76. Spain, S. G. & Cameron, N. R. A spoonful of sugar : the application of glycopolymers in therapeutics. *Polym. Chem.* **2,** 60–68 (2011).
77. Weigandt, K. M., Pozzo, D. C. & Porcar, L. Structure of high density fibrin networks probed with neutron scattering and rheology. *Soft Matter* **5,** 4321–4330 (2009).
78. Weigandt, K. M., Porcar, L. & Pozzo, D. C. In situ neutron scattering study of structural transitions in fibrin networks under shear deformation. *Soft Matter* **7,** 9992–10000 (2011).
79. Yanjarappa, M. J., Gujraty, K. V, Joshi, A., Saraph, A. & Kane, R. S. Synthesis of Copolymers Containing an Active Ester of Methacrylic Acid by RAFT : Controlled Molecular Weight Scaffolds for Biofunctionalization. *Biomacromolecules* **7,** 1665–1670 (2006).
80. Kirby, N. M. *et al.* research papers A low-background-intensity focusing small-angle X-ray scattering undulator beamline. 1670–1680 (2013). doi:10.1107/S002188981302774X
81. Hammouda, B., Ho, D. L. & Kline, S. Insight into Clustering in Poly (ethylene oxide) Solutions. *Macromolecules* **37,** 6932–6937 (2004).
82. Glinka, C. J. *et al.* The 30 m Small-Angle Neutron Scattering Instruments at the National Institute of Standards and Technology. *J. Appl. Crystallogr.* **31,** 430–445 (1998).
83. Kline, S. R. Reduction and analysis of SANS and USANS data using IGOR Pro. *J. Appl. Crystallogr.* **39,** 895–900 (2006).
84. Barker, J. G. *et al.* Design and performance of a thermal-neutron double-crystal diffractometer for USANS at NIST. *J. Appl. Crystallogr.* **38,** 1004–1011 (2005).

85. Terech, P. Structural Study of Cholesteryl Anthraquinone-2-carboxylate (CAQ) Physical Organogels by Neutron and X-ray Small Angle Scattering. *J. Phys. Chem.* **100,** 3759–3766 (1996).
86. Teixeira, J. Small-Angle Scattering by Fractal Systems. *J. Appl. Crystallogr.* **21,** 781–785 (1988).
87. Hammouda, B. & Horkay, F. Clustering and Solvation in Poly(acrylic acid) Polyelectrolyte Solutions. *Macromolecules* **38,** 2019–2021 (2005).
88. Dowling, M. B. *et al.* Biomaterials A self-assembling hydrophobically modi fi ed chitosan capable of reversible hemostatic action. *Biomaterials* **32,** 3351–3357 (2011).
89. Laudano, A. P. & Doolittle, R. F. Studies on synthetic peptides that bind to fibrinogen and prevent fibrin polymerization. Structural requirements, number of binding sites, and species differences. *Biochemistry* **19,** 1013–1019 (1980).
90. Lukyanov, A. N. & Torchilin, V. P. Micelles from lipid derivatives of water-soluble polymers as delivery systems for poorly soluble drugs. **56,** 1273–1289 (2004).
91. Rizvi, S. A. A. & Saleh, A. M. Applications of nanoparticle systems in drug delivery technology. *Saudi Pharm. J.* **26,** 64–70 (2018).
92. Kieler-ferguson, H. M. & Fr, J. M. J. Clinical developments of chemotherapeutic nanomedicines : polymers and liposomes for delivery of camptothecins and platinum (II). **5,** (2013).
93. Press, D. Effective use of nanocarriers as drug delivery systems for the treatment of selected tumors. 7291–7309 (2017).
94. Langer, R. Drug delivery and targeting. **392,** 5–10 (1998).
95. Montet, X., Funovics, M., Montet-abou, K., Weissleder, R. & Josephson, L. Multivalent Effects of RGD Peptides Obtained by Nanoparticle Display. 6087–6093 (2006). doi:10.1021/jm060515m
96. Lee, H., Fonge, H., Hoang, B., Reilly, R. M. & Allen, C. articles The Effects of Particle Size and Molecular Targeting on the Intratumoral and Subcellular Distribution of Polymeric Nanoparticles. **7,** 1195–1208 (2010).
97. Lamm, R. J. *et al.* Peptide valency plays an important role in the activity of a synthetic fibrin-crosslinking polymer. *Biomaterials* **132,** 96–104 (2017).
98. Devlin, J., Panganiban, L. & Devlin, P. Random peptide libraries: a sourse of specific

protein binding molecules. *Science (80-.).* **249,** 404–406 (1990).

99. Fan, S. *et al.* Curcumin-loaded PLGA-PEG nanoparticles conjugated with B6 peptide for potential use in Alzheimer ' s disease. *Drug Deliv.* **25,** 1044–1055 (2018).
100. Duvall, C. L., Convertine, A. J., Benoit, D. S. W., Hoffman, A. S. & Stayton, P. S. articles Intracellular Delivery of a Proapoptotic Peptide via Conjugation to a RAFT Synthesized Endosomolytic Polymer. (2010).
101. Chu, D. S. *et al.* As featured in : Biomaterials Science. (2015). doi:10.1039/c4bm00259h
102. Johnson, R. N. *et al.* Synthesis of Statistical Copolymers Containing Multiple Functional Peptides for Nucleic Acid Delivery. *Biomacromolecules* **11,** 3007–13 (2010).
103. Chu, D. S. H., Schellinger, J. G., Bocek, M. J., Johnson, R. N. & Pun, S. H. Optimization of Tet1 ligand density in HPMA-co-oligolysine copolymers for targeted neuronal gene delivery. *Biomaterials* **34,** 9632–9637 (2013).
104. Schellinger, J. G. *et al.* Melittin-grafted HPMA-oligolysine based copolymers for gene delivery. *Biomaterials* **34,** 2318–2326 (2013).
105. Kanaide, H. & Shainoff, J. R. Cross-linking of fibrinogen and fibrin by fibrin-stabilizing factor (factor XIIIa). *Transl. Res.* **85,** 574–597 (1975).
106. O'Brien-Simpson, N. M., Ede, N. J., Brown, L. E., Swan, J. & Jackson, D. C. Polymerization of unprotected synthetic peptides: A view toward synthetic peptide vaccines. *J. Am. Chem. Soc.* **119,** 1183–1188 (1997).
107. Hasson, C. J., Caldwell, G. E. & Emmerik, R. E. A. Van. NIH Public Access. *Motor Control* **27,** 590–609 (2009).
108. Studenovská, H., Šlouf, M. & Rypáček, F. Poly(HEMA) hydrogels with controlled pore architecture for tissue regeneration applications. *J. Mater. Sci. Mater. Med.* **19,** 615–621 (2008).
109. Kopeckova, P. Water soluble polymers in tumor targeted delivery. *J. Control. Release* **74,** 147–158 (2001).
110. Cunningham, V. J. *et al.* Poly(glycerol monomethacrylate) − Poly(benzyl methacrylate) Diblock Copolymer Nanoparticles via RAFT Emulsion Polymerization: Synthesis, Characterization, and Interfacial Activity. (2014). doi:10.1021/ma501140h
111. Save, M., Weaver, J. V. M., Armes, S. P. & Mckenna, P. Atom Transfer Radical Polymerization of Hydroxy-Functional Methacrylates at Ambient Temperature:

Comparison of Glycerol Monomethacrylate with 2-Hydroxypropyl Methacrylate. 1152–1159 (2002). doi:10.1021/ma011541r

112. Das, D. *et al.* RAFT polymerization of ciprofloxacin prodrug monomers for the controlled intracellular delivery of antibiotics. *Polym. Chem* **7,** 826–837 (2016).
113. Shin, H. C., Alani, A. W. G., Rao, D. A., Rockich, N. C. & Kwon, G. S. Multi-drug loaded polymeric micelles for simultaneous delivery of poorly soluble anticancer drugs. *J. Control. Release* **140,** 294–300 (2009).
114. Hughes, H. C. Swine in cardiovascular research. *Lab Anim. Sci.* **36,** 348–350 (1986).
115. Swindle, M. M., Makin, A., Herron, A. J., Clubb, F. J. & Frazier, K. S. Swine as Models in Biomedical Research and Toxicology Testing. *Vet. Pathol.* **49,** 344–356 (2012).
116. Pusateri, A. E. *et al.* Effect of a Chitosan-Based Hemostatic Dressing on Blood Loss and Survival in a Model of Severe Venous Hemorrhage and Hepatic Injury in Swine. *J trauma* **54,** 177–182 (2003).
117. Pusateri, A. E. *et al.* Advanced Hemostatic Dressing Development Program : Animal Model Selection Criteria and Results of a Study of Nine Hemostatic Dressings in a Model of Severe Large Venous Hemorrhage and Hepatic Injury in Swine. *J Trauma* **55,** 518–526 (2003).
118. Stern, S. *et al.* RESUSCITATION WITH THE HEMOGLOBIN-BASED OXYGEN CARRIER , HBOC-201 , IN A SWINE MODEL OF SEVERE UNCONTROLLED HEMORRHAGE AND TRAUMATIC BRAIN INJURY. *Shock* **31,** 64–79 (2009).
119. White, N. J., Wang, X., Liles, W. C. & Stern, S. Fibrinogen Concentrate Improves Survival During Limited Resuscitation of Uncontrolled Hemorrhagic Shock in a Swine Model. *Shock* **42,** 456–463 (2014).
120. Szebeni, J., Bed, P. & Rozsnyay, Z. Liposome-induced complement activation and related cardiopulmonary distress in pigs : factors promoting reactogenicity of Doxil and AmBisome. **8,** 176–184 (2012).
121. Szebeni, J. *et al.* A porcine model of complement-mediated infusion reactions to drug carrier nanosystems and other medicines ☆. **64,** 1706–1716 (2012).
122. Bertram, J. P. *et al.* Intravenous Hemostat : Nanotechnology to Halt Bleeding. (2009).
123. Boldt, J., Haisch, G., Suttner, S., Kumle, B. & Schellhaass, A. Effects of a new modifed, balanced hydroxyethyl starch preparation (Hextend). *Br. J. Anaesth.* **89,** 722–728 (2002).

124. Landskroner, K., Olson, N. & Jesmok, G. Cross-species pharmacologic evaluation of plasmin as a direct-acting thrombolytic agent: Ex vivo evaluation for large animal model development. *J. Vasc. Interv. Radiol.* **16,** 369–377 (2005).
125. Mitterlechner, T. *et al.* Prothrombin complex concentrate and recombinant prothrombin alone or in combination with recombinant factor X and FVIIa in dilutional coagulopathy: A porcine model. *J. Thromb. Haemost.* **9,** 729–737 (2011).
126. R. Baylis, J. *et al.* Rapid hemostasis in a sheep model using particles that propel thrombin and tranexamic acid. *Laryngoscope* **127,** 787–793 (2017).
127. Ngambenjawong, C., Gustafson, H. H., Sylvestre, M. & Pun, S. H. A Facile Cyclization Method Improves Peptide Serum Stability and Confers Intrinsic Fluorescence. *ChemBioChem* **18,** 2395–2398 (2017).
128. Von Maltzahn, G. *et al.* Nanoparticles that communicate in vivo to amplify tumour targeting. *Nat. Mater.* **10,** 545–552 (2011).
129. Liu, G. W. *et al.* Glomerular disease augments kidney accumulation of synthetic anionic polymers. *Biomaterials* **178,** 317–325 (2018).
130. Tabata, Y. & Ikada, Y. Effect of the size and surface charge of polymer microspheres on their phagocytosis by macrophage. *Biomaterials* **9,** 356–362 (1988).
131. Caliceti, P. & Veronese, F. P harmacokinetic and biodistribution properties of poly(ethylene glycol)–protein conjugates Paolo. *Adv. Drug Deliv. Rev.* **55,** 1261–1277 (2003).
132. Beier, J. I. *et al.* Fibrin accumulation plays a critical role in the sensitization to lipopolyccharide-induced liver injury caused by ethanol in mice. *Hepatology* **49,** 1545–1553 (2009).
133. Imokawa, S. *et al.* Tissue factor expression and fibrin deposition in the lungs of patients with idiopathic pulmonary fibrosis and systemic sclerosis. *Am. J. Respir. Crit. Care Med.* **156,** 631–636 (1997).
134. Brown, L. F., Dvorak, A. M. & Dvorak, H. F. Leaky vessels, fibrin deposition, and fibrosis: a sequence of events common to solid tumors and to many other types of disease. *Am. Rev. Respir. Dis.* **140,** 1104–7 (1989).
135. Hiramoto, R., Bernecky, J., Jurandowski, J. & Pressman, D. Fibrin in Human Tumors. *Cancer Res.* **20,** 592–593 (1960).

136. Fernandez, P. M., Patierno, S. R. & Rickles, F. R. Tissue factor and fibrin in tumor angiogenesis. *Semin. Thromb. Hemost.* **30,** 31–44 (2004).
137. Wallace, A. C. Demonstration of Fibrin in Early Stages of Experimental Metastases. *Cancer Res.* **36,** 1904–1909 (1976).
138. Dirix, L. Y. *et al.* Plasma fibrin D-dimer levels correlate with tumour volume, progression rate and survival in patients with metastatic breast cancer. *Br. J. Cancer* **86,** 389–395 (2002).
139. Chu, D. S. *et al.* MMP9-sensitive polymers mediate environmentally-responsive bivalirudin release and thrombin inhibition. *Biomater. Sci.* **3,** 41–45 (2015).
140. Warkentin, T. E., Greinacher, A. & Koster, A. Bivalirudin. *Thromb. Haemost.* **99,** 830–839 (2008).
141. Hejna, M., Raderer, M. & Zielinski, C. C. Inhibition of metastases by anticoagulants. *J. Natl. Cancer Inst.* **91,** 22–36 (1999).
142. Amirkhosravi, A. *et al.* Tissue factor pathway inhibitor reduces experimental lung metastasis of B16 melanoma. *Thromb. Haemost.* **87,** 930–936 (2002).
143. Kondapaka, S. B., Fridman, R. & Reddy, K. B. Epidermal growth factor and amphiregulin up-regulate matrix metalloproteinase-9 (MMP-9) in human breast cancer cells. *Int. J. Cancer* **70,** 722–726 (1997).
144. Svendsen, L., Blombäck, B., Blombäck, M. & Olsson, P. I. Synthetic chromogenic substrates for determination of trypsin, thrombin and thrombin-like enzymes. *Thromb. Res.* **1,** 267–278 (1972).
145. Reinhard, J., Brösicke, N., Theocharidis, U. & Faissner, A. The extracellular matrix niche microenvironment of neural and cancer stem cells in the brain. *Int. J. Biochem. Cell Biol.* **81,** 174–183 (2016).
146. Palumbo, J. S. *et al.* Platelets and fibrin(ogen) increase metastatic potential by impeding natural killer cell-mediated elimination of tumor cells. *Blood* **105,** 178–185 (2005).
147. Ogston, A. OGSTON, M.D., Surgeon. *J. Anat.* **16,** 526–567 (1882).
148. Lowry, F. D. Staphylococcus aureus Infections. *N. Engl. J. Med.* **339,** 520–532 (1998).
149. Lake, J. G. *et al.* Pathogen distribution and antimicrobial resistance among pediatric healthcare-associated infections reported to the National Healthcare Safety Network, 2011-2014. *Infect. Control Hosp. Epidemiol.* **39,** 1–11 (2018).

150. Weiner, L. M. *et al.* Antimicrobial-Resistant Pathogens Associated with Healthcare-Associated Infections: Summary of Data Reported to the National Healthcare Safety Network at the Centers for Disease Control and Prevention, 2011-2014. *Infect. Control Hosp. Epidemiol.* **37,** 1288–1301 (2016).
151. Lee, A. S. *et al.* Methicillin-resistant Staphylococcus aureus. *Nat. Rev. Dis. Prim.* **4,** (2018).
152. Jevons, P. M. 'Celbenin'-resistant Staphylococci. *Br. Med. J.* **1,** 124–125 (1961).
153. Hiramatsu, K. *et al.* Methicillin-resistant Staphylococcus aureus clinical strani with reduced vancomycin susceptibility. *J. Antimicrob. Chemother.* **40,** 135–146 (1997).
154. Huh, A. J. & Kwon, Y. J. 'Nanoantibiotics': A new paradigm for treating infectious diseases using nanomaterials in the antibiotics resistant era. *J. Control. Release* **156,** 128–145 (2011).
155. Loughman, A. *et al.* Roles for fibrinogen, immunoglobulin and complement in platelet activation promoted by Staphylococcus aureus clumping factor A. *Mol. Microbiol.* **57,** 804–818 (2005).
156. Mcdevitt, D. *et al.* Characterization of the interaction between the Staphylococcus aureus clumping factor (ClfA) and fibrinogen. *Eur. J. Biochem.* **247,** 416–424 (1997).
157. Que, Y. *et al.* Reassessing the Role of Staphylococcus aureus Clumping Factor and Fibronectin-Binding Protein by Expression in Lactococcus. *Infect. Immun.* **69,** 6296–6302 (2001).
158. Patti, J. M. A humanized monoclonal antibody targeting Staphylococcus aureus. *Vaccine* **22,** (2004).
159. Takeoka, S. *et al.* Function of fibrinogen gamma-chain dodecapeptide-conjugated latex beads under flow. *Biochem. Biophys. Res. Commun.* **312,** 773–9 (2003).
160. Okamura, Y. *et al.* Hemostatic effects of fibrinogen gamma-chain dodecapeptide-conjugated polymerized albumin particles in vitro and in vivo. *Transfusion* **45,** 1221–8 (2005).
161. Okamura, Y., Maekawa, I., Teramura, Y., Maruyama, H. & Handa, M. Hemostatic Effects of Phospholipid Vesicles Carrying Fibrinogen γ Chain Dodecapeptide in Vitro and in Vivo. 30–33 (2005).
162. Pease, D. C. An Electron Microscopy Study of Red Bone Marrow. *Blood* **11,** 501–526

(1956).

163. Wagner, B. C. L. *et al.* Analysis of GPIIb/IIIa Receptor Number by Quantification of 7E3 Binding to Human Platelets. (2015).

164. Nilsson, I. M., Patti, J. M., Bremell, T., Höök, M. & Tarkowski, A. Vaccination with a recombinant fragment of collagen adhesin provides protection against Staphylococcus aureus-mediated septic death. *J. Clin. Invest.* **101,** 2640–2649 (1998).

165. Stevens, K. A., Sheldon, B. W., Klapes, N. A. & Klaenhammer, T. R. Nisin treatment for inactivation of Salmonella species and other gram- negative bacteria. *Appl. Environ. Microbiol.* **57,** 3613–3615 (1991).

166. Millette, M., Le Tien, C., Smoragiewicz, W. & Lacroix, M. Inhibition of Staphylococcus aureus on beef by nisin-containing modified alginate films and beads. *Food Control* **18,** 878–884 (2007).

167. Hancock, R. E. W. Peptide antibiotics. *Lancet* **349,** 418–422 (1997).

168. Biscola, V. *et al.* Isolation and characterization of a nisin-like bacteriocin produced by a Lactococcus lactis strain isolated from charqui, a Brazilian fermented, salted and dried meat product. *Meat Sci.* **93,** 607–613 (2013).

169. Miao, J. *et al.* Membrane disruption and DNA binding of Staphylococcus aureus cell induced by a novel antimicrobial peptide produced by Lactobacillus paracasei subsp. tolerans FX-6. *Food Control* **59,** 609–613 (2016).